The Impact of a Scleral Lens on the Eye

by

Maria K Walker

A dissertation submitted to the Vision Science Department,

College of Optometry

in partial fulfilment of the requirement for the degree of

DOCTOR OF PHILOSOPHY

in Physiological Optics

Chair of Committee: Rachel R. Redfern, OD, PhD

Committee Member: Jan PG. Bergmanson, OD, PhD

Committee Member: Alan Burns, PhD

Committee Member: Langis Michaud, OD, MSc

University of Houston
May 2021

DEDICATION

To my scleral lens patients.

ACKNOWLEDGMENTS

First and foremost, I would like to extend my sincere gratitude to the University of Houston College of Optometry and to Dr. Laura Frishman for accepting me into the Graduate program and fostering interests and ambitions throughout my time in the program. I would also like to thank my committee chair and PhD advisor Dr. Rachel Redfern. The countless days, nights and weekends that she has spent helping me to write grants, plan experiments, evaluate data, edit manuscripts, and more, have been integral to my success in the program. Beyond the scientific mentorship, Rachel has always been a kind and thoughtful friend to me, sharing birthdays, holidays, and helping guide me along each step of my professional path. I am greatly appreciative of her mentorship and guidance over the past several years.

I also thank Dr. Carolina Lema for her extremely patient and kind approach to teaching me valuable lab techniques and practices. She has also spent many long hours working with me to make experiments work in the lab, troubleshoot protocol challenges, or scrutinize the results to make sense of the outcomes. Always enjoying a good laugh or cry during our conversations about current events and family, I will fondly remember my times in the lab with Carolina.

Dr. Jan Bergmanson has been a strong mentor to me since I arrived at UHCO in 2014. Having a robust history of contact lens research and a scleral lens background, he has offered invaluable advice and mentorship many times during my time in the PhD program. He is always willing to discuss new and interesting scleral lens projects and is continuously eager to collaborate on studies that will improve the outcomes with scleral lens wear. I also appreciate his light-hearted approach to life, and his good company at dinners, conferences, and in the halls of UHCO.

When I started the PhD program, I understood very little about the complicated interactions of inflammatory proteins and cells on the ocular surface. Many productive conversations over the years with Dr. Alan Burns have helped change this, and whether it be brainstorming on his

whiteboard or learning hidden gems from the contents of his well-stocked bookshelf, I always come away with a fresh perspective after visiting with Dr. Burns.

As I was first inspired to begin research with scleral lenses and began to read the peer-reviewed literature, I was immediately drawn to the research of Dr. Langis Michaud. He has consistently and prolifically studied broad aspects of research related to scleral lenses, and I am continuously inspired by his work in the field. I am lucky to have gotten to know him over the years, and always enjoy our dynamic conversations about scleral lens research at conferences and meetings. He continues to be a role model for me, and I thank Dr. Michaud for his continued mentorship and for serving on this dissertation committee.

I have many research and clinical colleagues that have supported me tremendously over the past several years. Drs. Karen Lee, Matt Kauffman, and all of the other faculty and staff working in the contact lens department at UHCO have been continuously supportive and have helped me to administrate my clinical research endeavors. Dr. Kathryn Richdale has been a great friend and mentor to me over the past few years, often taking our dogs for long walks to discuss future project directions and grants. Dr. David Berntsen, who initially encouraged me to come to UHCO to work on his BLINK clinical trial, has continuously provided advice and direction in navigating my career in clinical research. I offer all of these colleagues my heartfelt gratitude.

Lastly, I would like to thank my family and friends for all of their support. My wonderful and supportive parents, Danny and Kitty, who have never yielded in their encouragement of my education, establishing it as a keystone in my life from a young age. Kevin Cohn, my supportive partner, who has continuously provided the daily support I've needed to achieve this goal. From cooking dinner, to taking care of the dogs while I've worked late tending to an experiment or trying to finish a manuscript, he has always been there. My sisters, Liz and Katie, whose accomplishments and merits have always inspired me and challenged me to seek my fullest potential. I thank all of you for your love and support.

ABSTRACT

Purpose: There are several gaps in understanding ocular effects of a scleral lens (SL), particularly in the composition of the fluid reservoir (FR) that bathes the cornea and the impact of the landing zone radius (LZR) on the eye. The purpose of this dissertation is to (1) identify and compare molecules in the FR to basal tears, (2) determine the composition of the FR in midday fogging (MDF), and (3) determine if conjunctival compression from the LZR changes the intraocular pressure (IOP) and optic nerve head minimum rim width (MRW).

Methods: (1) In normal subjects (n=15) wearing SL for 8-hour, basal and FR tear samples were collected, and immunomodulatory molecules were quantitated using Luminex multiplex immunoassay and compared between tear sample types. (2) In normal subjects (n=13) wearing SL, optical coherence tomography (OCT) was used to quantitate MDF, which was then correlated to relative lipid and protein abundances (mass spectrometry), SL parameters, and ocular surface health outcomes. (3) In normal subjects (n=26) wearing a SL on one (test) eye, MRW and IOP were measured using OCT imaging and iCare tonometry, respectively, at baseline, 2- and 6-hours SL wear and compared to the untreated (control) eye.

Results: (1) Matrix metalloproteinase (MMP)-9 and MMP-10 were significantly greater in the FR, reaching 62.7 and 25.8 ng/ml, respectively, after 8-hours SL wear. (2) MDF samples were positively correlated to levels of wax esters ($r = +0.76$, $P = 0.01$) and hydrophobic lipids, negatively correlated to conjunctival compression ($r = -0.59$, $P = 0.048$), and not correlated to negative ocular surface health outcomes. (3) MRW thinning was not different in the test eyes after 6-hours of SL wear (-8 μm) vs control (-6 μm) eyes ($P = 0.09$). Mean IOP increased 2 mmHg post-SL removal ($P = 0.02$).

Conclusions: In normal SL wearers, the FR is distinct from the basal tears and may retain inflammatory molecules. Hydrophobic lipids are primarily correlated to MDF, supporting the need for development of a lipophilic solution in the SL bowl to reduce the risk of MDF. Despite a modest increase in IOP post-SL removal, MRW is not significantly impacted during SL wear.

TABLE OF CONTENTS

LIST OF TABLES

LIST OF FIGURES

LIST OF ABBREVIATIONS

Abbreviation	Full name
AH	Aqueous humor
AS-OCT	Anterior segment - optical coherence tomography
AV	Aqueous veins
BC	Base curve
BMO	Bruch's Membrane opening
CC	Collector channels
CE	Cholesterol ester
ECM	Extracellular matrix
FR	Fluid reservoir
GP	(corneal) gas permeable lens
IL	Interleukin
IOP	Intraocular pressure
LZR	Landing zone radius
MDF	Midday fogging
MGD	Meibomian gland dysfunction
MMP	Matrix metalloproteinase
MRW	Minimum rim width
MS	Mass spectrometry
MSREC	Mass spectrometry research and education center
OAHFA	(O-acyl)-ω-hydroxyl fatty acids
OCT	Optical coherence tomography
OZR	Optic zone radius
PC	Phosphatidylcholine
SAG	Sagittal depth
SC	Schlemm's canal
SL	Scleral lens
SV	Scleral veins
TAG	Triacylglycerols
TIMP	Tissue inhibitor of MMP
TM	Trabecular meshwork
TZR	Transition zone radius
WE	Wax ester

Chapter 1. Background & Introduction

The history of scleral lenses

A rigid contact lens to provide stable and optimal optics for an irregular cornea is not a novel concept, and in fact the first type of rigid lens was a scleral bearing, large diameter (15. 0-22.0 mm) glass lens, developed between 1887 to 1889 by three independent men in Europe[1–3]. In 1887, at the firm of F. Ad. Müller & Söhne of Wiesbaden, Germany, the first SL was manufactured for a patient with lagophthalmic keratitis in the right eye due to cancerous destruction of the lower eyelid. This therapeutic, blown glass shell was worn on an extended wear basis and probably had a total diameter of about 25.00 - 30.00 mm[4]. In 1888, Adolf Fick designed a ground shell with a total diameter of 20.00 mm in a series of five patients with corneal scarring and one with keratoconus, only one of them achieving visual improvement[1]. In the same year, Photinos Panas reported that his junior colleague, Eugène Kalt, had obtained a significant increase in visual acuity with a shell in a case of keratoconus[5]. Examination of Kalt's shells revealed that they had a mono-curve back surface construction with a total diameter of 16.00–22.00 mm[6]. In 1889, August Müllerwas the first clinician to correct refractive error with a contact lens, when he neutralized his own high myopia using a ground SL having a total diameter of 20.00 mm[3].

SL fitting in Europe expanded slowly over the next 30-40 years, and in the 1920s a German firm (Carl Zeiss) developed the practice of fitting SLs using a trial set. They offered a choice of four alternative specifications of ground glass lenses to correct keratoconus[7]. Within a decade the fitting set expanded to 39 lenses to allow correction of refractive errors[8]. While there was a range of base curve radii and back surface scleral radii, each lens had the same primary optic diameter of 12.00 mm and the same overall diameter of 20.00 mm. Successful eye impressions were first made by István Csapody in 1929[9] and the manufacture and fitting of molded SL using this approach was developed by József Dallos a decade later[10]. The earliest report of the successful clinical use of a plastic polymer to manufacture a SL was in 1939 by Petrus Their using polymethyl methacrylate (PMMA)[11] .

The major limitation of both glass and PMMA contact lenses is their negligible gas transmissibility, which has been associated with hypoxic complications for patients wearing them from the late 19th until the latter part of the 20th century. For this primary reason, the SL was largely replaced by corneal bearing lenses from about 1920 until the late 20th century, since these smaller diameterlenses allow tear exchange and don't cover the entire cornea. In the mid-1970s, the first rigid gaspermeable (GP) contact lens material (cellulose acetate butyrate) was developed[12], and the evolution of more GP materials followed. Siloxymethacrylate and fluoromethacrylate materials were developed with greatly increased oxygen permeability, and eventually the most commonly used GP material today, fluorosilicone acrylate, was developed. Even with the development of newer GP materials, the re-emergence of scleral contact lenses did not gain momentum until the late 1990's and early 2000's.

The SL manufactured in GP materials first emerged in 1983 when Donald Ezekiel of Perth, Australia described fitting gas permeable SL on 43 patients[13]. In the rest of the world, pioneering specialists led the advancement of SL for refractive correction in post-surgical and keratoconic eyes, including Perry Rosenthal of the United States, Ken Pullum of the United Kingdom, and Rients Visser of The Netherlands[14–16]. These innovators realized the potential of the SL modality and have led practitioners to embrace this new application of a historical concept. Today there are hundreds of worldwide SL specialists and the SL continues to expand market share and utilization[17–19].

The volume of scientific research on SL has increased significantly during the past decade[20,21], as the use of these lenses has expanded into community eye care practice[22]. Early literature on SL consisted primarily of case reports and retrospective reviews describing outcomes of SL therapy in advanced corneal disease[15,23–27]. More recently, study scopes have expanded to evaluate interactions between SL and ocular surface tissues, in healthy and diseased eyes. For example, studies evaluating the oxygen tension beneath a SL and corneal edema during lens wear[28–37], and those studying the effects of a SL on anterior ocular anatomy[38–44], have been primary interests of researchers. Yet despite the developing body of scientific literature on SL and the growing number

of eye care providers who are utilizing these lenses[22], gaps remain in the eye care community's understanding of the impact that SL may have on ocular surface tissues, specifically regards to the fluid reservoir (FR) beneath the SL and the effect of the lens landing area (on the conjunctiva/sclera) during SL wear.

Features of a SL fit

Despite their differences, the optical performance of a SL is similar to that of a corneal GP lens, which has long been the standard of care when fitting corneal diseases. They are both made of the same rigid plastic materials, but in comparison to the corneal GP, the SL has superior comfort and visual stability[19,45–49], making it a more desirable option for many patients. The superior comfort is attributed to the SL landing on the conjunctiva, which has markedly less pain nerve receptors compared to the highly sensitive cornea[50,51], as well as minimal amount of movement when the SL is on the eye. However, despite the favorability of the lens modality, the unique fitting system of the SL presents potential complications that are not observed with any other types of contact lenses[17,52,53], such as midday fogging (MDF) of the FR[52,54] and compression of conjunctival tissue[38].

A SL is fitted on the eye in a manner unique from all other types of contact lenses. The relatively thick GP plastic lens is approximately 300 µm centrally and vaults over the cornea by about the same amount, landing on the spongy conjunctival tissue overlying the sclera (Figure 1.1 and Figure 1.2). Due to this vault over the cornea, a SL is customarily filled with preservative free saline, which mixes with the tears on the ocular surface to form the tear fluid reservoir (FR). The FR is much thicker (typically 200-400 µm) than the tear layer which exists beneath traditional soft contact lenses (~5 µm) and corneal GP lenses (~20 µm). Beyond the thickness of the FR, there is increasing evidence that the exchange rate of the FR is quite limited[55–58], which is important to consider in the context of the cornea that relies on the tear fluid for much of its oxygen, microbial protection,and other nutritional support[51,59].

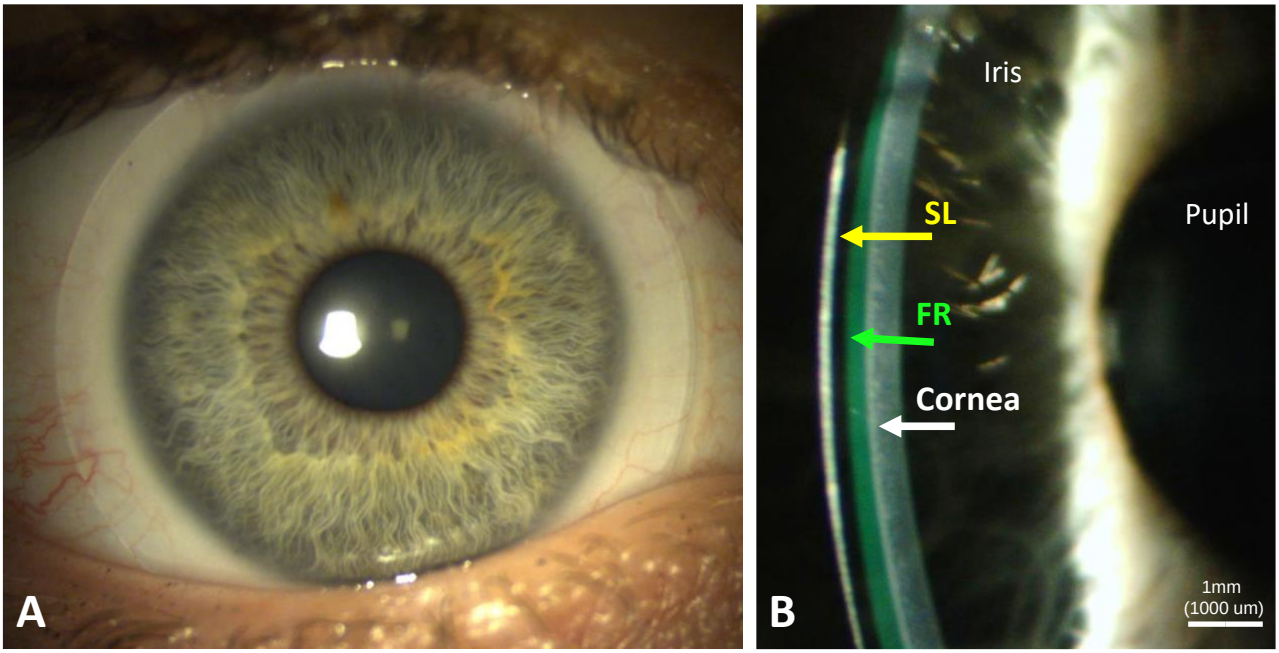

Figure 1.1. A scleral lens on the eye. The SL is shown using biomicroscopy in white light low magnification (A) which shows the landing of the lens on the conjunctiva. In higher magnification, an optic section can be used to view the width of the cornea (B), the tear fluid reservoir (FR) and scleral lens (SL) can be evaluated.

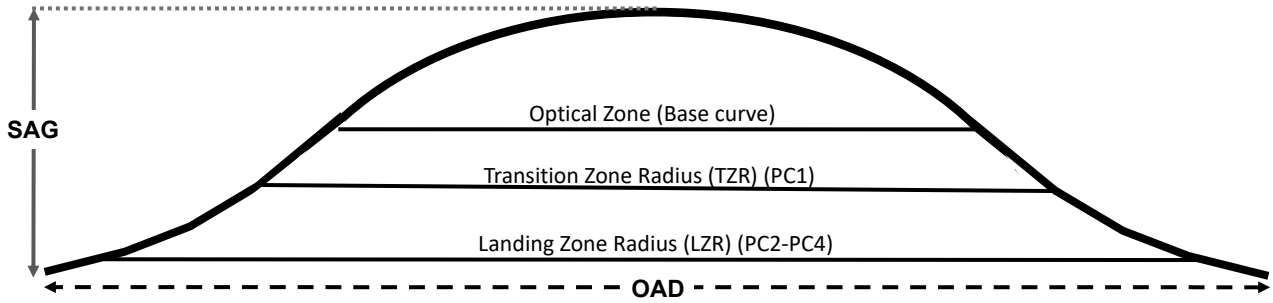

Figure 1.2. Cross-sectional schematic of a scleral lens. The SL has three distinct zones. The optic zone is the central (~8.5 mm) zone of the lens; the transition zone radius (TZR) is located inthe mid-periphery of the SL, and most peripheral area of the lens is the landing zone radius (LZR), which lands on the conjunctival tissue during SL wear. Note that radius refers to radius of curvature of the back surface of the lens rather than a linear radius measurement. SAG: sagittal depth; OAD: overall diameter; PC: peripheral curve

SL indications and uses

The SL is used to treat a variety of ocular surface conditions, with well-established benefits of visual quality, comfort, and ocular surface protection[17,48,60–62]. The most common indication for SL wear is keratoconus, and SL are also used in other conditions that create irregular corneal astigmatism (i.e., pellucid marginal degeneration, post-infectious scarring, post-transplant irregularities, and post-

refractive surgery complications). All of these conditions can create severe visual distortion and require rigid contact lenses to neutralize optical aberrations. The benefit of SL for these patients is to provide optical correction that cannot be achieved with other refractive modalities. Beyond irregular astigmatism, SL are increasingly used to treat systemic diseases that create severe ocular surface dryness such as Sjögren's Syndrome, Steven's Johnson Syndrome, and graft-versus-host disease, as well as eyelid malformations or deformities that create ocular exposure[63–68]. Individuals suffering from these conditions often experience extreme pain and damage to the ocular surface due to severe dryness, which the SL can relieve by vaulting over the exposed cornea and providing a liquid bandage in the FR.

The success and expansion of the SL due to the visual clarity and stability achieved has motivated its use in cases of complicated but normal eyes, such as in patients with high ametropia, astigmatism, and presbyopia[69,70]. While examples of visual success are acclaimed with SL wear,and the capacity to rehabilitate the ocular surface is exceptional[67,71–73], alongside these successesare accounts of adverse events and an increasing concern for potential side effects[31,40,52,74–77]. Consequently, there is an increasing interest in the effects of these custom devices on the ocular surface and adnexa[20,78]. In light of this, and considering the diseased eyes for which they are indicated[14,49,61,79–83], it is imperative to understand both the positive and negative ocular health impacts of the SL.

The tear fluid and scleral lenses

Function and composition of the natural tear film

The human tear film is an essential component of the ocular surface, providing nutrition, lubrication and protection for the corneal and conjunctival epithelial cells. Specifically, the primary functions of the tear film are to prevent desiccation, protect from invading microorganisms, and provide an optically smooth refractive interface. These functions are facilitated by the physiological activity of the proteins, peptides, lipids, electrolytes, gases and metabolites that compose the fluid, as well as by the physical properties of the tear film.

The high-water content mixture of proteins and metabolites, mainly produced by the lacrimal gland, are considered aqueous and typically deliver nutrition and antimicrobial protection. The mucins, which are shed or secreted by epithelial and goblet cells[84,85], help to tether the tear film to the ocular surface. The lipids, primarily secreted from the Meibomian glands (aka tarsal gland) as meibum[86], help reduce evaporation of the tear fluid. The aqueous and mucin are often considered a mucoaqueous gel when closest to the cornea[87], with lipids present throughout but mostly concentrated at the surface in a 40 nm lipid layer[88]. Overall, the mixture of the tear components provides a nutritious fluid that protects and nourishes the underlying ocular surface, which will bediscussed in chapters 2, 3 and 5.

Over the past 20 years more than 1500 proteins have been detected in the human tear film[89–91]. Most of these proteins originate from the lacrimal gland, but many are also secreted from the conjunctival and corneal cells[90]. Of these proteins, the most abundant are lactoferrin, lysozyme, and lipocalin A[90,92–95], which primarily exhibit anti-microbial activity[95]. Beyond these common tear proteins there are cytokines, chemokines, proteases and other small proteins and peptides that are variably present during different times of day and during periods of inflammation or infection. The concentrations of these proteins are often studied in the open and closed eye environments, and many are targeted in protein quantification studies as indicators of inflammation and disease[96] (Table 1.1).

Human tear lipids are primarily responsible for reducing evaporation of the tear film. Although different types of classifications exist, in one of the most common classification systems (LIPID MAPS® Lipid Classification System) lipids are classified into 8 major categories (Table 1.2). Each category contains hundreds of classes, subclasses, and species. Lipids from all 8 classes and as many as 236 unique species have been identified in the human tears[97,98]. Some of the primary lipid classes studies in the tears include wax esters (WE) and other fatty acyls, cholesterol esters (CE), triacylglycerols (TAG), phosphatidycholines (PC), and sphingomyelins (SM). Most of these lipids are believed to originate from meibum, the holocrine secretions from Meibomian glands that contribute most of the lipids to the tear film, although there is some contribution from secretory cells on the

ocular surface[98,99]. There is controversy on the exact composition of the tear lipids, but most sources agree that the majority are WE and CE that originate through the meibum secreted by the Meibomian (Tarsal) glands[97–100]. In general, many studies agree that WE and CE comprise about 40% of the tear lipids each, with the remaining 20% being primarily a mixture of TAGs, OAHFAs and phospholipids[101]. Lipids have been found to be irregular in patients with ocular surface disease, specifically dry eye disease[102] and Meibomian gland dysfunction[103,104] and have been implicated in contact lens discomfort[105]. In SL wear, they have not been evaluated in the peer-reviewed literature. Lipids and proteins are assessed in the FR using mass spectrometry (MS), in Chapter 3.

Table 1.1. Common proteins studies in disease and contact lens wear.

Protein	Function	Change in disease or CL
Lactoferrin	Iron binding and antimicrobial	⇵ Sjogren's Syndrome[106,107]; ↑ GPC[108]; ↓ dry eye ↻ SCL wear[106,107] discomfort[108]
Lysozyme-C	antimicrobial	↓ dry eye; ↻ SCL[109,110]
Lipocalin-1	lipid-binding[111,112]	⇵ Sjogren's Syndrome[106,107]; ↑ CL intolerance[113]
Serum Albumin	osmotic pressure regulation	↑ dry eye[114]
Secretory IgA	lipid-binding[111,112]	↓ dry eye; ↻ SCL[109]
sPLA2	Staphylococcal-cidal	↑ CL intolerance[113]
EGF	cell proliferation, differentiation, viability	↓ Sjogren's Syndrome[115]
EBP	may be related to epi staining	↓ Sjogrens[116]; ↻ SCL[109]
PIP	vague function, may degrade ECM	↑ dry eye[114] ↓ blepharitis[117], Kc[118], CL discomfort[119]
Immunoglobulins (many)	Immune functions	⇵ in Kc[120], ↑IgA in CL wear[121]
Colony stimulating factors GM-CSF, G-CSF, M-CSF	Leukocyte production/proliferation	↑ SCL[122]
Pro-Inflammatory Cytokines IL-1α,IL-1β,IL-4, IL-12p70,IL-13,IL-15IL-16,IL-17,IL-22, IL-6sR, IL-33, TNF-α, TNF- β, IFN-γ	Immune functions	⇵ SCL[123–125]
Proteases MMP-1, -2,-3,-5,-7,-9,-10; TIMP 1-4	ECM degradation	⇵[126]
VEGF (many)	Angiogenesis, endothelial migration	↑ CL discomfort[122]

Fibronectin	Tissue repair	↑ SCL[127]
Cystatin SA – III	Cysteine protease inhibitor	↓ blepharitis[117]
Proline rich 4	Unknown function[128]	↓ CL dry eye[114]
Secretoglobin 1D1	Steroid binding and transport	↓ CL dry eye[114]
Secretoglobin 2A2	Unknown, possible steroid binding	↑ CL dry eye [114]
Lacritin	Pro-secretory functions[129]	↓ blepharitis[117], CL dry eye [114]
β-2 microglobulin	expression/stability of MHC class I	↓CL dry eye [114]

G-CSF: Granulocyte-colony stimulating factor; GM-CSF: Granulocyte-monocyte-colony stimulating factor; EGF: epidermal growth factor; EBP: epidermal binding factor; VEGF: vascular endothelial growth factor
↻: no change found; ⇵ variably altered in studies

Table 1.2. Major lipid categories and classes identified in human tear lipids.

Relevant Classes	Relevant Classes	Estimated Meibum Abundance[101,130] (%)
Sterols	Cholesterol esters (CE)	30
	Steroids	<1
	Cholesterol & derivatives	3.5 – 19.2
Sphingolipids	Ceramides	<1
	Sphingomyelin	Found minimally
Fatty acyls	Wax esters (WE)	41 – 68
	Carnitines	Found minimally
	Fatty Amides	Found minimally
	Free fatty acids	0.1
	OAHFA	4.0
Glycerolipids	Monoradylglycerols (MAG)	Trace – 2.6
	Diracylglycerols (DAG)	Trace – 3.3
	Triracylglycerols (TAG)	1.0 – 9.8
Glycerophospholipids	Phosphotidylcholine	Found minimally
	Phospholipids	0.1 – 14.8
Prenols Saccharolipids & Polyketides	Minimal or no detection in tears	

In addition to proteins and lipids, approximately 100 minerals and metabolites have been identified in the tear film including amino acids, electrolytes, and arachidonic acid derivatives[89,131]. Two studies have evaluated metabolites in SL wear. One study in 1977 observed no difference in tear calcium levels between patients wearing soft, corneal GP, or SL, when compared to non-lens wearers[132]. More recently, Carracedo et al. found a reduced concentration of diadenosine tetraphosphate (Ap_4A), a nucleotide associated with dry eye disease[133], after 8 hours of SL wear in keratoconus subjects[39], although the significance of an alteration in this or other metabolites associated with SL wear is not clear. Metabolites in the tear film are not specifically evaluated in this dissertation, although Chapter 5 Discussion summarizes future directions for evaluating tear metabolites in SL wear.

The SL fluid reservoir

There is a conspicuous lack of understanding in the eyecare community with regards to the FR. The FR bears little resemblance to a normal tear film and is instead a deep reservoir which may harbor

a composition of proteins and lipids that is considerably different than the ocular surface tears. The fluid begins as a mixture of ocular surface tears with the non-preserved sterile saline or other non-preserved ocular lubricants used as the application solution[134]. One recent study measured leukocytes in the reservoir after SL wear[135], and another evaluated the tear fluid outside the lens margin[39], but otherwise there are no published reports that have quantified the composition of the FR itself. The potential physiological impact of bathing the entire cornea with a fluid that does not mimic natural tears is not yet fully understood. Chapters 2 and 3 of this dissertation focus on examining the composition of the FR in SL wear.

The FR is substantially thicker than the normal tear film. The ideal thickness of the FR over the cornea is a matter of some debate[30,32], but in clinical practice it can range from 100-1000 µm overlying different areas of the cornea in successful SL wearers[136,137]. However, most experts recommend limiting the reservoir to approximately 200 µm over the apex of the cornea. Factors such as ocular surface and corneal contour, centration of the lens, and other lens parameters can affect FR thickness. Variations in the thickness are also observed over time, as SL tend to settleinto the conjunctiva during wear[138–140]. Physiological implications of the presence of this thick tear film for long-term SL wear have yet to be comprehensively examined.

There are favorable and unfavorable reports of the tear FR and its effect on the ocular surface, and although there have only been a couple studies assessing the molecular composition of the FR, many groups have indirectly assessed this layer by evaluating the protective and healing effects of the fluid. Perry Rosenthal first published on the use of a SL for a rehabilitation device for persistent epithelial defects in 2000, and there has been expansion into treatment of neovascularization[141] and potential treatment of severe infection[62] using the FR[141–143]. Yet while the presence of a (largely stagnant) tear FR may provide protection for and facilitate healing of the cornea, it may also have detrimental effects on corneal health. Tear stagnation may contribute to the development of microbial keratitis[144,145], or an accumulation of carbon dioxide and other metabolic waste products in the post-

lens FR[146]. Increased concentration of these waste products can lead to changes in corneal pH and stromal acidosis[147]. The importance of understanding the composition and influences of the tear FR is ever apparent as the use of the SL continues to expand.

The most common complication associated with the FR is the accumulation of debris in the fluid, referred to as midday fogging (MDF, Figure 3) due to its typical presentation after 3-4 hours of lens wear[52,148]. MDF is reported by 26-46% of SL wearers[135,148,149], but peer-reviewed publication on this topic is limited, and there is some confusion as to exactly what it is and how it should be managed. There was one study, of the two that have evaluated tears in SL wear, which identified leukocytes in the FR but not greater in MDF[135], but no other studies have explored the specific cells or analyte composition of the FR during MDF. Chapter 3 of this dissertation evaluates the composition of MDF and its association with other SL parameters.

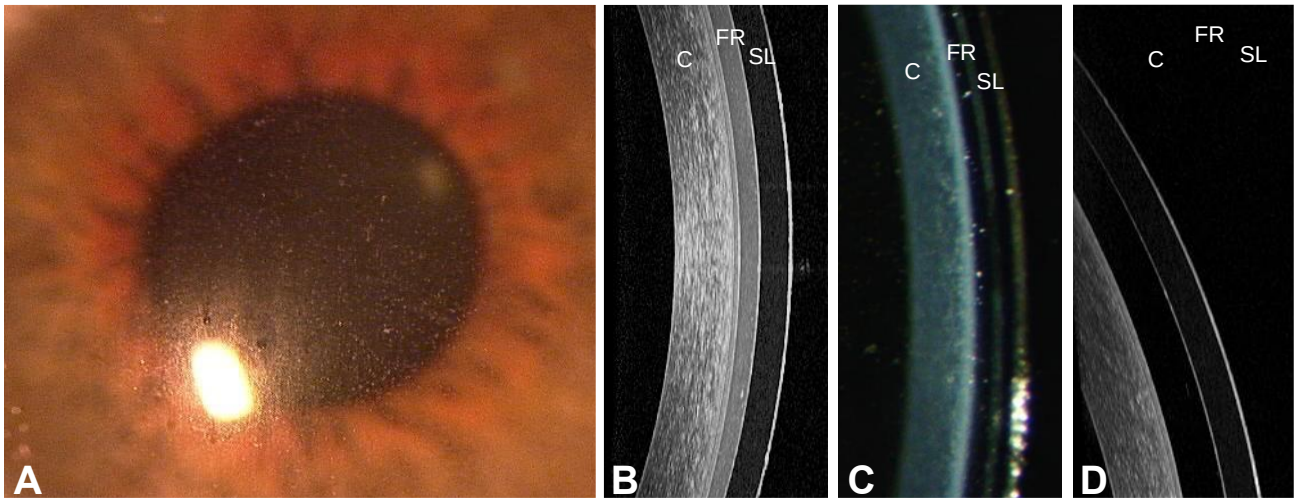

Figure 1.3. Midday fogging in SL wear. A white light biomicroscope full illumination image at 10x shows debris visible over the pupil in a patient wearing SL who is experiencing MDF (A). An OCT image (B) and white light 40x biomicroscope optic section (C) of the same patient show a layer of debris in the FR. An OCT image of a patient without MDF is shown for comparison (D).

Anterior segment morphology and scleral lenses

In addition to trapping a significant FR over the cornea, SL land on the soft and spongy conjunctiva overlying the sclera, perilimbally around the cornea. This unique interaction creates uncertainty regarding the impact of pressure and the weight of the SL on this deformable tissue. This area of landing is superficial to the anterior chamber structures that are responsible for aqueous humor (AH) outflow, and thus maintaining the intraocular pressure (IOP) of the eye (Figure 1.4). Pressure overlying these structures could in theory create increased resistance to outflow (most likely at the level of the episcleral veins), and potentially increase IOP. There is conflicting data in support or rejection of this hypothesis, although there is no real consensus on the experimental approach in this relatively new area of research. Here we will review the AH outflow pathways and associated structures, including the conjunctiva but also the most vulnerable downstream structure, the optic nerve head, which could be affected by increased IOP. In Chapter 4, we report the findings from a clinical study that evaluated the effect of SL on the downstream optic nerve head morphology.

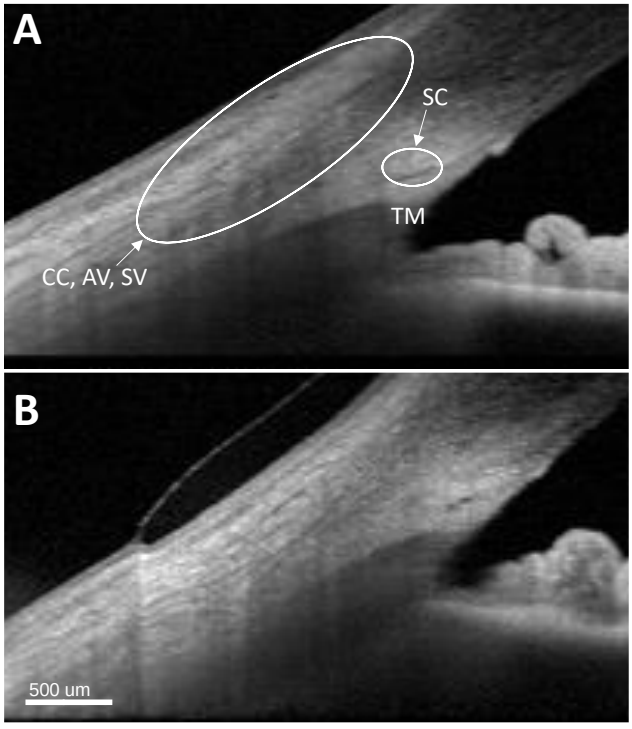

Figure 1.4. OCT image of the anterior chamber angle. An OCT image shows the anterior chamber angle in the area that the SL lands. In image (A), the angle is shown without a lens on the eye, with the locations of anatomical structures labeled (estimated based on histological understanding of the anatomical region). In (B), the same structures with a scleral lens in place.

CC: collector channels
AV: aqueous veins
SV: scleral veins (including episcleral veins)
SC: Schlemm's canal
TM: trabecular meshwork

The conjunctiva and sclera

The well-fitted SL lands on the bulbar conjunctiva overlying the sclera. The primary functions of this tissue are (1) ocular surface lubrication through mucous contributions to the tear film, (2) mechanical protection, and (3) immune defense. This anterior-most aspect of the conjunctiva covers the globe and consists of 2-4 layers of non-keratinized stratified cuboidal epithelial cells around goblet and Langerhans cells[51,150], the former of which are greater in abundance further from the limbus and in the fornix and palpebral conjunctiva[51]. It is highly vascularized, with anterior ciliary arteries feeding into the episcleral arterial plexus which in part eventually branches to supply oxygen and nutrients to the peripheral cornea[151]. The venous vasculature drains into numerous peripheral veins that connect with the eyelid's venous system, and also drain directly into the episcleral venous network. The sensory nerve fibers innervating the bulbar conjunctiva are contained in the ophthalmic (upper conjunctiva) and maxillary (lower conjunctiva) branches of the trigeminal nerve (CN V), and there is also both sympathetic and parasympathetic autonomic innervation (primary to regulate the blood vessels in the region)[51]. The terminal nerves consist of free as well as complex, corpuscular nerve endings, which are located immediately beneath the epithelium in the anterior stroma[51,152]. The corpuscles are often within the palisades of Vogt and are most numerous within a 0.5 to 1.5 mm annulus around the limbus[51,152] (i.e., a subepithelial plexus that is in the approximate location of the inner landing zone for smaller diameter scleral lenses). These mechanoreceptors are sensitive to touch[51], and given their proximity to the limbus may be more responsive to SL landing close to the limbus. In addition, bulbar conjunctival vessels and episcleral vessels may become dilated or constricted if the LZR is not appropriately aligned with the underlying tissue.

The sclera underlying the bulbar conjunctiva is also important to consider in SL wear, as the LZR of the lens overlies this tissue in the perilimbal region. The episclera is the outermost layer of the sclera that lies between Tenon's capsule (and also connects with the conjunctiva at the limbus) and the scleral stroma[153]. It primarily consists of loosely arranged collagen bundles and is ~15-20 µm thick

at the limbus and thinner posteriorly[154]. The scleral stroma is composed primarily of dense bundles of collagen of varying fibril diameter in a random arrangement with a similar percentage and type of collagen observed anteriorly and posteriorly. Near the limbus scleral collagen bundles are arranged in concentric circles, which is thought to allow some flexibility in response to changes in intraocular pressure or biomechanical stress transmitted from the extraocular muscle[153]. Despite a similar collagen content, the anterior sclera adjacent the limbus is typically stiffer than the tissue at the equator or posterior[155], and a chemically induced stiffening of the posterior sclera results in greater elevations in intraocular pressure during experimental IOP challenges in animal models[156].

Anterior chamber & aqueous humor pathway

The pathway of AH starts at production by the ciliary body[157] in the posterior chamber, out through the pupil, through the anterior chamber and outflowing primarily through the trabecular meshwork (TM). The TM is a complex tissue located in the iridocorneal angle at the junction of the cornea and iris root, consisting of a scaffolding of connective tissue with a dense extracellular matrix (ECM) and lamellar sheets sandwiched between endothelial cells[51,158]. There are three functional sections of the TM: the uveal meshwork, corneoscleral meshwork, and the juxtacanalicular tissue (JCT). The uveal and corneoscleral meshworks have 3 and 8-15 layers of fenestrated sheets, respectively[159], with fenestrations in these tissues becoming more narrowly spaced as they approach the JCT that lies between the inner wall of Schlemm's canal and the last trabecular lamellae. The JCT is denser than the rest of the TM and consists of 2-5 amorphous cell layers in a loose ECM, providing the greatest resistance to AH outflow[158–163]. The ECM plays a dominant role in controlling the rate of AH outflow through the TM, containing collagens, proteoglycans, fibrillin, fibronectin, elastin, laminins, and proteins such as integrins that act as mechanoreceptors, which sense changes in the ECM that indicate an increase or decrease in pressure in the TM[162,164–168]. These structural and organizational components collectively provide the matrix which allows controlled passage of AH from the anterior segment to Schlemm's canal.

The TM leads to Schlemm's canal (SC), which has the first (endothelial) membrane that the AH can pass through. Some of the AH fluid passes through the endothelium of SC through vacuoles and pinocytosis, pressure driven by the forces from the anterior chamber. The SC also drains into 24-35 collector channels[169,170] that connect to more conventional outflow pathway through aqueous veins and episcleral veins. The aqueous veins are at the end of the outflow pathway and are small vessels that function as the final transporter of the AH to the venous drainage of the eye[170,171]. As clear AH enters the general blood circulation in the episcleral veins, a diluted blood colored gradient of fluid is often observed. Approximately half of these small veins are found in the deep limbus[171], and the remainder of them originate in the anterior limbal loops and from the more posterior sclera. Intrascleral and episcleral veins carry the AH outflow into the vortex veins to exit the eye[172]. The episcleral veins are more anterior and typically considered as the primary outflow pathway. There are also small tributary episcleral veins that drain aqueous veins and join larger episcleral veins before reaching the venous system. These tributary vessels normally contain blood and maintain an oscillatory pressure equilibrium with the aqueous veins[172,173], but aqueous can enter them when the pulsatile pressure increases in the downstream outflow structures (i.e., episcleral veins)[174]. In a normal functioning eye, when the resistance to outflow in the episcleral veins increases, upstream structures of the outflow system (TM, SC) increase pulsatile pressure to maintain AH outflow.

Beyond the primary outflow pathway through the TM, the uveoscleral pathway is an alternate route for AH outflow[175,176]. In this pathway, AH outflows through the iris root and the connective tissue of the ciliary muscle. From there the AH diffuses through supraciliary and suprachoroidal spaces, exiting to the venous system through ciliary muscle and episcleral veins[51,177], and in small amounts through the choroidal circulation.

The anatomy and physiology of the conjunctiva, as well as of the aqueous humor outflow pathway, are of particular relevance to SL wear, primarily because the conjunctival tissue in conjunction with the underlying sclera supports the weight of the LZR. The blanching of small blood vessels and

compression of conjunctival tissue can be easily observed in many individuals during SL wear (Figure 1.5). This compression could affect the important functions of the conjunctiva such as ocular surface protection and immune regulation[178], and has major potential implications for the impact on IOP and the homeostasis of AH outflow.

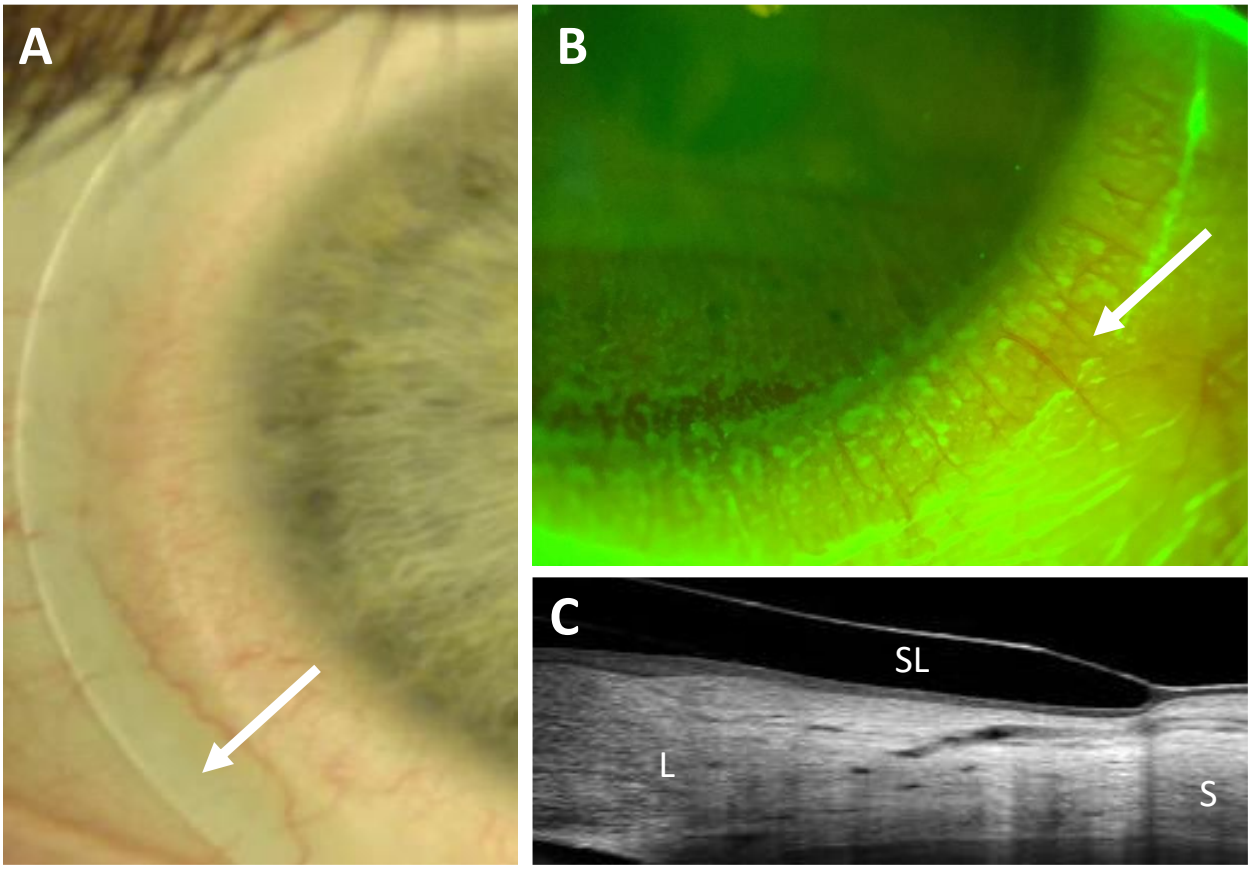

Figure 1.5. Conjunctival compression in SL wear. Compression of the conjunctiva can be observed with SL. White light biomicroscopy shows areas with restricted blood flow (A) evidencedby the blanched appearance at the LZR (arrow). When the lenses are removed and the ocular surface stained with NaFl (B), indentation of the conjunctiva is observed where the lens edge was (arrow). Using OCT (C), the compression can be assessed quantitatively and measured with software calipers. SL: scleral lens; L: limbus (approximate location); S: sclera.

Intraocular pressure and the optic nerve head

The regulation of IOP is a vital homeostatic process and dysregulation can result in ocular hypertension and glaucoma. The process is controlled in the anterior segment, where the balance between the inflow and outflow of AH determines IOP[179]. Anything that increases production or impedes outflow of AH may disrupt this balance, and thus it has been suggested that SL wear may

cause IOP elevation. In 1951, Huggert reported that IOP increased by up to 30 mmHg in patients wearing glass SL for 25 minutes[180]. Miller, Carroll and Holmberg hypothesized that the suction force that holds a SL on the eye (referred to as “scleral cling”) could lead to compression of episcleral vasculature and could therefore impede the evacuation of aqueous from the eye through those vascular structures[181]. More recent studies have also raised concerns that a SL may lead to elevated IOP due to increased resistance to AH outflow[182,183], or due to the forces generated by the sub-atmospheric pressure beneath the lens[182].

The primary challenge in assessing IOP during SL wear is that the lens lands overlying the cornea, which is the tissue that most tonometers are calibrated to. This makes it all but impossible to glean a true IOP measurement noninvasively while the lens is in place. Therefore, researchers must consider other ways to evaluate any changes, or effects thereof, in IOP during SL wear. In recent years, optical coherence tomography (OCT) has made it possible to reliable quantify microscopic changes in optic nerve morphology. The minimum rim width (MRW) is the minimum distance between Bruch’s membrane opening (BMO) and the inner limiting membrane (Figure 1.6). This metric has been shown to have excellent repeatability and sensitivity to detect subtle changes due to fluctuations in IOP[184–187]. When IOP increases, it causes thinning of the MRW due to the stress of the pressure. Changes can be noted within minutes of IOP change and have been shown to be dose-dependent in primate models[184]. It has been suggested that change may be detected with IOP fluctuations of as little as 5 mmHg. In Chapter 4, this parameter will be assessed in SL wearers to determine if SL wear causes transient changes to MRW.

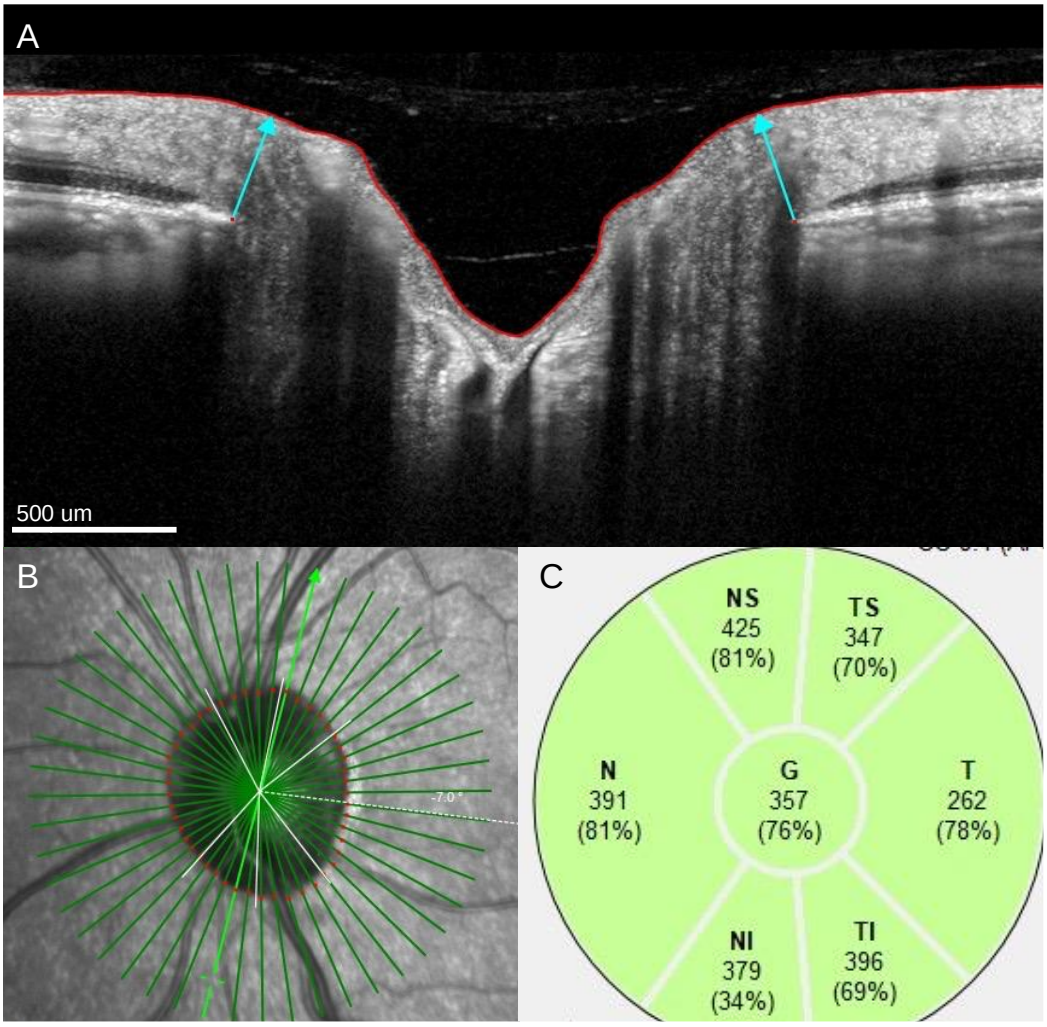

Figure 1.6. Minimum rim width of the optic nerve head. Using optical coherence tomography (OCT), a cross section of the optic nerve head (ONH) can be imaged (A). To measure the MRW,a 24-line radial scan of the optic ONH was acquired (B). From each of the 24-line scans, the MRW is calculated as the distance from the Bruch's membrane opening to the inner limiting membraneof the retina (teal arrows in A). The detection arrows can be manually adjusted as needed[168], and the software automatically measures the length of the arrows for each scan in µm. The average MRW can then be calculated (C) and split into sectors or averaged globally (the middle "G" section of the sector map). Due to the variation in the different sectors that can be observed based on ONH size and shape, this global "G" MRW, which is an average of all 24 scans, is a better representation of the entire ONH and is a single value that can be used to represent MRW of an eye.

Overview of dissertation

SL are an increasingly utilized medical device to treat normal and diseased eyes, and there remain large gaps in the understanding of how they affect the eye. The purpose of this dissertation is to provide an in-depth assessment of SL on the anterior ocular surface tissues and tears, and to determine the normal response of an eye to SL. We explore the effects of SL in a normal population

with the goal of understanding how these devices affect normal tissue and to develop a platform to study them in disease. The central hypothesis of our research is that standard SL treatment alters the composition of the tear fluid and IOP homeostasis that may lead to negative sequelae in patients wearing SL. The hypothesis was examined with the following specific aims:

SA1. To measure the inflammatory proteins in the tears and FR after acute SL wear in normal eyes. Tear samples were collected from the basal tears and the FR before and after 8 hours and 4 days of SL wear in normal neophyte eyes. The levels of inflammatory markers were quantitated using Luminex assays. Corneal staining, conjunctival hyperemia, subjective comfort, and visual acuity were also assessed and compared to the tears.

SA2. To evaluate the impact of short-term SL wear on the anterior segment morphology and FR composition. The curvature of the conjunctiva will be measured using scleral topography (sMap 3D) after an 8-hour SL wearing period and several days of SL wear. The FR will be assessed for midday fogging using OCT in all subjects to determine if there is a relationship between compression and midday fogging. Additionally, select samples will be quantified for proteins and lipids using mass spectrometry. Concentrations of proteins and lipids will be compared to levels of compression to determine the relationship between conjunctival/scleral compression and the occurrence of midday fogging in the FR.

SA3. To determine the impact of short-term SL wear on the posterior segment morphology (MRW) and IOP. The MRW at the optic nerve head rim tissue will be measured before, during, and after 6 hours of SL wear, and the change will be measured and compared between a test eye and a non-SL wearing control. IOP will also be measured after lens removal to determine if the amount of MRW changes have any relationship with post-removal IOP.

The data from this study will significantly expand the knowledge of the FR and increase our understanding of its composition. We will also learn if the amount of SL compression can influence the

FR composition, specifically MDF. Furthermore, understanding theimpact of a SL on IOP and ONH morphology is paramount to managing risks and benefits of wearing SL. This study is significant because it will contribute to the characterization of the components of the tear fluid beneath the SL and lead to a better understanding of the eye's response to SL wear in normal eyes.

Chapter 2. Scleral lens wear: measuring inflammation in the fluid reservoir

Published January 2020 in Contact Lens Anterior Eye

Maria K Walker
Carolina Lema
Rachel Redfern

Introduction

The scleral lens (SL) is an ocular surface device manufactured in gas-permeable plastic and placed on the eyes of individuals with corneal disease. They were originally manufactured in glass and used to treat high myopia and irregular corneas in Europe during the late 19th century, but it wasn't until the development of gas-permeable materials in the late 20th century that the SL became a widely viable option; in the past 15-20 years the gas-permeable SL has dramatically integrated into clinical practice. Modern applications of the SL remain to manage irregular corneal disorders like keratoconus[19,61,188] and have expanded to include s/p corneal surgeries[81,189] and the treatment of ocular surface compromise caused by Sjögren's syndrome[72,190], ocular cicatricial pemphigoid[191,192], graft-versus-host disease[189,193], and other environmental exposure-related or dry eye diseases[72,194,195]. Over the past two decades, the use of the SL has soared with the global realization of the superior comfort and visual stability it can provide[72,196,197].

The expanding use of the SL has led to an increase in case reports that establish the benefits of their use[74,198–200], but also in the reports of clinical conundrums that raise important questions about the side effects of the SL on the ocular surface[74,76,201–208]. The need for additional prospective research focused on the impact of SL on ocular health is recognized by both researchers and clinical practitioners[76,182,209], and the basis of the need is the unique SL fit, which can lend way to several ocular surface sequelae that are not observed with any other ocular medical devices. When a SL is fit to the ocular surface, the large diameter, relatively thick (~300μm) plastic lens vaults over the cornea, landing on the conjunctiva and harboring a relatively thick post-lens tear fluid reservoir (FR) between the SL and the cornea. Prior to application, the concave portion of a SL is filled with a preservative-free solution (customarily saline), which mixes with the ocular surface tears during SL application to form the FR. This layer is often considered beneficial to the cornea as a protective fluid barrier from the environment, also helping to neutralize higher order aberrations seen in patients with irregular corneal shape. The FR is commonly between 200 and 400 μm in axial depth (thickness),

with an estimated volume of approximately 200 to 400 µL. During SL wear, the FR often has minimal exchange with the outer basal surface tears[210–214], meaning that the SL may sequester inflammatory and other tear film components in the FR that would otherwise be refreshed during blinking. Several complications associated with SL wear do in fact occur within the FR, such as midday fogging[198,215,216] epithelial toxicity[81], and underlying corneal edema[217–219]. A recent study reported the presence of leukocytes in the FR of SL wearers experiencing midday fogging suggesting inflammation could be occurring on the ocular surface[216]. The composition of the FR and how it differs from the basal ocular surface tear film is otherwise unknown.

The current evidence supports the hypothesis that SL wear traps normally refreshed tear film components in the FR leading to elevated levels of inflammatory mediators overlying the cornea and perilimbal conjunctiva. To test this hypothesis, we determined if pro-inflammatory cytokines (Interleukins: IL) and matrix metalloproteinases (MMPs), which are often used as biomarkers for inflammation in the tear film[220–224], are increased in the FR after 8 hours and 4 days of SL wear in normal individuals.

Methods

Participants

This study was compliant with the tenets of the Declaration of Helsinki and was approved by the University of Houston's Institutional Review Board. All enrolled subjects signed an informed consent prior to participation. A total of sixteen normal, habitual soft contact lens wearers (SL neophytes) were recruited and seen at the University of Houston, College of Optometry (UHCO). Inclusion criterion was daily soft contact lens wear to ensure that all eyes were accustomed to a contact lens being applied to the eye (spherical, soft, or multifocal power). Subjects with a history of extended wear soft contact lens wear were excluded, as with those with a history of corneal gas permeable or hybrid contact lens wear.

Scleral lens fit and wearing schedule

Subjects reported to The Ocular Surface Institute (TOSI) at UHCO for a complete anterior segment examination which included assessment of the cornea, conjunctiva, sclera, eyelids and lashes, anterior chamber, and iris. All subjects were determined to have good ocular health and were then fitted with SLs. A diagnostic fitting set with 14.8- and 15.4-mm SLs was used to determine the lens parameters for each subject (Zenlens RC, Alden Optical, Rochester, NY, USA) and selection of diameter was based on horizontal visible iris diameter (HVID). Subjects were fitted into 14.8 mm lenses if their HVID was <11.8 mm, and 15.4 mm lenses when their HVID was ≥11.8 mm. Sagittal depth (SAG) was determined by applying various diagnostic lenses and determining which lens vaulted the apical cornea nearest to 300 µm. During the diagnostic fitting, the investigator also examined the transition zone radius (TZR) and the landing zone radius (LZR), two peripheral lens areas overlying the limbus and the sclera, respectively, to determine if the lens was adequately vaulting the cornea and landing evenly on the conjunctiva. Toric TZR and LZR designs were ordered when meridional asymmetries of compression or excess lift were observed. An ideal SL fit vaulted over the cornea, clearing the limbus by approximately 30-50 µm and landing on the conjunctiva without impingement of blood vessels. Over-refraction was conducted to determine best SL power. Custom SL were ordered and finalized for each subject prior to beginning the experimental visits.

Subjects were instructed to discontinue soft contact lens wear for a 3-day washout period prior to the start of the SL experimental visits, to allow the eye to return to a relative baseline state and avoid interference of any inflammation caused by a soft contact lens fit. On the morning of the first experimental day, baseline testing was done (ocular surface tear collection, comfort, vision and ocular health), and the SL were dispensed between 7:30 and 8:30 AM to be worn continuously before returning for the 8-hour (8h) follow-up visit that evening. At the 8h visit, all initial testing was repeated, and in addition the FR was collected during SL removal. At the completion of the 8h visit, subjects wore the SL at least 8h per day for 3 consecutive days, returning after 8 hours on the 4th day for the

4-day (4d) visit to evaluate a potential adaptive response. During this wearing period subjects were instructed to remove the SL at night and use a hydrogen peroxide disinfection and cleaning solution to disinfect SL daily (ClearCare®, Alcon Laboratories, Ft Worth, TX, USA). Each morning the SL was filled with sterile saline solution prior to application (Purilens, Freehold, NJ, USA).

Tear collection

Basal ocular surface tears (T_b) were collected using a 10 µL microcapillary tube placed in the lower temporal fornix, taking care to avoid the eyelid margin and reflex tearing. Capillary action facilitates movement of tears into the tube. The T_b were collected at the baseline visit (prior to SL wear) and at the 8h and 4d visits (T_b samples at 8h and 4d were collected prior to SL removal). The FR samples (T_{FR}) were collected as the SL was removed by the investigator (using a micropipette) (Figure 2.1). For each sample type (basal, FR), left and right eyes were pooled for each subject in a single Eppendorf tube and frozen at -80^{0}C until analysis. Samples were pooled to maximize FR volume, which is fixed and can have low yield. In total, five tear samples (three T_b and two T_{FR}) were collected for each subject. No samples were pooled between subjects.

Figure 2.1. Basal tear and tear film reservoir collection. A microcapillary tube was placed in the temporal fornix to collect basal tears (Tb) from the exposed ocular surface prior to SL removal when applicable (A). The SL was carefully removed using a small plunger (B) and the tear fluid reservoir (TFR) was collected from the lens basin using a pipette (C).

Cytokine and MMP Luminex assay

All tear samples (2 to 140 µL) were frozen immediately after collection and thawed at the time of analysis. Two- microliters of undiluted sample were used to determine total protein concentration by

the use of the Direct Detect® infrared spectrometer (EMD Millipore, San Diego, CA, USA). Levels of IL-4, IL-8, MMP-7, MMP-9, and MMP-10 were quantitated in tear samples using customized magnetic beads-based Luminex assays (R&D Systems, TC. Minneapolis, MN, USA). All assays were performed according to manufacturer instructions. Briefly, standards, quality controls and samples were pipetted into individual wells of a 96-well plate and thoroughly mixed and incubated with antibody-immobilized beads at room temperature for 2h. Then, a cocktail of biotinylated detection antibodies specific to the analytes of interest was added to all wells, thoroughly mixed and incubated for 1h. Next, development was done by adding a streptavidin-phycoerythrin (SAPE) conjugate, which was thoroughly mixed into each well and incubated for 30 min at room temperature. Each incubation step was followed by proper washing to remove unbound sample components or reagents. Finally, SAPE-analyte-binding magnetic beads were re-suspended in sheath fluid and the 96-well plate was analyzed with a MAGPIX instrument and xPONENT software (Luminex Corporation, Austin, TX, USA). Quantitation of each analyte per sample was determined using the Milliplex Analyst software (EMD Millipore). For all Luminex assays, a total of 10 µg of total protein was loaded per well in technical duplicates or triplicates. Therefore, to calculate the final analyte concentration in each sample, the individual dilution factor (that resulted from each sample being diluted to reach 10 µg of total protein per well) was applied, and it is shown as ng/mL for all analytes. The volume of undiluted sample used per Luminex assay ranged from 2 to 12 µL depending on its total protein concentration which varied from 1.80 to 12.97 µg/µL.

Comfort & ocular health evaluation

Comfort, visual acuity, and ocular surface staining were quantified at baseline and follow-up visits. Contact lens discomfort is the primary reason for discontinuation of contact lens wear in the US[225], and was measured as an assessment of SL satisfaction using two surveys: The Contact Lens Dry Eye Questionnaire (CLDEQ-8) and a custom Visual Analog Scale (VAS). The VAS asked participants to rate their ocular comfort on a 100 mm scale (the left-most limit of the line indicating

the SL “extremely uncomfortable”, and the right-most limit indicating “extremely comfortable”). Vision was assessed using a high contrast, high luminance logMAR visual acuity chart. Visual acuity was measured with habitual spectacle wear at baseline, and with SL at initial application, 8h, and 4d.

Bulbar conjunctival staining was measured in 4 quadrants (nasal, temporal, inferior, and superior) after instillation of Lissamine Green (Green Glo, HUB Pharmaceuticals, Rancho Cucamonga, CA, USA). A modified NEI staining scale of 0 to 3 was used for each quadrant, with a potential total score ranging from 0 to 12. Corneal staining was graded after instillation of sodium fluorescein (Soft Glo, HUB Pharmaceuticals) in a total of 5 corneal areas (central, nasal, temporal, inferior, and superior) using a modified Oxford grading system of 0 to 5 in each area for a total possible score of 25.

Statistics and data analysis

Statistical analysis was performed using GraphPad Prism 7.0 (GraphPad Software, La Jolla, CA, USA). The D’Agostino-Pearson omnibus K2 normality test was used to determine normality, and tear analytes were compared using one-way ANOVA and Friedman test for multiple comparisons of non-parametric data. The non-parametric uncorrected Dunn’s test was used for post-hoc multiple comparisons.

Sample size was determined based on feasibility of the study and to collect pilot data, since no preliminary data was available on inflammatory analyte levels in the FR of a SL. Therefore, a sample size of 15 was determined with a goal of 12 complete subjects, the recommended sample size when little is known about the expected outcome[226]. However, due to limited volume of several FR samples, only 10 subjects that had complete datasets and were analyzed. A minimum of 10 individuals was considered acceptable as it has been reported by previous similar pilot studies[227–229], and given the novelty of this type of data. Post-hoc sample size analysis was done using the outcomes from MMP-10 and show post-hoc power of 77.2% for this data.

Results

A total of 16 subjects were recruited for this study and 15 completed all study visits (one subject relocated before completing). However, data is only shown for the 10 subjects with a complete collection of tear samples. The mean subject age was 26 years (range 22 to 29 years) and 60% (n=6) were female. On average, subjects wore the SL for 8.1 ± 0.2 hours on the first day of wear, approximately 8 hours per day on the 2nd and 3rd days, and 8.5 ± 0.4 hours on the 4th and final day of SL wear. All subjects reported wearing the SLs for at least 8 hours each day during the 4-day study period. The study population demographics are shown in Table 2.1.

Table 2.1. Subject demographics and SL parameters.

Subject Demographics	
Age (range)	26 (22-29)
Gender (% female)	60%, n=6
Hours SL wear: Day 1	8.1 ± 0.2
Hours SL wear: Day 4	8.5 ± 0.4
SL Parameters	
Brand	Zenlens RC & Toric RC
Manufacturer	Alden Optical, B&L
Material	Boston XO_2
Dk, barrer	141
Power range, diopter	+1.00 to -7.75
Diameter, mm	14.8 and 15.4
SAG range, µm	3600 to 4500
Altered TZR, # lenses (%)	1/20 (5%)
Altered LZR, # lenses (%)	7/20 (35%)
Central SL Clearance	
Apical Clearance (at dispense), µm	293 ± 41
Apical Settling (8h), µm	145 ± 30
Apical Settling (4d), µm	140 ± 32

Values shown as mean ± SE unless otherwise indicated. SL: scleral lens; SAG: sagittal depth; TZR: transition zone radius; LZR: landing zone radius.

SL fitting characteristics

Two subjects (4 eyes) were fitted into 14.8 mm SL and the remaining 8 subjects (16 eyes) were fitted in 15.4 mm SL. One out of 30 SL (5%) was steepened in the TZR to increase clearance over the limbus; no toric TZR were ordered. In the LZR overlying the conjunctiva and sclera, a total of 7 SL

(35%) were designed as toric, and the remaining 14 lenses (70%) had a spherical LZR. Mean apical clearance over the center of the cornea was 293 ± 41 µm at dispense, settling at 145 ± 30 µm on day 1 after 8h, and 140 ± 32 µm after 4d of SL wear (Table 2.1). Average apical clearance after 8h of SL wear on day 4 was 157 ± 88 µm.

Total tear protein analysis

A complete set of 5 tear samples were required to test whether the concentrations in the T_b were different than in the T_{FR}. Full sample sets were collected in 10 subjects, with those excluded having one or more missing either T_{FR} (n=4) or T_b (n=1) samples. Mean T_b volume collected was 17 ± 2 µL prior to SL wear and 18 ± 1 µL after SL wear; mean T_{FR} volume was 30 ± 5 µL. Total protein concentration (TPC) was greatest in the T_{FR} samples (7.8 ± 0.5 µg/µL) but it was not significantly different from the concentration of the baseline tears collected prior to SL wear (6.2 ± 0.7 µg/µL) or the T_b samples taken prior to SL removal (5.8 ± 0.6 µg/µL) (p=0.14) (Table 2.2).

Table 2.2. Tear collection volumes and total protein concentration (TPC).

	Baseline	8h		4d	
	T_b	T_b	T_{FR}	T_b	T_{FR}
Volume (µL)	17 ± 2	19 ± 2	24 ± 4	18 ± 1	36 ± 12
TPC (µg/µL)	6.2 ± 0.7	5.72 ±	7.02 ± 3.13	5.87 ± 3.49	7.81 ± 2.52

A total of five tear samples were collected from each subject. Baseline basal tears (T_b) were collected prior to SL fitting and dispense. The basal and tear film reservoir (T_{FR}) tear samples were then collected after 8h and 4d of SL wear. Data shown as mean ± SE.

Cytokine and MMP Luminex assay

To determine pro-inflammatory cytokines on the ocular surface during SL wear, we measured and compared the concentrations in the T_b and T_{FR} samples, at both 8h and 4d. The two cytokines tested in all subjects, IL-4 and IL-8, both showed higher concentrations in the T_{FR} than the T_b. The median concentration of IL-4 at 8h was 3.1 ng/mL in the T_{FR} and 2.2 ng/mL in the T_b. At the 4d visit, T_{FR} concentration was 3.5 ng/mL and T_b concentration was 0.9 ng/mL. IL-8 concentrations were lower in general at the 8h (0.4 ng/mL in the T_{FR} and 0.1 ng/mL in the T_b) and 4d visits (0.2 ng/mL in the T_{FR} and 0.0 ng/mL in the T_b). There were no statistical differences found between these analytes. In addition, the number of subjects who showed more than a 2-fold greater concentration in the T_{FR} were counted. After both 8h and 4d of SL wear, the concentration of IL-4 was >2-fold more in the T_{FR} in 6 out of 10 subjects. When comparing IL-8 in the T_b and T_{FR}, 4 of 10 subjects had >2-fold IL-8 in the T_{FR} after 8h, and only 3 out of 10 after 4d. While not all subjects showed this magnitude of increase in the T_{FR}, the remaining subjects showed similar or scattered levels of analytes in the T_b and T_{FR}, and there were no trends toward greater concentrations of IL-4 or IL-8 in the T_b (Figure 2.2).

Due to the association of MMPs with ocular surface epithelial defects and inflammation, we examined the concentration of MMPs -7, -9 and -10 (Table 5, Figure 2.3). There were no significant differences in MMP-7 levels at any of the samples. MMP-9 and -10 were both greater in the T_{FR} samples, showing a significant difference at 8h (p-value=0.047 and p<0.001, respectively), and for MMP-10 only at 4d (P = 0.047) (Figure 2.3). MMP-9 levels were >2x higher in the T_{FR} than the T_b in 8 out of 10 subjects at the 8h and 4d visits. MMP-10 trends were similar, and after 8h SL wear the concentration was greater in the T_{FR} in 10 out of 10 subjects, and after 4d SL wear 9 out of 10 subjects had >2x concentration of MMP-10 in the T_{FR} (Figure 2.4).

Table 2.3. Tear cytokines and MMPs

Analyte[a]	Pre-SL	8h SL wear			4d SL wear		
	T_b	T_b	T_{FR}	*p-value*	T_b	T_{FR}	*p-value*
IL-4	3.7 (0.7; 6.6)	2.2 (0.5; 5.6)	3.1 (0.8; 10.5)	*0.20*	0.9 (0; 9.3)	3.5 (0.9; 12.3)	*0.09*
IL-8	0.2 (0; 2.6)	0.1 (0; 0.8)	0.4 (0; 3.1)	*0.40*	0.0 (0; 0.7)	0.2 (0; 1.6)	*>0.99*
MMP-7	50.7 (30.4; 132.7)	46.0 (8.1; 126.0)	54.4 (16.5; 183.8)	*>0.99*	34.2 (8.9; 104.9)	87.5 (27.7; 240.7)	*>0.99*
MMP-9	31.5 (0; 94.4)	15.2 (0; 85.1)	62.7 (13.7; 300.7)	*0.047**	0 (0; 10.5)	18.4 (5.7; 86.1)	*0.24*
MMP-10	13.0 (1.3; 18.7)	2.8 (0.6; 8.8)	25.8 (6.8; 45.2)	*<0.001***	2.1 (0.7; 4.3)	17.2 (2.8; 55.1)	*0.047**

[a] concentration shown as median ng/mL (interquartile range)
* significant p-value comparing the T_b to the T_{FR} using Dunn's multiple comparisons test ($p<0.05$)
** significant p-value ($p<0.01$)
T_b: basal ocular surface tears. T_{FR}: fluid reservoir tears

Concentrations of IL-4, IL-8, MMP-7. -9 and -10 in each of the 5 tear samples collected from 10 subjects, shown as ng/mL. Significant differences were seen between the T_b and T_{FR} in MMP-9 after 8h SL wear, and in MMP-10 after 8h and 4d wear. No other significant differences were observed between sample types.

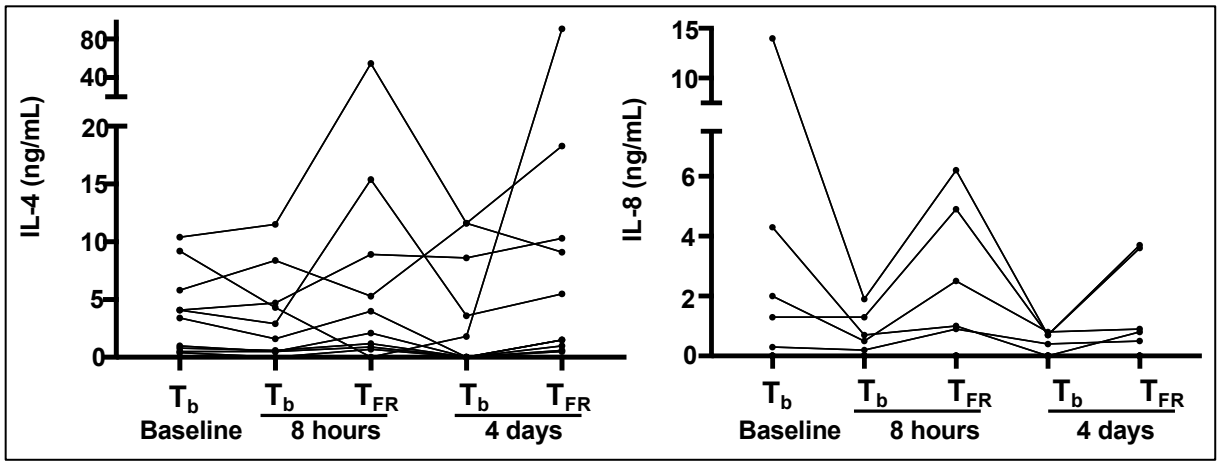

Figure 2.2. Changes in IL-4 and IL-8. IL-4 and IL-8 levels for subjects at each study visit (baseline, after 8h and after 4d of SL wear) collected from the basal ocular surface tears (Tb) and the SL fluid reservoir (FR).

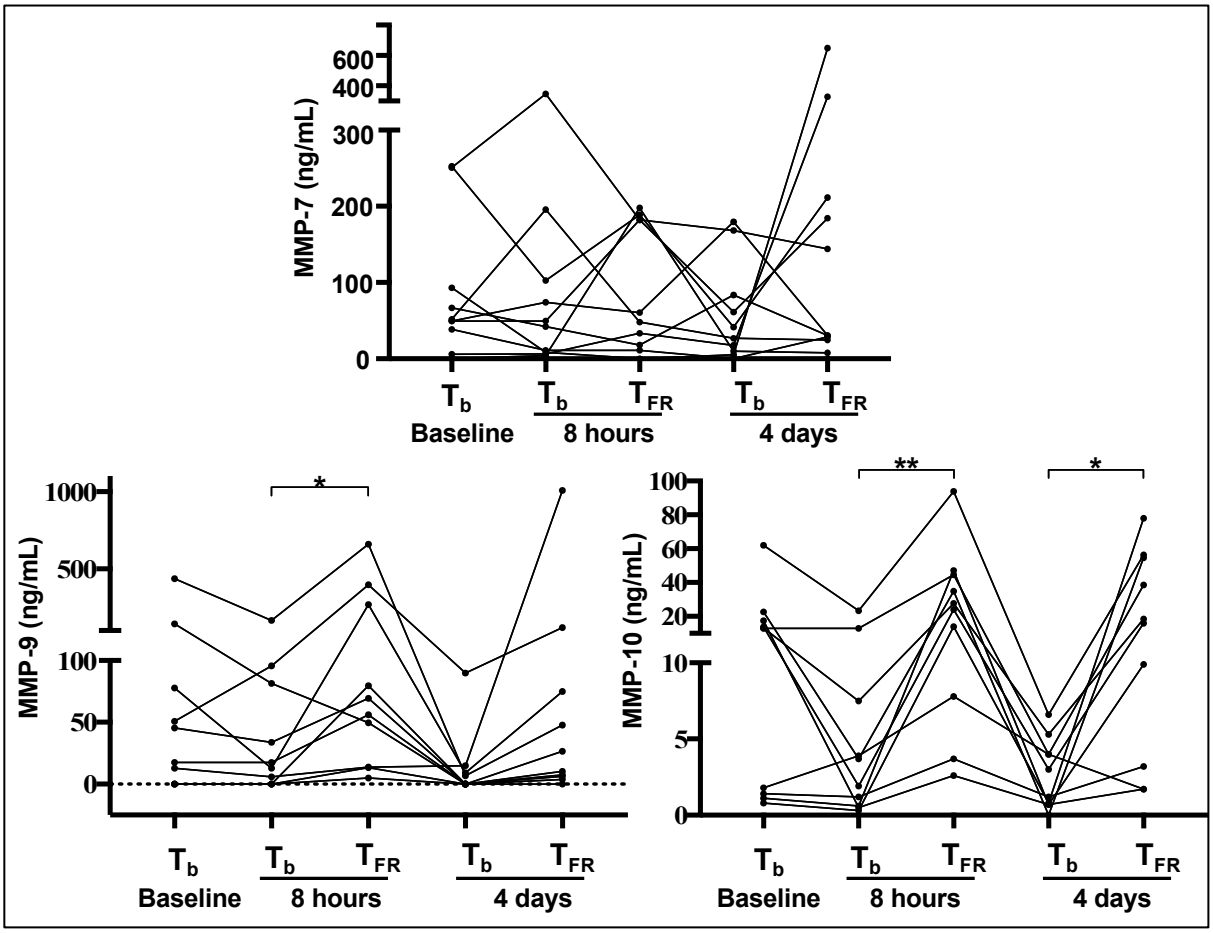

Figure 2.3. Changes in MMP-7, -9, and -10 with SL wear. Matrix Metalloprotease (MMP) levels for subjects at each study visit (baseline, after 8h and after 4d of SL wear) collected from the basal ocular surface tears (Tb) and the SL fluid reservoir (TFR). *$p \leq 0.05$, **$p < 0.01$

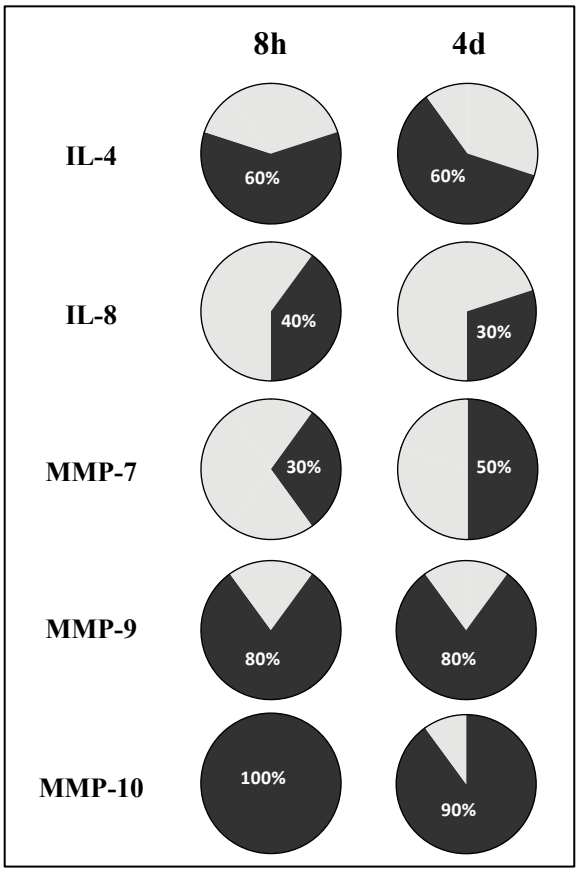

Figure 2.4. Percent subjects with >2-fold concentration in the FR compared to the Tb. The FR are represented in dark grey for each analyte at both timepoints. Non-shaded areas represent all other subjects that showed more similar concentrations, or greater concentration in the Tb.

TIMPs were only tested in selected samples when remaining volume after cytokines/MMPs analysis was available. Due to a lack of entire sample sets for TIMP data, it is not included in the analysis. The range of the MMP-9 and MMP-10 ratios that were calculated with TIMP-1 and TIMP-2 concentrations did not show any patterns and were relatively consistent across all samples except the Day 4 basal tears, in which the ratios were lowest. No conclusions can be made about the TIMP data in this study, but this should be tested in future studies to show the inhibition of MMPs during SL wear.

Comfort & ocular health evaluation

To evaluate basic satisfaction of neophytes following SL wear, comfort and vision data were analyzed for the 10 subjects that underwent tear analysis. There were no differences between the

average CLDEQ score measured pre-SL (11 ± 2) compared to after 8h (10 ± 2) or 4d (14 ± 2) of SL wear (p = 0.19) (Table 2.4). The average VAS score prior to SL was 80.35 ± 6.99 out of the 100-point scale. After 8h of SL wear the VAS comfort was 65.79 ± 6.42 and after 4d it was 60.72 ± 7.87, reduced but not significantly (p = 0.09).

Table 2.4. Comfort, staining and visual acuity.

	CLDEQ-8	VAS	Cornea (NaFl)	Conjunctiva (Lissamine)	Visual Acuity (logMAR)
Pre-SL	11 ± 2	80.35 ± 6.99	1.6 ± 0.9	3.0 ± 0.5	-0.09 ± 0.01
8h SL	11 ± 2	65.79 ± 6.42*	1.6 ± 0.5	4.1 ± 0.6	-0.07 ± 0.01
4d SL	14 ± 2	60.72 ± 7.87*	1.4 ± 0.6	3.3 ± 0.7	-0.11 ± 0.02
p-value	0.19	0.09	0.72	0.24	0.16

*significant difference compared to pre-SL wear using ANOVA with Dunnett's post hoc multiple comparison test (≤0.05). Data is shown as mean ± SE.

Shown at baseline and after 8h and 4d SL wear. Staining scores are a modified NEI grading scale (conjunctiva) – scoring each of 4 quadrants on the 1-3 scale and adding them for a total possible score of 12; and a modified Oxford grading scale (cornea) – scored in 5 corneal areas on a 1-5 scale for a total possible score of 25.

Change in comfort score was also calculated, positive values indicating improved comfort after SL wear. On average, change in CLDEQ comfort was +2 ± 2 after 8h of wear (range -11 to +8) and -3 ± 3 after 4d of SL wear (range -13 to +12). Change in VAS comfort score was -14.56 ± 9.13 after 8h of wear (range -63.15 to +38.95) and -19.63 ± 10.68 after 4d of wear (range -71.35 to +37.61). The CLDEQ and VAS scores were compared to each other for each subject, to test correlation of the two testing methods. The inversely related scoring systems were not strongly correlated at baseline (r = -0.573, p = 0.08) but did have significant correlation at 8h (r = -0.752, p = 0.01) and 4d post-SL wear (r = -0.744, p = 0.01).

There was no change in vision with SL wear compared to spectacle acuity measured at the SL dispense (p = 0.16). Ocular surface staining was evaluated for all subjects at each time point. Conjunctival staining (total potential score of 12) did not change from baseline (3.0 ± 0.5) to 8h (4.1 ± 0.6) or 4d (3.3 ± 0.7) of SL wear (p=0.24). Corneal staining (total potential score of 25) was 1.6 ±

0.9 pre-SL wear, 1.6 ± 0.5 after 8h, and 1.4 ± 0.6 after 4d of SL wear (p=0.72). No subjects showed a single sector staining score of greater than 2 for corneal or conjunctival staining, indicating that there was no severe staining associated with SL wear in this study.

There were no relationships between comfort, visual acuity or staining with the levels of the tear analytes tested in this study. For example, of the 6 subjects with the greatest increase of MMP-9 in the T_{FR}, 2 of them reported improved comfort, 2 of them reported worse comfort, and 2 of them didn't report a clear change in comfort at all. For MMP-10, the 9 subjects with over 2x greater concentration in the T_{FR} at 4d also showed no clear relationship between improved comfort (n = 2), worse comfort (n = 4), or no change in comfort (n = 3). Similar trends were seen for vision and corneal/conjunctival staining scores when they were compared to the tear analytes.

Discussion

Ocular surface inflammation in SL wearers is a growing concern and understanding the relationship between SLs and the inflammatory state of the eye is essential. This is the first study to determine the differences between the FR microenvironment and the local basal tears. The results show that after 8h and 4d of SL wear there are greater concentrations of MMP-9 and -10 in the FR, and that the increase is dampened after 4 days. The SL were fitted on normal eyes to collect pilot and control data, following standard guidelines to avoid inflammation due to a poor fit.

There were no fitting characteristics (e.g., apical clearance, landing zone appearance) that indicated a risk of increased inflammation with a specific fit, although this study was not designed to test this. The peripheral fit of the SL was designed to reduce excessive conjunctival compression, with 35% of SL manufactured with toric peripheral curves to accommodate uneven scleral curvature. Lenses had adequate apical clearance to avoid mechanical interaction with the cornea. A study using variable SL fits (e.g., 200 vs. 600 µm apical clearance, different lens diameters) would show whether certain fitting relationships create more or less inflammation in the FR[216]. Unfortunately, corneal

thickness and topographical analysis were not evaluated during the present study to assess for hypoxia, but studies have shown that SL create mild, subclinical hypoxia in normal eyes[218,219].

IL-4 and IL-8 were evaluated due to their role in inflammatory eye conditions. IL-4 is associated with angiogenesis and allergies, increased in the presence of contact lens related allergies such as giant papillary conjunctivitis[230]. IL-8, secreted by epithelial cells and inflammatory cells[224,231], can be elevated during soft contact lens wear[125]. No significant changes in IL-4 or IL-8 were observed after SL wear, and no corneal infiltrates were observed. The variability of IL-4 in the FR is justification for future studies to look at this marker in a larger cohort and in diseased eyes.

Due to the implications of MMP-9 in dry eye, inflammation, and reduced epithelial barrier function, it is a commonly used as inflammatory marker in the tears[228,232]. In the present study, MMP-9 levels were elevated in FR samples collected after SL wear for 8h and 4d, although only significantly after 8h. Compared to a clinical threshold, 40 ng/mL as used in the InflammaDry® test to indicate clinically significant inflammation[233], MMP-9 levels are greater only after 8h of SL wear in the FR (median: 62.7 ng/mL). The wide range of MMP-9 was greatest in the FR, which was as high as 659 ng/mL after 8h and >1000 ng/mL after 4d of SL wear. It should be noted that levels do normally increase into those ranges overnight, as have been measured immediately upon awakening by Markoulli et al.[234], who also measured midday concentrations of 9.8 $\pm$ 14.2 ng/mL in the same cohort. The concentration of MMP-9 and the diurnal variations in the FR should be studied further, specifically in diseased eyes which may tend to produce more of this potentially damaging analyte.

MMP-10 is not as well studied in the tear film or cornea, compared to MMP-9. The protease is implicated in wound healing and tissue remodeling and can be elevated after corneal surgery in diabetic patients[235] and during desiccating corneal stress[236]. Several studies in other tissues have suggested a regulatory role of MMP-10 which may contribute to reducing excessive and potentially damaging effects of inflammation[237]. Here, MMP-10 was markedly elevated in the FR, and its

presence may represent a response to SL wear in order to regulate inflammation in the FR. Again, these findings merit the need for future studies to explore the specific origin and implication of increased MMP-10 in the FR.

The increased MMP-9 and -10 in the FR may be due to trapped fluid on the ocular surface when the SL is applied. Alternatively, there may be increased production of MMP-9 and MMP-10 by the corneal epithelial cells during SL wear, which can accumulate in the FR. Both hypotheses imply that there is minimal tear exchange within the subjects fitted in this study, which is consistent with other published reports of SL wear[210,238]. The FR concentrations were often more similar to the early morning tears, which may harbor an increased inflammatory load due to the closed eye overnight environment[239,240], although subjects were awake for at least 45-60 minutes prior to morning tear collection. Measurement of the protease activity of MMP-9 in FR by the use of gel zymography to determine the levels of MMP-9 inactive and active forms might provide further functional information but could not be accomplished in the present study due to limited sample amount.

The concentration of tissue inhibitors of MMP (TIMPs) are important to consider when assessing the impact of increased MMP in the tears. As the MMP/TIMP ratio increases, it can be indicative of increasing inflammatory state[241]. In the present study, only limited TIMP data was available and most MMP/TIMP ratios could not be calculated. The ratios that were calculated were less than 0.5, which is not particularly indicative of an inflammatory state; however, the limited available data does not allow for any conclusive interpretation. Larger studies including more subjects and simultaneous quantification of MMPs and TIMPs are needed to draw conclusions about TIMP regulation of MMPs during SL wear.

This study shows that comfort was reduced after 4d of SL wear in 53% and 80% of normal subjects, according to the CLDEQ and VAS, respectably. While it has not been formally investigated in SL, contact lens discomfort is the primary reason for discontinuation of soft contact lens wear in the

US[225], and symptoms are usually quite similar to that of dry eye disease, which is known to have an inflammatory component[242]. However, conversely to dry eye, the contribution of inflammation to the discomfort response experienced by contact lens wearers remains unclear. In this study, no correlation was observed between SL discomfort and inflammatory mediator levels in tears. Comfort was highly variable with SL, somewhat contradictory to reports of improved comfort with SL in diseased eyes[196]. This is likely explained by relative responses; individuals with diseased eyes naturally compare the SL to classically uncomfortable alternatives they've become adapted to (e.g., corneal GPs), whereas here the subjective comfort rating was coming from individuals accustomed to soft contact lenses which are typically more comfortable. Care should be taken to accurately state the comfort of the SL in light of the population they are intended for and the alternatives available to that population.

There are some limitations of this study, which was the first to compare several different types of tear samples during SL wear. First, the sample size was small, in part due to challenges of collecting the samples. Sample size analysis using this data recommends 20 subjects for future studies, or 40 if there is a normal group compared to a diseased test group. All subjects had normal eyes, and would not typically be fitted into a SL. However, data derived from normal individuals allows for controlled normative data to be determined. This data will be used for development of a similar study in diseased eyes (e.g., keratoconus) who present high variability and a wide range of abnormalities in their tear fluid. There was also not a good baseline to compare without SL wear, since the only pre-SL measurements were taken in the morning which are subject to diurnal variation. However, this study did not compare the tears pre- and post-SL, rather were comparing the tears beneath and outside the SL. Tears were also pooled between eyes, which was necessary due to the risk of not always having enough FR volume beneath each lens. Since these were normal eyes, it was assumed that there was not a significant difference in response between the eyes, but future studies may wish

to keep eyes separate especially if incorporating lens fit into the analysis of the tear response to SL wear.

Conclusion

The results from this study found MMP-9 and MMP-10 were increased in the FR when compared to the basal tears on the ocular surface outside the SL margin. These results suggest inflammatory mediators can become trapped in the FR, which could compromise the ocular surface integrity with prolonged wear. This scenario could be amplified if placed on a diseased eye where MMPs and inflammatory mediators could become chronically trapped in the FR. Therefore, it is imperative that future studies continue to evaluate inflammation in the FR during SL wear, in both normal and diseased eyes.

Chapter 3.The protein and lipid composition of midday fogging and correlations with scleral lens fitting characteristics (manuscript in preparation).

Introduction

Scleral lenses (SL) have unique fitting characteristics that are not observed with any other contact lens modalities, specifically in the manner of vaulting the cornea and limbus, trapping a thick fluid reservoir (FR) and landing peripherally upon the easily deformable conjunctival tissue. In contrast to hybrid or soft contact lenses, the rigid SL does not yield to the shape of the anterior eye, so alignment of the lens to the ocular surface with minimal compression is of critical importance. The compression and sinking of a SL increases over the course of lens wear and has been implicated in sealing the post-lens FR and contributing to the occurrence of midday fogging (MDF)[148,243].

MDF occurs in one-third of SL wearers and there is an urgency to understand and mitigate it due to the visual reduction it causes as well as the unknown physiologic effects[56,135,149,244,245]. It has been defined as the accumulation of particulate debris in the post-lens FR, typically occurring gradually with a dense turbidity developing in the FR after a few hours of SL wear (hence the name midday fog). The composition of the FR in MDF is unknown, with confusion as to exactly what it is and therefore how it should be managed. Some clinicians have hypothesized that MDF occurs at least in part due to compression of goblet cells in the conjunctiva, leading to excessive mucin secretion into the FR[246,247]. Alternately, a small pilot study conducted in 2014 suggested that lipids may be present in greater abundance in MDF, although no specific classes were identified[248]. Another more recent study detected several types of leukocytes in the FR of SL wearers, although not significantly more in the MDF samples compared to those without[135]. A robust understanding of the composition of the FR in MDF has yet to be accomplished.

Although there has not been a comprehensive analysis of lipids in the FR during MDF, it is a reasonable hypothesis that they may be increased in MDF. First, they are often hydrophobic in nature and do not mix well with aqueous solution. When a SL is applied to the eye, sterile saline is used to fill the lens bowl and it is this aqueous fluid that mixes with the ocular surface tears to form the FR. All tears on the surface of the eye at the time of application, including the lipids (which

functionally prevent evaporation of the underlying aqueous tears), are mixing with the saline to form the FR. These lipids may become trapped and precipitate out of the aqueous FR over several hours of wear. Furthermore, patients with different amounts and/or types of lipids on their ocular surface when the SL is applied or being worn may have different susceptibilities to experiencing MDF. This study will use mass spectrometry to provide a comprehensive analysis of lipids as well as proteins in the FR, comparing the abundances to the severity of MDF.

In addition to identifying the components of the FR in MDF, it is useful to evaluate for associations between MDF and certain SL fitting characteristics. The amount of conjunctival compression, for example, could affect MDF if this compression led to increased cellular expression or secretion, or if the compression influenced the amount of tear exchange occurring between the FR and the ocular surface tears. The amount of conjunctival compression that occurs during SL wear varies between individuals and even between quadrants in a single individual[243,249,250]. The amount of compression can be measured grossly using a biomicroscope but more specifically using optical coherence tomography (OCT)[38,251] or the more recently developed scleral topography[249,252]. Reports of conjunctival compression with SL range from about 10 µm to greater than 100 µm, depending on the location evaluated, the SL designs, and the instrument used to take the measurement. The sMap 3D is a scleral topographer that was developed to measure the shape of the conjunctival tissue[253] and can be used to calculate the change in curvature of the conjunctival in the area where the SL lands on the tissue. The instrument measures scleral topography across a ~18-20 mm horizontal plane and a slightly smaller distance in the vertical dimensions[211–213]. In addition to the primary purpose of the instrument to measure the scleral shape for customizing lens designs, these measurements can also be taken repeatedly over time to evaluate changes in the shape. Indeed, a customized software within the instrument allows two maps to be compared to determine the change in conjunctival curvature caused by SL wear.

This study has three goals: (1) to characterize the major lipid and protein components contributing to MDF; (2) to measure the amount of compression occurring after SL wear; and (3) to determine the correlation between amount of conjunctival compression and level of MDF in the FR, testing the hypothesis that greater conjunctival compression will be associated with increased MDF. Collectively these findings will expand the understanding of MDF in SL wear and lead to better evidence-based management of this complication.

Methods

Subject selection and experimental overview

This study was compliant with the tenets of the Declaration of Helsinki and was approved by the University of Houston's Institutional Review Board. All enrolled subjects signed an informed consent prior to participation. A total of thirteen normal subjects were recruited and seen at the University of Houston, College of Optometry (UHCO). Sample size determination was made based on expected change in conjunctival morphology, since there are no available data on quantifying lipids and proteins in MDF. Based on calculations made to detect a change of at least 0.1 mm curvature change and considering similar studies which have been well-powered with 8-12 subjects, we set a sample size at 13 to power the study at 80%. Inclusion criterion was a normal ocular surface including the cornea and conjunctiva. Soft contact lens wear was permitted but subjects discontinued lens wear for at least 3 days prior to beginning the experiments, considered an appropriate timeline for the eyes to return to baseline health based on recommendations from other studies[254–256]. All subjects were SL neophytes and were excluded if they were unable to wear SL for 8-hours per day, had a known sensitivity to Fluress® ophthalmic drops (which contains 0.25% sodium fluorescein (NaFl) and 0.4% Benoxinate HCL), or had a history of any ocular disease or surgery including refractive surgery within the past 2 years.

There were several subject visits prior to and during the experimental phase of this study (Figure 3.1). At the enrollment visit, sMap scleral topography was completed and diagnostic SL over-refraction was done to determine the appropriate SL power and shape parameters to determine the appropriate SL power and shape parameters (i.e., curvatures, widths of zones). Custom SLs (Europa, Visionary Optics, Front Royal, VA) were ordered based on the scleral topography and refraction calculations. All SL were manufactured in the Optimum Extreme material (Dk = 125), and were designed with 5 different zones, each with different curvatures and widths (see schematic in Chapter 1, Figure 1.2). These curvatures (primarily the central base curve and most proximal peripheral curve) were customized for each individual SL in order to ensure a similar SL fit on the variable eye shapes of different subjects. The LZRs of the lenses were designed to land on the conjunctiva without bearing or impingement of blood vessels, which was accomplished with either toric (i.e., 2 different peripheral curvatures 180 degrees apart) or spherical (i.e., single LZR curvature) based on the curvature of the sclera/conjunctiva. The lenses were manufactured with lens diameter between 15.5 and 16.5 mm, determined based on the size of each subjects' cornea (which was measured via the sMap), with the aim of designing lenses that fit all subjects in the same way: clearance over the cornea and limbus with a smooth symmetrical landing on the conjunctiva, creating minimal compression and blanching of the conjunctival blood vessels. The toric or spherical landing curvatures were automatically designed by the sMap software and adjusted as needed in the SL fitting and training sessions (pre-experimental) to provide the most optimal fitting SL for each subject.

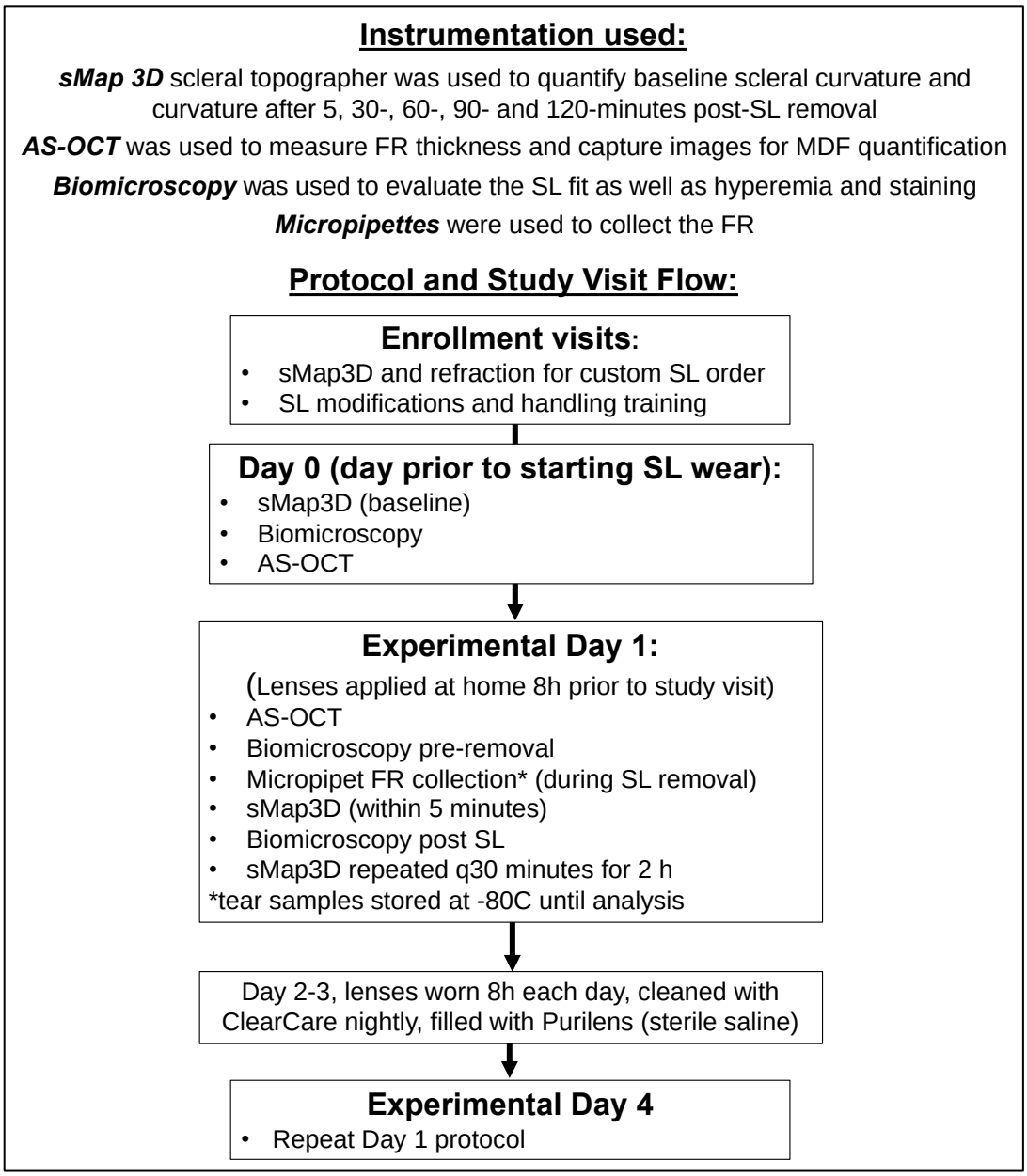

Figure 3.1. Flowchart of experimental protocol. The flowchart maps out the sequence of testingcompleted for the subjects, starting with pre-experimental lens fitting and ending with post-SL removal sMap testing.

The day prior to beginning SL wear, subjects reported to UHCO between 4-6 pm (Day 0), wearing spectacles, for a baseline scleral topography using sMap scan and final SL assessment using biomicroscopy and AS-OCT. Overnight the lenses were disinfected with ClearCare, and on the next morning, Experimental Day 1, subjects applied their lenses using buffered sterile saline as the application solution (Purilens, LifeStyle Co., Freehold, NJ, USA) 8 hours prior to their scheduled visit.

When arriving for the study visit, AS-OCT images were acquired, the SL were evaluated using white light biomicroscopy, and then the SL were removed with the investigator collecting the FR during removal. sMap topography was done (within 5 minutes of removal) to determine the conjunctival curvature and magnitude of conjunctival compression. Ocular surface health assessment was repeated post-removal. The sMap was then repeated every 30 minutes for 2 hours to determine the rate of decompression as a secondary outcome. The study visit was then complete, and subjects left wearing spectacles. For the next three days, subjects wore the lenses for 8 hours per day, filling with Purilens prior to application and disinfecting with ClearCare each night. On the fourth day of SL wear, subjects presented for a repeat of Day 1 testing. At the completion of the Day 4 experimental visit, SL wear was discontinued. The methodologies used for each of the aforementioned outcomes are more thoroughly described in the sections below.

Anterior segment OCT and midday fogging assessment

AS-OCT images (Visante OCT™, Carl Zeiss, Germany) were acquired to measure the FR depth and to quantify MDF. Measurements were taken initially at lens dispense visit (Day 0,SL worn for <5 minutes), and again at the beginning of each experimental study visit (after 8h SL wear). From the images, the FR thickness was measured at the dispense and after 8 hours of SL wear, at the location of the corneal apex, using built in software calipers.

MDF scores were calculated using two techniques in this study. In the preliminary (subjective) scoring, which was done in order to bin the samples into 2 groups for MS analysis, the OCT images were subjectively scored and designated as “MDF” or “non-MDF”. For this initial analysis,OCT images were masked and graded by an investigator (MKW) using a preliminary scale created previously developed but not validated (Figure 3.2). The investigator estimated severity based on this 5-category scale of MDF severity: none (1), trace (2), mild (3), moderate (4), or severe (5). Moderate and severe grades were deemed in the “MDF” group, and none, trace, or mild were deemed “non-MDF”.

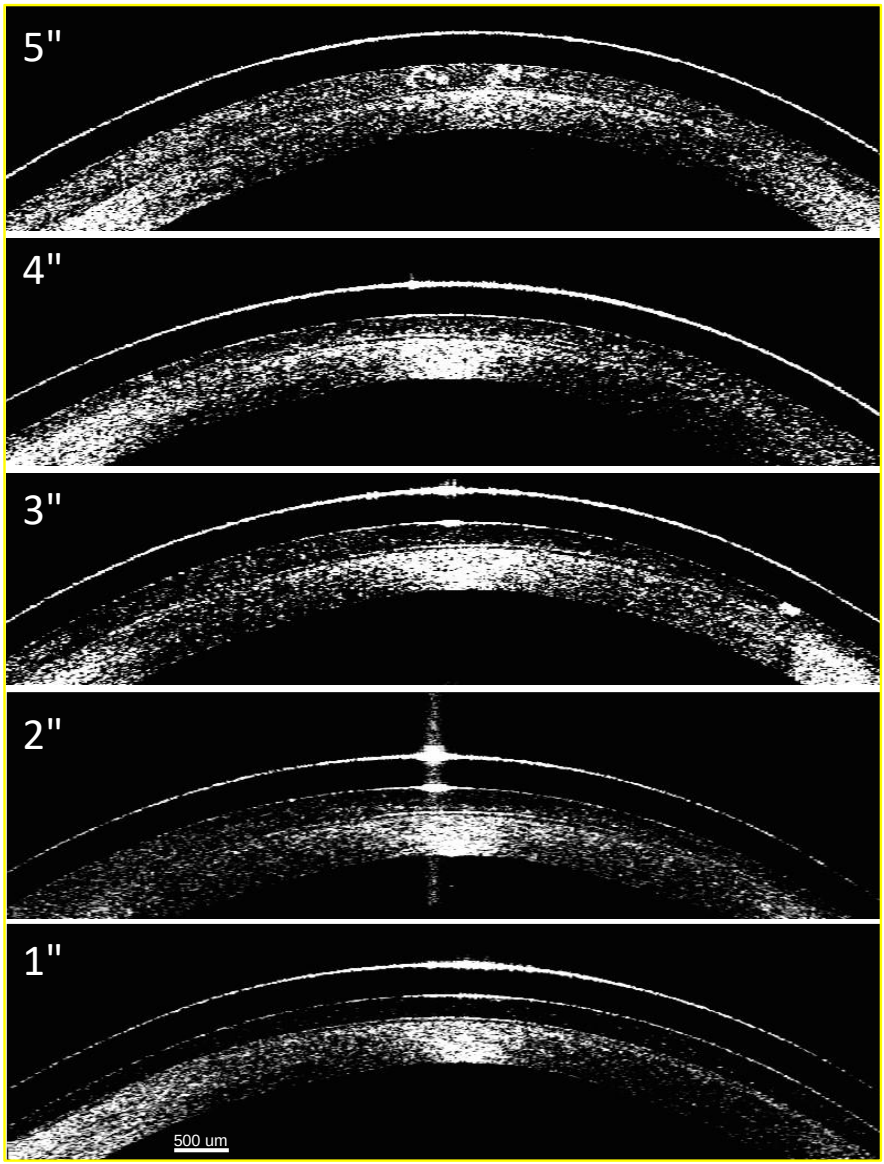

Figure 3.2. Subjective MDF grading scale. The 5-point scale used for subjective grading of MDF images in the preliminary subjective grading. Note that this scale has not been validated and was used for preliminary grouping of MDF subjects only.

The MDF scores were later quantitatively scored from the OCT images using a custom ImageJ protocol. This was done due to the range of MDF observed in the images, making it difficult to truly form two distinct groups. For this analysis, the OCT images were exported to ImageJ and quantified using a custom protocol (Figure 3.3). The scores were determined by calculating the net gray value in the FR (subtracting the background noise), and are presented as calibrated optical units, or simply “units”. The MDF scores were averaged between the two days for the final score for each eye, which allowed comparison of the scores to the FR compositional data (protein and lipid), since

the FR samples were pooled within each eye for mass spec analysis. In post-hoc analysis, the subjective scores were compared to the quantified ImageJ MDF scores to compare the scoring methods.

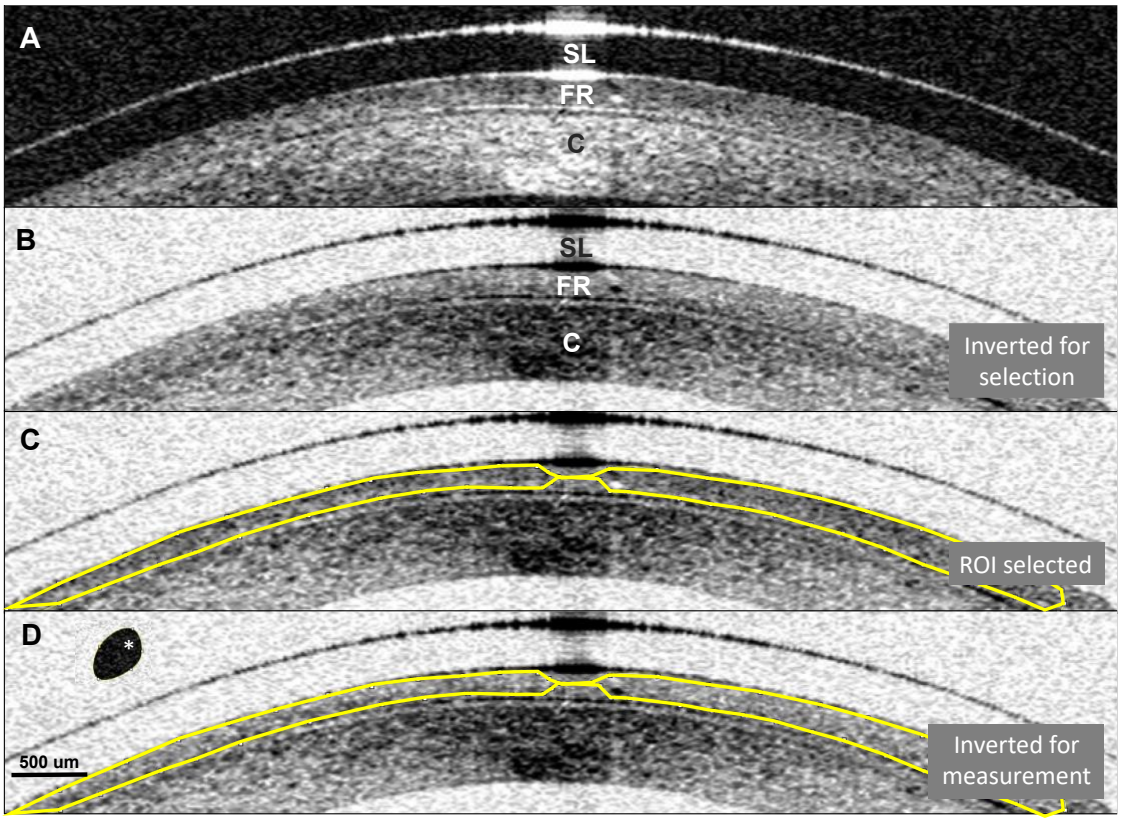

Figure 3.3. Processing of AS-OCT images to determine MDF score. First, the raw image was imported into ImageJ (A). Next in the image processing, the images were inverted to improve contrast (B). The region of interest (ROI) was selected using the polygon selection tool and splinefit (C). The entire FR area was selected (yellow outline), although areas of reflection and distortionwere avoided (i.e., the central reflection observed centrally). Lastly, the selected ROI was inverted again, and the mean gray value was measured in "calibrated optical units". Additionally, due to the noise of the images, a small area in the periphery of the imaging screen was randomly selected (D, white star), and mean gray value was measured using the same technique as the ROI, which was later subtracted from the FR value to determine the final score for each image. Scores were measured two times by two different masked examiners and averaged for the final score. C: cornea; FR: fluid reservoir; SL: scleral lens

Ocular surface health assessment & fluid reservoir collection

Prior to SL removal, visual acuity was recorded using a high contrast, high luminance Snellen acuity chart. White light biomicroscopy was performed to assess global and limbal hyperemia, graded based on the CCLRU grading scale[257]. The scleral LZR was assessed for blood vessel blanching

and impingement. After biomicroscopy and prior to sMap, SL were removed, and the FR was collected during removal. The collection was done by a single investigator (MKW) using the same method from Chapter 2 (see Figure 2.1). The tear samples were stored (DNA LoBind Eppendorf Tubes) and frozen at -80^{o}C for up to 6 months prior to analysis. After the SL were removed and the initial sMap scan was completed, evaluation of the cornea and conjunctiva was done using biomicroscopy. Corneal surface integrity was determined using NaFl vital dye and staining patterned was graded using the CCLRU scale. Both global and limbal hyperemia, as well as corneal staining, were graded subjectively using 0.1-unit scales. This specificity of grading has been shown to increase the repeatability of the subjective measurement[258] however, it should be noted that there is debate whether it is more precise to use a 0.5-unit scaling[259].

Fluid reservoir analysis with mass spectrometry

A total of 12 tear samples (7 with MDF, 5 non-MDF) were sent to the Mass Spectrometry Research and Education Center (MSREC) at the University of Florida Department of Chemistry,where they were analyzed for protein and lipid content. For each analysis type, 5 µL of FR (total 10 µL) was shipped on dry ice to the MSREC. Lipid samples were transferred to a glass tube and then extracted using an isopropanol extraction method. Total lipid concentration was determined by a sulfo-phospho-vanillin assay, and the sample loading was normalized for 0.1 µg total lipid content (i.e., sample volume was varied based on the estimated lipid concentration so that the same amount of lipid was loaded for each sample). After being extracted and normalized, the lipid eluent was analyzed on the Bruker QTOF-MS (Impact II quadrupole-quadrupole-time-of-flight (QqTOF) mass spectrometer). The resultant lipid data was then searched using lipidomic libraries in Metaboscape and SimLipid. Total protein was determined on a Qubit^{TM} and the appropriate volume of each sample was taken to equal 20 µg total protein for digestion. Nano-liquid chromatography tandem mass spectrometry (Nano-LC/MS/MS) was performed on a Thermo Scientific Q Exactive HF Orbitrap mass spectrometer equipped with an EASY Spray nanospray source (Thermo Scientific) operated

in positive ion mode. The LC system was an UltiMate™ 3000 RSLCnano system from Thermo Scientific. All MS/MS samples were analyzed using Sequest (XCorr Only) (Thermo FisherScientific, San Jose, CA, USA; version IseNode in Proteome Discoverer 2.2.0.388). Scaffold (version Scaffold_4.9.0, Proteome Software Inc., Portland, OR) was used to validate MS/MS based peptide and protein identifications. Peptide identifications were accepted if they could be established at greater than 95.0% probability by the Peptide Prophet algorithm[260] with Scaffold delta-mass correction. Protein identifications were accepted if they could be established at greater than 99.0% probability and contained at least 1 identified peptide. Protein probabilities were assigned by the Protein Prophet algorithm[261].

Ocular surface curvature and compression using sMap topography

The sMap scans were taken a total of 12 times on each eye of all subjects during the experimental time. To acquire each scan, the investigator first applied 200 µL Fluress® to the ocular surface, which is a viscous NaFl emulsion with topical anesthetic. This allows a relatively stable layer of NaFl to coat the ocular surface and for the patient to keep their eyes open and gaze steady on the target during acquisition. A total of three images were acquired for each eye: straight gaze, upgaze, and downgaze. These three images were automatically montaged together by the software (Figure 3.4), which detects the limbus of each image to determine like locations (to facilitate the montage processing). The first acquisition was used for SL design and not in the compression analysis. The second scan, taken the day prior to starting SL wear, served as the baseline scan, taken in close proximity and at the same time of day as the experimental acquisitions to reduce noise from diurnal variations in conjunctival shape[262]. After removal of the SL of Day 1, a scan was acquired within 5 minutes, and then subsequently at 30-, 60-, 90-, and 120-minutes post-SL removal. This was repeated again on Day 4. At the end of Day 4, subjects were asked to return for a follow-up sMap scan every 24 hours for the next 3 days, to determine the time it takes for full rebound to baseline conjunctival curvature.

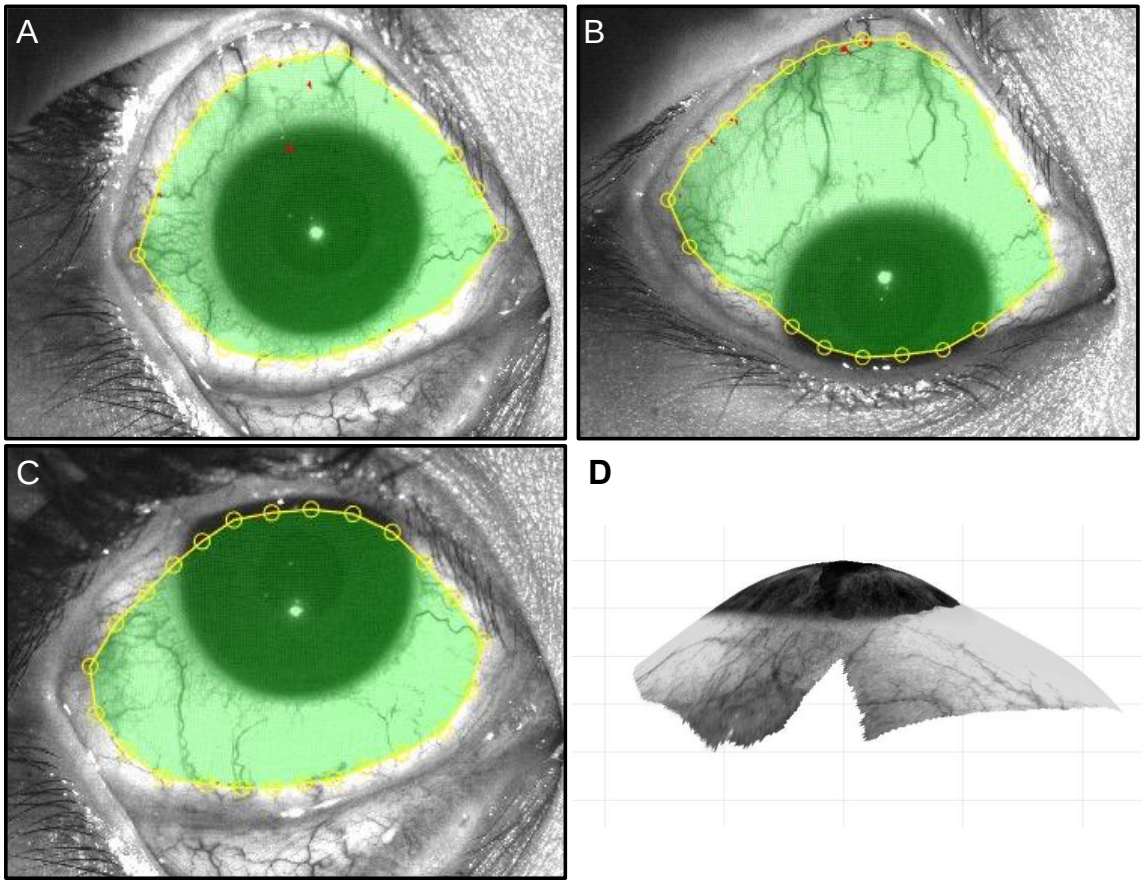

Figure 3.4. sMap imaging technique. To acquire the scleral topography imaging with the sMap,sodium fluorescein (NaFl) is instilled to illuminate the tear film overlying the conjunctiva. Images are acquired in straight gaze (A), downgaze (B), and upgaze (C). After acquisition in the three gaze positions, the images are montaged together (based on limbus detection) to form a 3D topographical map of the sclera and corneal surface (D).

Data and statistical analysis

Normality of all outcomes were evaluated using the Shapiro-Wilk test. Curvature of the conjunctival surface was compared between all 4 quadrants before and after SL wear using the non-parametric version of ANOVA for paired outcomes, the Friedman test. Post-hoc testing was done using Dunn's multiple comparison test to determine where the differences were significant. Visual acuity was measured with a Snellen chart and converted to logMAR for analysis at baseline and experimental visits. Significance was set at $P \leq 0.05$.

To analyze the FR composition in MDF, relative abundance of lipids and proteins were compared to MDF scores. The tear samples used for MS were initially grouped subjectively into MDF and non-

MDF groups for initial bulk analysis of the MS data, and subsequently the MDF was quantified in each sample to allow correlations to be made with specific lipids and proteins. This quantification was done using ImageJ, which measured the mean gray value of the FR as calibrated optical units. The quantitative Objective scoring of MDF using ImageJ is novel and has not been previously validated; therefore, to determine repeatability and reproducibility of the methodology, two masked examiners graded each image twice using an identical protocol. The intra-observer repeatability was measured by calculating the within-subject standard deviation of the measurements made on the same subject[263,264], and inter-observer reliability was calculated by dividing the square of the between subject SD by the sum of the squares of the between subject SD[264]. MDF scores between Day 1 and Day 4, as well as between the two eyes of each subject, were assessed for correlation using the Spearman rank test for nonparametric data.

Lipids and proteins in the FR were identified using Metaboloscape and Simlipid databases (lipids), and Scaffold (proteins). Post-processing sorting and analysis was done in Microsoft excel and GraphPad Prism. To evaluate the correlation between MDF and the other outcomes (compression, FR depth and settling), right eyes only were selected for the analysis and correlation was measured with the Spearman rank test.

Results

A total of 26 eyes from 13 subjects were included in the analysis. The SL diameter for 70% of subjects (n = 9) was 16.0 mm, and those subjects with significantly smaller or larger than average horizontal visible iris diameter (11.8 mm) were made SL with smaller (15.5 mm, n = 1) or larger (16.2 mm, n = 1; 16.5 mm, n = 2) diameters. All SL were designed to vault the cornea including limbus and land without impingement or blanching of blood vessels on the conjunctival surface. All lenses were manufactured with a central 8.5 mm wide optic zone and a 2.1 mm wide adjacent peripheral curve, both with variable radii of curvature depending on the power and sagittal depth (SAG) of the lens (see Figure 1.2 in Chapter 1 for SL schematic). The average lens SAG was 4368 ± 244 µm. A

total of 18 lenses were designed with toric (rotationally asymmetric) LZRs, and 8 lenses were designed with spherical (rotationally symmetric) LZRs; mean toricity in the LZR was 127 ± 114 µm. Table 3.1 shows the SL parameters, fitting characteristics, and ocular health outcomes for subjects with and without MDF.

Table 3.1. Scleral lens parameters and characteristics

Outcome	At SL Dispense (All subjects)	Post-SL wear		Correlation* r (P-value)
		MDF (scores 39-92)	Non-MDF (scores 6-24)	
Mean lens SAG (µm)	4368 ± 244	4240 ± 191	4405 ± 256	-0.36 (0.22)
Mean LZR toricity^ (µm)	127 ± 114	191 ± 109	103 ± 108	+0.32 (0.12)
Visual acuity	-0.03 ± 0.13	-0.03 ± 0.10	-0.01 ± 0.06	+0.31 (0.29)
Corneal Staining	0.1 ± 0.1	0.2 ± 0.1	0.3 ± 0.3	+0.07 (0.83)
Limbal Hyperemia	0.5 ± 0.2	1.1 ± 0.5	0.8 ± 0.8	-0.06 (0.83)
Global Hyperemia	1.0 ± 0.7	1.9 ± 0.7	1.6 ± 0.6	+0.11 (0.71)
Apical Clearance (µm)	293 ± 84	336 ± 117	265 ± 69	-0.06 (0.85)
FR settling Day 1 (µm)	n/a	81 ± 75	88 ± 42	-0.16 (0.63)
% mild blanching	8%	12.5% (n=1)	11% (n=2)	-
% severe blanching	0	0	0	-
% excessive movement	0	0	0	-
% excessive LC^{+}	19%	50%	11%	-

*correlation with MDF using Spearman rank correlation testing, using right eyes only
^mean toricity in the area of the LZR over the conjunctiva
$^{+}$excessive limbal clearance (LC) estimated in at least one quadrantSAG: sagittal depth; FR: fluid reservoir

AS-OCT analysis: FR settling and MDF scoring

AS-OCT images were captured and analyzed for all 26 eyes at the SL dispense visit and at each experimental visit. Mean FR thickness at SL dispense (0 hours wear) was 285 ± 90 µm (336 ± 117 µm in the MDF group and 265 ± 69 µm in the non-MDF group), and after 8 hours of lens wear it was 254 ± 81 µm and 183 ± 67 µm, settling an average of 81 ± 74 µm and 88 ± 42 µm, respectively in

the MDF and non-MDF groups. When compared to the quantified MDF score, the FR thickness and settling amounts were not significantly correlated to increasing MDF (Table 3.1).One eye that settled 240 µm had no clearance after 8 hours lens wear on either experimental day, therefore was not analyzed for MDF.

In subjective grading, a total of 7 eyes met the criteria (a score greater than 2) for MDF, and 19 eyes were considered non-MDF. Once MDF was quantified using ImageJ, the subjective scores were compared to the objective to determine an appropriate "cutoff score" in distinguishing MDF from non-MDF (Figure 3.5).

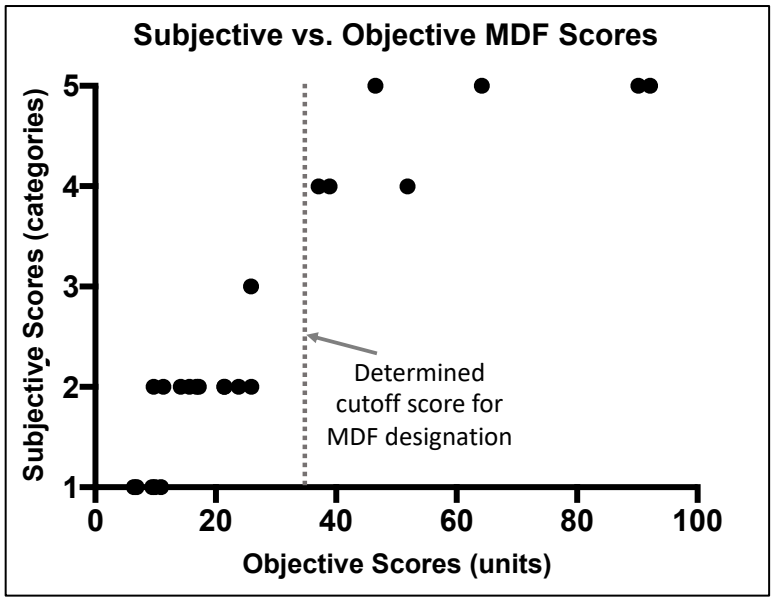

Figure 3.5. Subjective vs. objective MDF. The subjective categories are compares to the continuous variable objective scores, showing that the subjective scoring was in agreement with those objective scores. However, the objective scores are more able to discriminate between severity within each of the subjective categories. Note the subjective score equal to 1, which has several different scores all in the same category, or the score of 4 which also has a wide range of severities.

In the quantitative analysis using ImageJ, MDF is reported as calibrated units of optical density (units). On Day 1 the mean MDF score was 33 ± 29 units (range 7 – 96) and on Day 4 they were 28 ± 24 units (range 6 – 91); Day 1 and 4 scores were strongly correlated between eyes ($r = +0.94$; $P < 0.001$), and mean right and left MDF scores were also strongly correlated ($r = +0.94$; $P < 0.001$) (Figure 3.6). The cutoff for MDF was determined to be 35 units, with those scores greater being considered MDF and those below considered non-MDF. Repeatability and reproducibility of the ImageJ quantification of MDF were evaluated by comparing the intra- and inter-observer

measurements. Intra-observer repeatabilityof the measurements was 0.97 and 0.39, respectively, for the two examiners. Inter-observer repeatability was even better, 0.3.

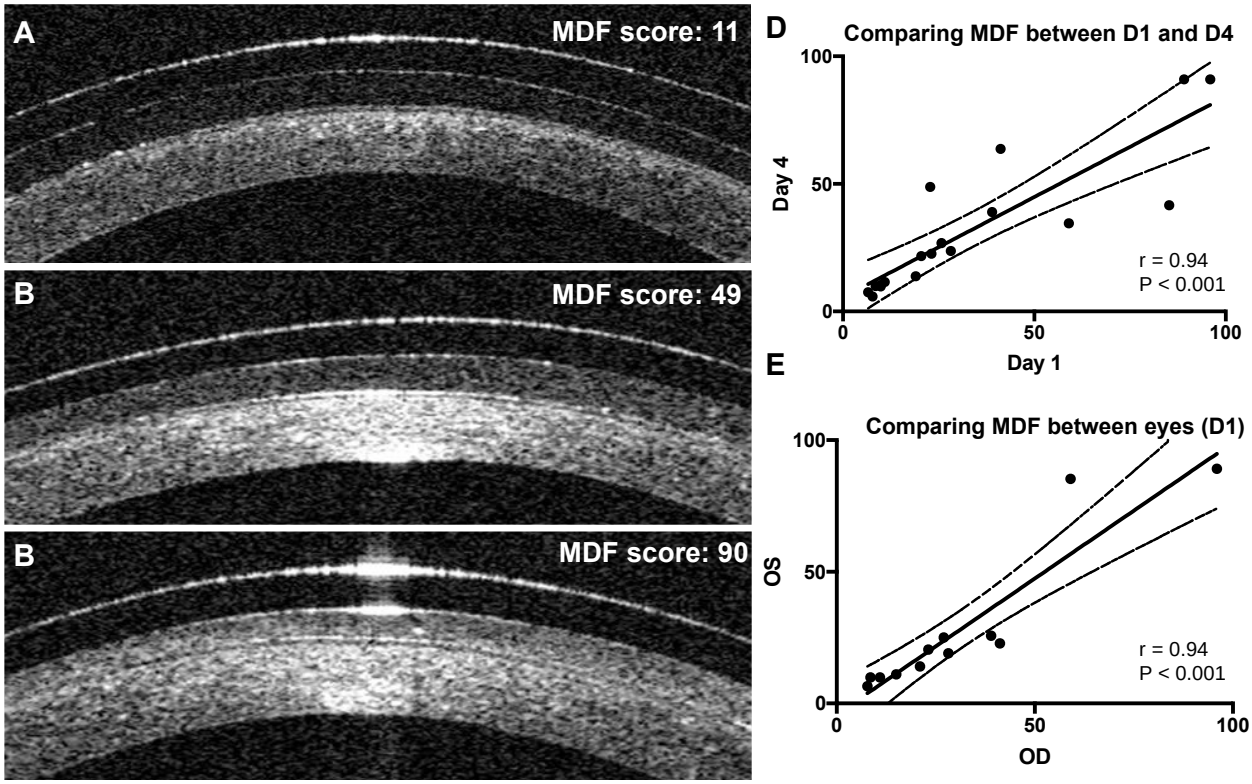

Figure 3.6. AS-OCT images showing MDF scores and correlations between days and eyes. Examples of MDF scores from the subjects in the study (A-C) are shown, and the correlations between the eyes on day 1 and 4 (D) as well as between eyes on day 1 (E) were very strong.

Lipid & protein analysis

A total of 12 FR samples (7 with MDF, 5 with no MDF) were analyzed for lipids and proteins using MS. The overall mean lipid and protein concentrations were 32.3 ± 32.0 µg/mL and 36.5 ± 46.3 µg/mL, respectively, with no differences in concentration observed between the MDF and non-MDF group (P = 0.83 for lipids, P = 0.25 for proteins). A total of 1175 distinct lipids and 1491 proteins were identified in the samples, and the relative abundances were compared to MDF scores to determine which lipids and proteins were positively or negatively correlated to increasing MDF severity. The subjective grouping of MDF and non-MDF samples was only used for initial gross observation of the MS data, and once the images were quantified, those scores were used for MS data comparison. The average quantified score in the MDF group was 60 ± 23 units (range 36 to 92) and in the non-

MDF control group it was 14 ± 7 units (range 7 to 23); no subjects showed non-zero values for MDF score. Observation of the grouped MS chromatograms (Figure 3.7) shows several distinct differences in the overlapping peak graphs for the MDF and non-MDF grouped samples in the lipid data. No observable differences in chromatograms between the two groups were observable in the protein data.

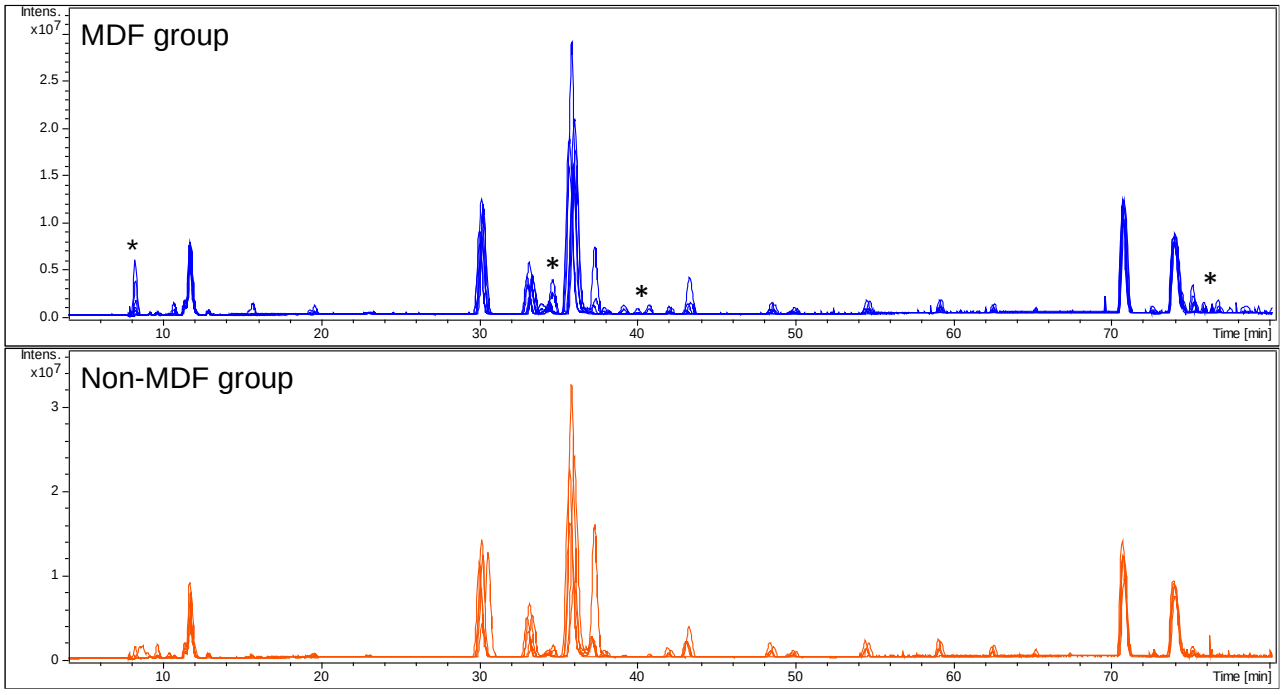

Figure 3.7. Mass spec chromatograms for lipid testing. The top is an overlay of the chromatograms for all subjects deemed in the MDF group (mean MDF score: 60 ± 23 units; range 39-52), and the bottom chromatogram is an overlay of the subjects deemed in the non-MDF group(14 ± 7 units; range 6-24). Asterisks are shown in the top graph to indicate where the peaks differ most between groups.

Several categories and classes of lipids were represented in the tear samples (Figure 3.7). The sterols showed the greatest abundance, with large proportions of glycerophospholipids, glycerolipids, fatty acyls, and sphingolipids. Several of the classes of lipids within these categories were seen in greater abundance in subjects with greater levels of MDF. Saturated cholesterol esters (CE), wax esters (WE), fatty amides, and carnitines (from the sterol and fatty acyls classes) were among the most abundant lipids that were correlated to increasing MDF. When evaluating the relative abundance of each lipid class in the FR, the only class which showed a difference in the

percent of total lipid abundance were the WE, which comprised approximately 10% of lipids in the MDF group and only 4% of lipids in the non-MDF group. The findings in each lipid category are summarized in the sections below, and a summary of the primary classes and species that were increased in MDF are shown in Table 3.2.

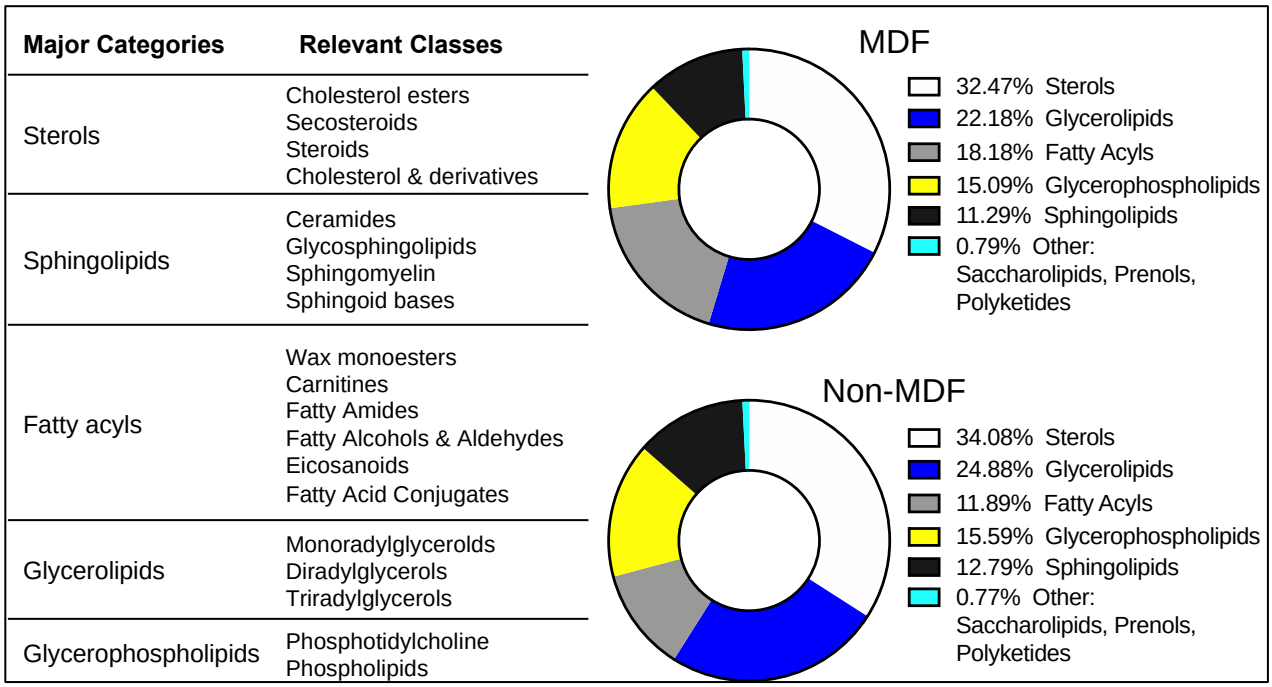

Figure 3.8. Major lipids categories and classes found in the scleral lens fluid reservoir. The major lipid categories and the primary classes of lipids that were found in the FR samples are shown on the left. Percent abundance of each categories are shown on the right for the MDF samples (top) and the non-MDF samples (bottom). Steroids were the most abundant, followed by glycerolipids. Fatty acyls (mostly WE) were more abundant in the MDF samples.

Sterols

Approximately 75 different species of sterols were detected in the FR samples, primarily sterol esters (i.e., CE, steroids), secosteroids (i.e., vitamin D derivatives), as well as cholesterols and their derivatives. The CE made up approximately 13% of total lipids, 12% unsaturated and 1% saturated, the latter of which were positively correlated to MDF ($r = +0.68$, $P = 0.02$). The unsaturated CE, which were more abundant, were not correlated to MDF ($r = +0.31$, $P = 0.32$), although several of the unsaturated CE species (i.e., CE 19:1, 20:1, 22:1, 24:1), while not highly abundant, showed a positive correlation with MDF (Table 3.2). In addition to evaluating abundance of certain classes and

species of sterol, the ratio of saturated: unsaturated CE was also measured and ranged from <0.01 to 0.13, with greater values indicating an increasing level of saturated compared to unsaturated CE. This increasing ratio was significantly correlated to increasing MDF (r = +0.73, P = 0.02).

Another class of sterol lipid found in the FR were the steroids, although overall they were not correlated to MDF. Certain types of steroids that can be irritants (C18 and C19) were present in small quantities and showed no relationship to MDF. However, select C21 steroids, for example 18-oxocortisol, were seen in greater abundance in the MDF samples (r = +0.60; P = 0.04). The secosteroids (i.e., vitamin D derivatives) represented approximately 20% of the lipid abundance but were not correlated to MDF, and neither were cholesterol or their derivatives. Overall, no sterols were found to have a significant negative correlation to MDF.

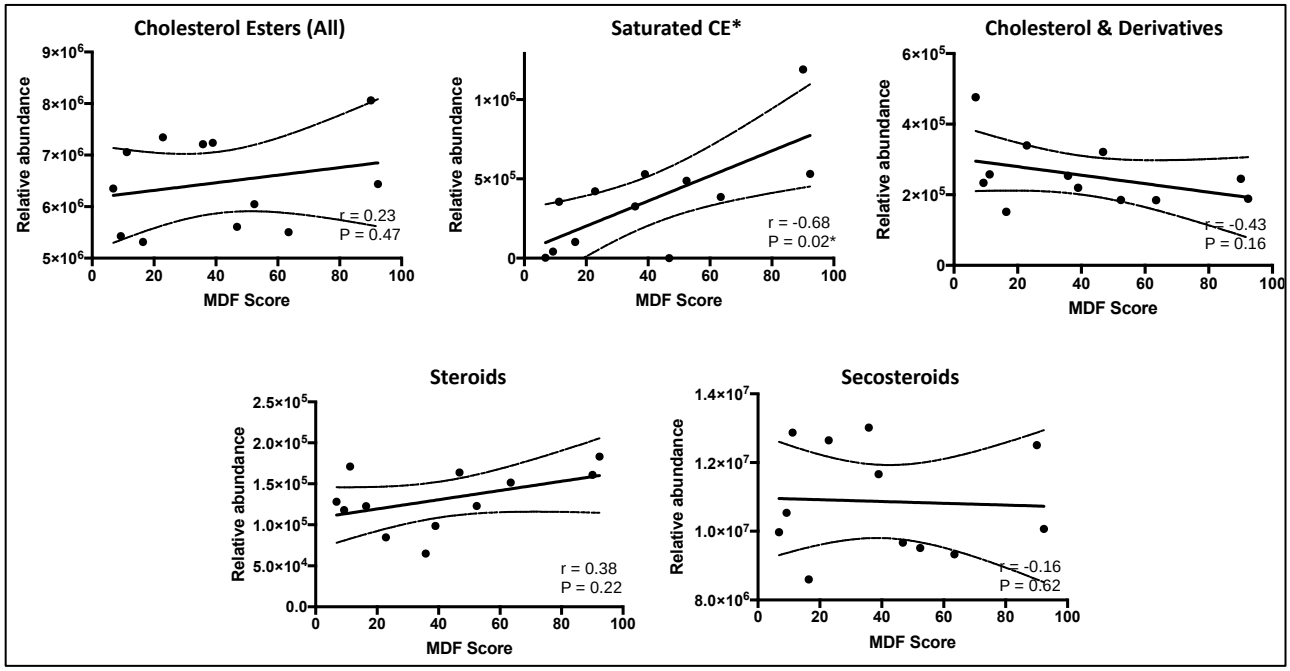

Figure 3.9. Sterols vs. MDF. The relative abundances of various classes of lipids from the sterol category. These lipid classes of interest in the FR are plotted against the MDF scores. The only correlation observed between the MDF and lipid classes were the saturated cholesterol esters (CE), which are shown to increase with increasing MDF (P = 0.02).

Fatty acyls

Several hundred species of fatty acyls were found in the FR samples, including fatty esters such as wax esters (WE) and carnitines, as well as hydrocarbons, eicosanoids, fatty alcohols &

aldehydes, and fatty acid conjugates. Several of these classes and species of fatty acyls were correlated to increasing MDF. Fatty amides for example, were significantly correlated to MDF, as were fatty esters such as WE and carnitines ($r = +0.75$, $P = 0.01$ for all three classes). The WE class of lipids were the most compelling in the FR of subjects with MDF. Over 75 different species of WE were detected, making up ~10% of all total lipids in MDF samples and only ~4% in non-MDF grouped samples. Over 50% of these WE, mostly unsaturated, were highly correlated to increasing MDF (Table 3.2), and many of the fatty acyl lipids (including WE) that were increased are considered “branched chain fatty acids”, which are fatty acids with at least one methyl branch. Similar to the observations in CE, the ratio of saturated: unsaturated WE were also measured (range +0.004 to +0.17), which showed an increasing ratio with increasing MDF ($r = +0.70$, $P = 0.01$).

Additional classes of lipids within the fatty acyl category included eicosanoids, fatty alcohols, fatty aldehydes, and hydrocarbons. Eicosanoids, which include prostaglandins and leukotrienes, were not overall shown to be correlated to MDF, although select species were positively correlated to increasing MDF (Table 3.2). Fatty alcohols and aldehydes, as well as hydrocarbons, were not detected in high abundancy in the FR samples and there were no species correlated to MDF.

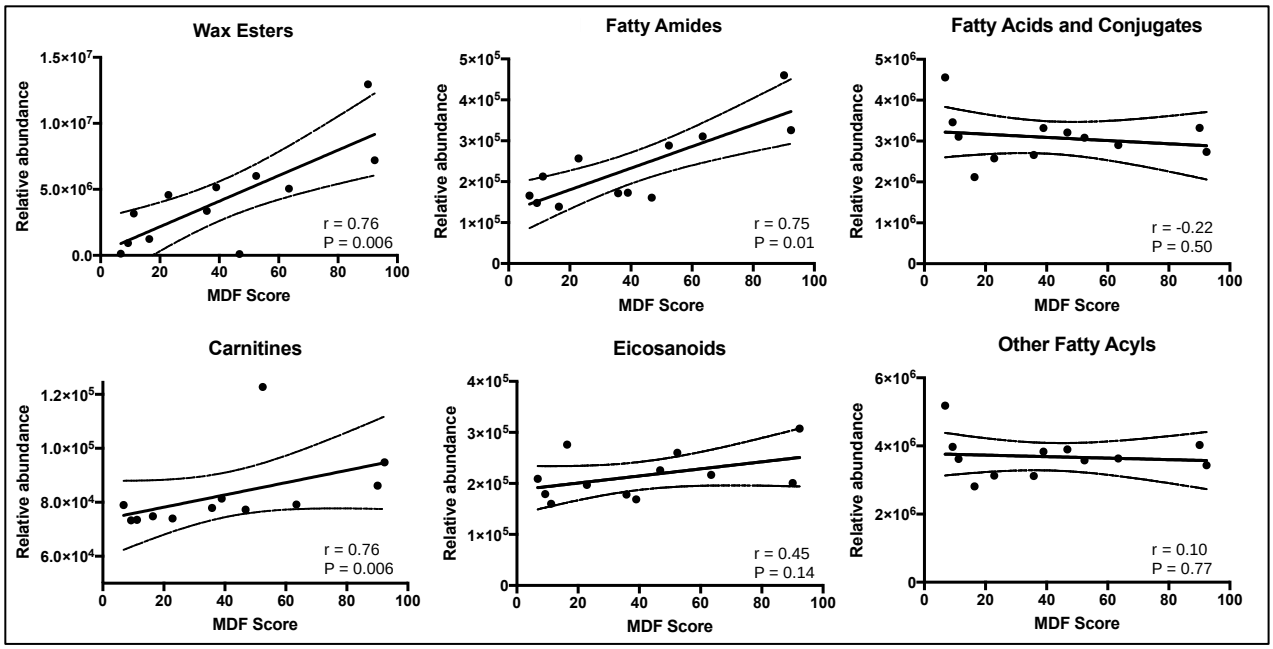

Figure 3.10. Fatty acyls vs. MDF. The relative abundances of the fatty acyls of interest in the FR are plotted against the MDF scores. In this category of lipids, there are several classes (WE, fatty amides, carnitines) that show positive correlations to increasing MDF.

Glycerolipids, sphingolipids and glycerophospholipids

Glycerolipids, sphingolipids and glycerophospholipids were all detected in various abundances in the FR samples, although none showed strong correlations to the MDF severity in thesamples. Glycerolipids include monoradylglycerols (MAG), diradylglycerols (DAG), and triacylglycerols (TAG), the latter of which typically the most studied type of glycerolipids in the tear fluid. In these samples, TAGs were one of the most abundant species of lipid in the FR (21% of detected lipids), but there was no correlation to MDF (Figure 3.11). Sphingolipids and glycerophospholipids made up approximately 12 and 15% of the lipids detected in the FR samples, respectively. Sphingolipids, which include ceramides and sphingomyelin, were abundant in the FR but their levels did not correlate to MDF. Ceramides were not significantly correlated to MDF (r = +0.53, P = 0.08). The glycerosphospholipid species in the samples were primarily from the phosphotidylcholine (PC) class, which comprised approximately 12% of total lipids detected and was not overall correlated with increasing MDF. The phospholipid class of lipids, while only comprising ~0.5% of total lipids, was interestingly found to be negatively correlated to increasing MDF (r = -0.64; P = 0.03).

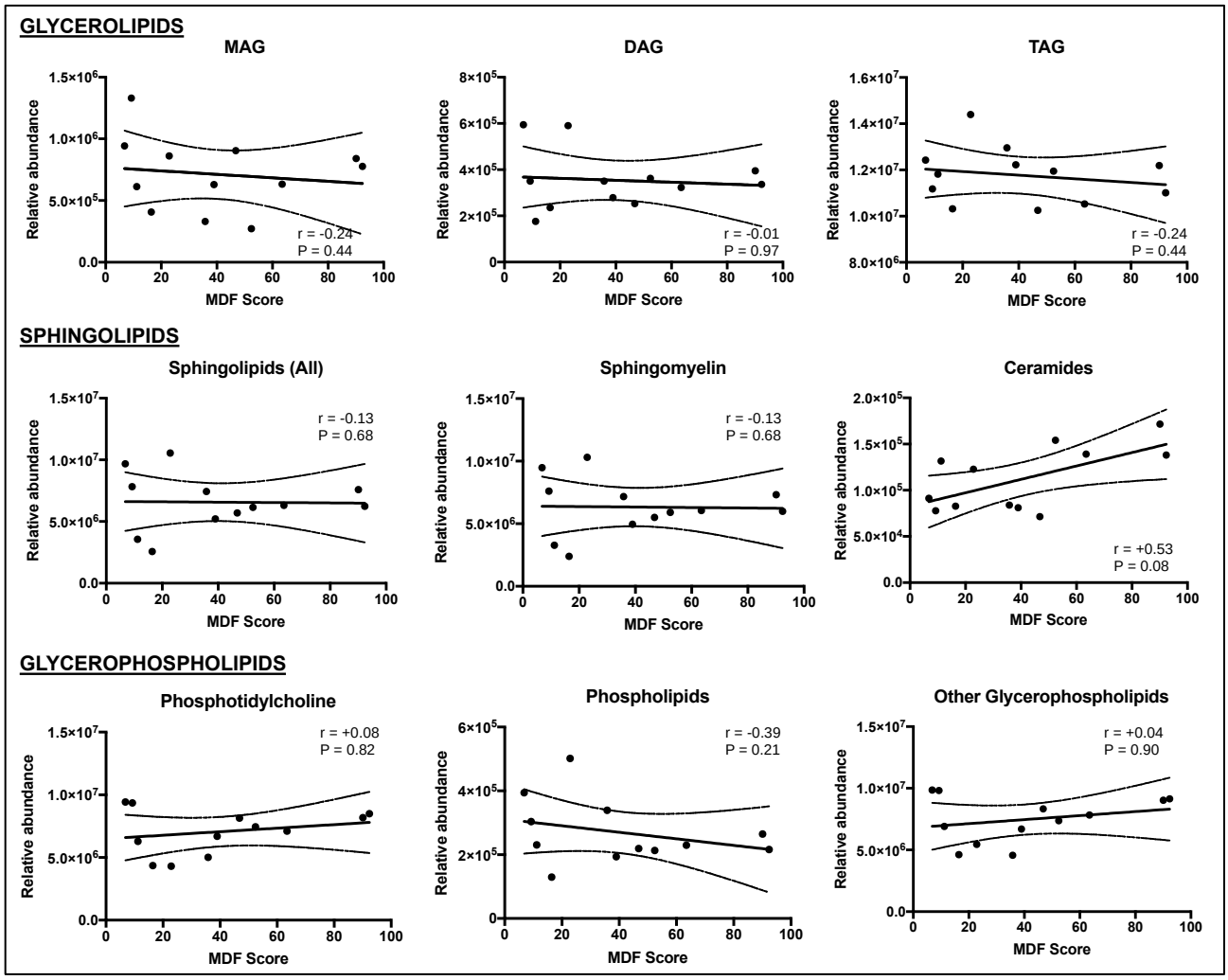

Figure 3.11. Glycerolipids, sphingolipids and glycerophospholipids vs. MDF. The relative abundances of select classes of glycerolipids, sphingolipids and glycerophospholipids are shown plotted against the MDF scores. In these categories, no classes were correlated to MDF. FR: fluid reservoir; MDF: midday fogging.

Table 3.2. Lipid classes/species that are different in MDF.

Lipid Category Class / *Species*	Properties & Function	% of FR	r (P-value)
	STEROLS		
Saturated CE		1	+0.69 (0.02) *
Unsaturated CE	Nonpolar esters formed from fatty acids with sterols[101]; hydrophobic in nature Prevent tear film evaporation; tend to form separate phase in aqueous solution[101]	12	+0.31 (0.32)
CE 18:1		*10*	-0.57 (0.06)
CE 19:1, 20:1, 22:1, 24:1		*<1*	+0.75 to +0.76 (0.01) *
18-Oxocortisol	Steroid with similar functions as aldosterone[265,266], regulatory role in salt/water balance	<1	+0.60 (0.04) *
Cholestanone	Cholesterol derivative with no known function in tears	<1	+0.75 (0.01) *
	FATTY ACYLS		
Saturated WE	Esters formed from fatty acids with alcohols; Hydrophobic in nature, nonpolar	1	+0.50 (0.10)
Unsaturated WE			
34:1, 37:1, 38:1, 39:1, 43:1, 44:1, 34:2, 37:2, 39:2, 40:2, 40:3, 44:2, 43:2, 43:3, 47:2, 48:2, 48:3	Prevent tear evaporation, often found on outer surface of organisms and create sealed barrier[101,267]	11	+0.78 (<0.01) * +0.61 to +0.82 (<0.01 to 0.05) *
Linoleyl myristate	Wax monoester and unsaturated fatty acid	<1	+0.61 (0.04) *
Carnitines	role in lipid transport and energy production; found in ECM membranes	<1	+0.75 (0.01) *
Fatty amides	Believed to be low in concentration in meibum[99,101], unknown function in tears	4	+0.75 (0.01) *
Sativic acid	Hydroxy fatty acid	<1	-0.64 (0.03) *
	SPHINGOLIPIDS		
Ceramide	relatively hydrophobic, do not interact with aqueous in tears[268], high melting point; Amphiphilic, can be elevated in dry eye[102], often bound to lipocalin in tears[269]	2	+0.53 (0.08)
	GLYCEROPHOSPHOLIPIDS		
Phospholipid	Polar; help to stabilize the interface of lipid and aqueous tear components[270]	*<1*	-0.64 (0.03) *

CE: cholesterol ester, WE: wax ester

There were a total of 1491 proteins detected in the FR samples and there was no positive correlation observed in comparison to increasing MDF. Two proteins, immunoglobulin fragments, showed a significantly negative correlation to MDF, although there were several hundred fragmented immunoglobulins detected and overall, there were no other significant correlations other than those two fragments. The 14 most abundant proteins detected, as well as other proteins of interestdue to their relevance in contact lens-associated inflammation, are listed in order of abundance in the FR (Table 3.3). In addition to the proteins listed, there were two unidentifiable protein products, one which was 9% of the protein abundance and the other which was 3% of the abundance.

Table 3.3. Major tear protein findings.

Protein	Primary tear function	Abundance in FR (%)	MDF Correlation	
			r	P-value
Lactoferrin	Antimicrobial iron binding[108,271]	13.1	-0.16	0.63
Serum Albumin	Permeability marker	12.1	-0.40	0.23
Ig light chain, partial	Immune function	4.2	-0.72	0.02 *
Lipocalin-1	Antimicrobial lipid binding[269,272]	4.0	+0.31	0.36
Transmembrane secretory component	Unknown	4.1	-0.36	0.27
Lysozyme-C precursor	Antimicrobial	3.7	-0.16	0.65
Complement C3	Inflammatory indicator	2.3	-0.35	0.30
Transferrin	Permeability marker	2.1	-0.21	0.53
Prolactin induced protein	Unknown	2.0	-0.51	0.11
IgG light chain	Immune function	1.7	-0.76	0.01 *
Cystatin Precursor	Protease inhibitors[112,273]	1.6	-0.07	0.84
Zinc-a-2-glycoprotein	Possible role in inhibiting cell proliferation[274]	1.5	-0.60	0.06
Serpin peptidase inhibitor	Unknown[275]	1.3	-0.40	0.22
Mammoglobin-B precursor	Unknown	1.0	+0.15	0.67

Conjunctival compression

The conjunctival curvature changed by an average of -0.10 ± 0.03 mm^{-1} on Day 1 and -0.08 ± 0.05 mm^{-1} on Day 4 of SL wear, measured within 5 minutes of lens removal on each day and averaged between the 4 quadrants. These changes in curvature were significant in all 4 quadrants (Figure 3.12 and Figure 3.13) and represent a downward compression of the tissue (increasing the negative curvature values of the tissue shape). The sMap algorithm measures curvature of the surface directly, which is inversely related to radius of curvature. The change of 0.1 mm curvature change seen represents ~10D change in radius of curvature. The change is negative since the tissue is compressed inward, which will effectively steepen the curvature in that region. The change was greatest in the nasal meridian (-0.11 ± 0.02 mm^{-1}) but was not significantly different from the superior (-0.10 ± 0.03 mm^{-1} flattening) or temporal quadrants (-0.10 ± 0.02). The average inferior quadrant change was the least at -0.07 ± 0.02 mm^{-1}. By the 90-minute post-SL removal time on both Day 1 and 4, mean curvature was nolonger significantly different from baseline, and eyes were 90-95% rebounded at 2hrs post-SL removal. The superior and inferior compression rebounded at approximately the same rate (approximately 7 x 10^{-4} mm^{-1}/sec), which was more quickly than the nasal (5 x 10^{-4} mm^{-1}/sec) andtemporal quadrants (6 x 10^{-4} mm^{-1}/sec). In all quadrants, rebound rate was greatest in the first 30 minutes.

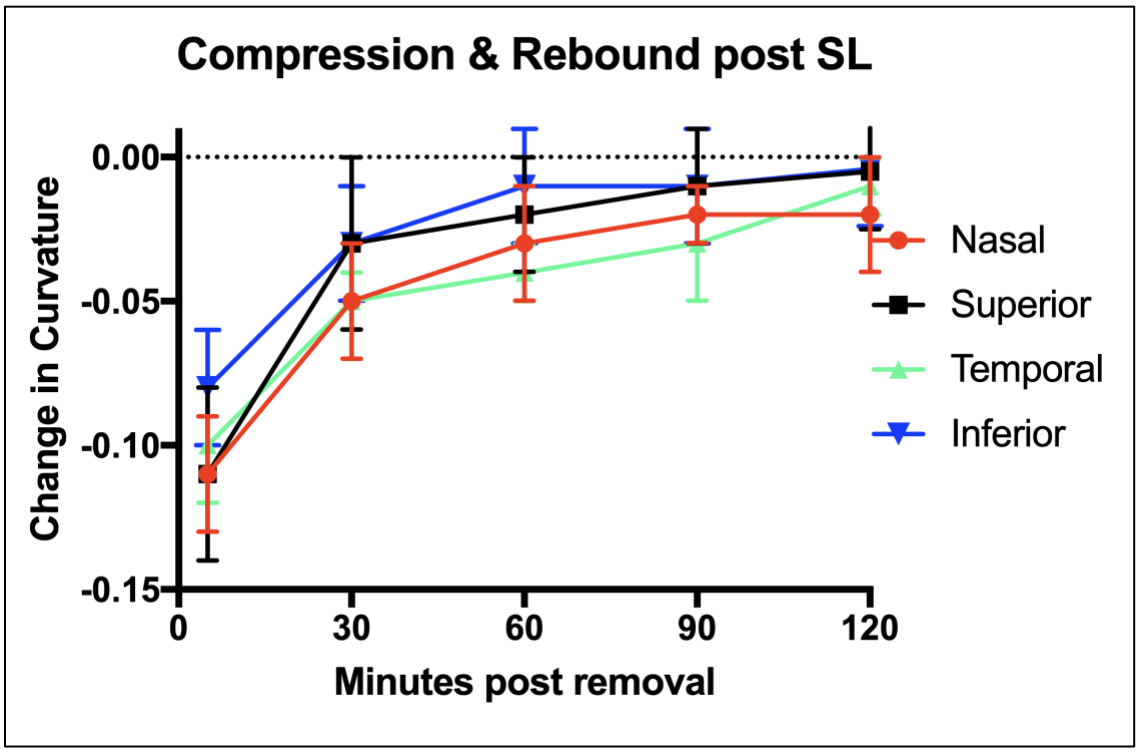

Figure 3.12. Conjunctival compression and rebound after 8 hours of scleral lens wear. Change in conjunctival curvature are shown for all four quadrants after 8 hours of SL wear of Day 1. The timepoints measured started from 5 minutes post removal up and go up to 120 minutes post-removal. Curvature was significantly different from baseline in all quadrants (Dunn's multiple comparisons test) until 90 minutes post-SL removal. Eyes were approximately 90-95% rebounded back to baseline curvature after 120 minutes post-SL removal.

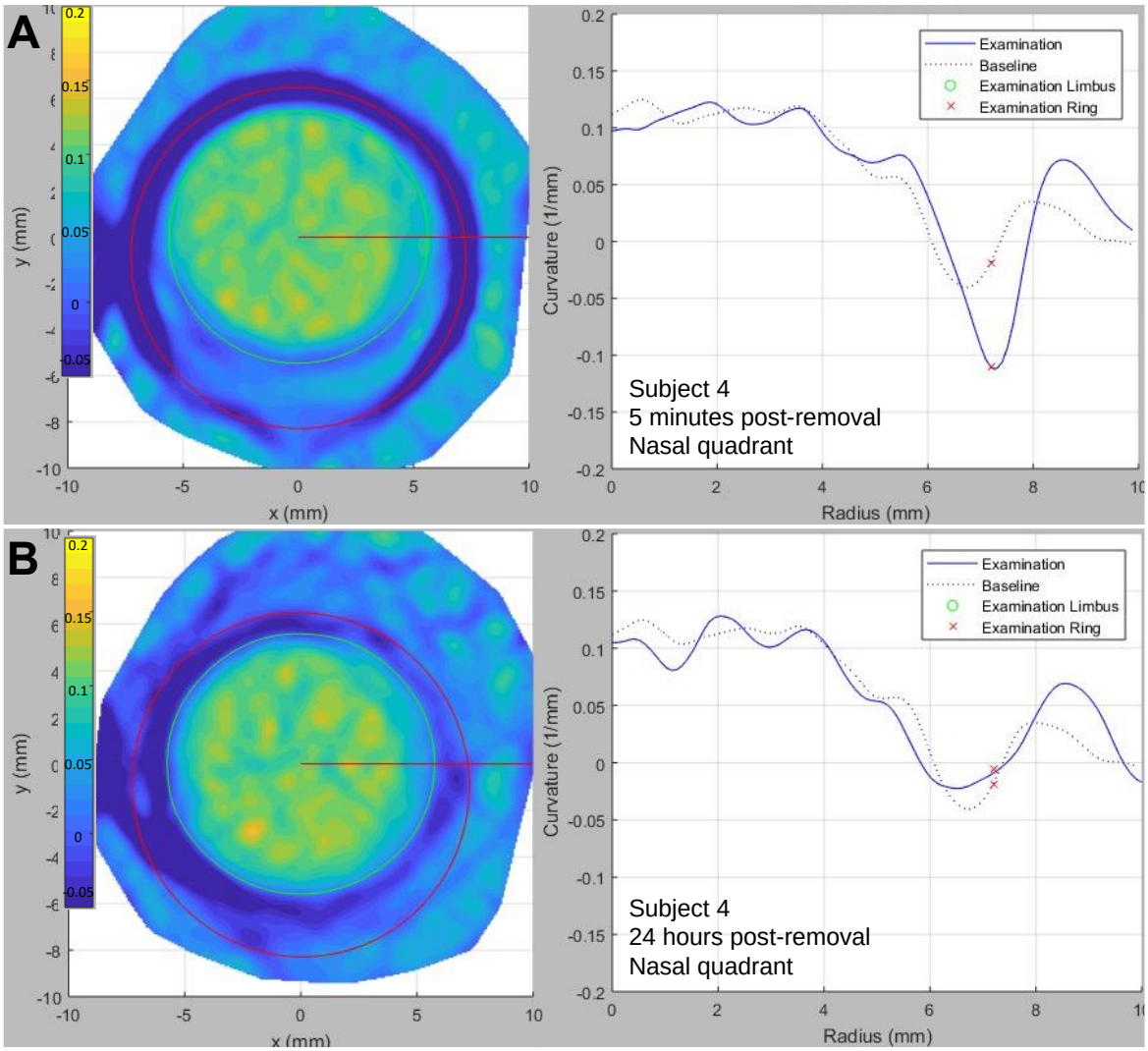

Figure 3.13. Conjunctival compression display. Color maps and graphical representation takenwith the sMap, showing the amount of compression for subject 4, taken 5 minutes post-SL removal (A), as well as after 24 hours post-removal (B). A cross-section of the map (red line) is shown in graph form to compare the measured curvature to the baseline. For each subject, the compression ring was at a slightly different location, so the ring was manually aligned for each subject.

Correlations between outcomes

The MDF scores were compared to other parameters of the SL fit to determine if certain fitting characteristics were associated with the occurrence of MDF. Only right eyes (n = 13) were used for this analysis. The primary outcome of interest was the mean change in curvature in the landing area, as determined by sMap. On Day 1, conjunctival curvature change at 5 minutes post-removal was not significantly correlated to the amount of MDF on Day 1 (r = -0.46, P = 0.13). On Day 4,

there was a negative association between conjunctival compression and increasing MDF (r = -0.59; P = 0.049), although with high variability and many subjects that fell outside the 95% CI. In other words, subjects with greater amounts of curvature change after SL removal did not show a strong correlation to increasing MDF. In post-hoc analysis, each quadrant was evaluated individually and the superior quadrant on Day 4 showed the greatest negative correlation (r = -0.62; P = 0.03), with the nasal quadrant on both days showing the least correlation to MDF (P = 0.75 and 0.74 on Day 1 and 4, respectively).

MDF was also compared to several of the lens fitting and ocular health parameters. The amount of initial FR depth, measured using OCT, was not found to be significantlycorrelated to MDF (r = -0.06, P = 0.85), and neither was the amount of FR settling that occurred (r = -0.16, P=0.63). Limbal clearance, although not measured objectively and just subjectively evaluated as excessive or not, did appear to be excessive in 4 out of 7 eyes with MDF (57%) and only 2 out of 18 eyes (11%) without MDF. Additionally, there were no correlations between increasing MDF and visual acuity (r = +0.30, P = 0.14), global hyperemia (r = +0.11, P = 0.70) or limbal hyperemia (r = -0.06, P = 0.84). There were 8% (n = 3) of eyes that experienced blood vessel blanching in any quadrant, 2 eyes with MDF and 1 eye without. These are not enough subjects with blanching for it to be reasonably compared to MDF scores.

Discussion

The findings of this study suggest that lipids, primarily nonpolar fatty acyls (i.e., WE), are contributory toward MDF in the FR of SL wearers. Additionally, there is some evidence of a difference in inflammatory protein activity within the MDF and non-MDF samples, although it is not clear what that difference truly is. When compared to SL fitting and ocular health outcomes, the only correlation observed was between the amount of compression and MDF and it was a negative correlation, which seems to indicate that a looser fitting lens (i.e., one that causes less tissue compression) has more of an association with MDF than a tighter SL fit. Overall, these

findings suggest that MDF is correlated to an increase of hydrophobic fatty acids in the FR and is not strongly related to the amount of conjunctival curvature change during SL wear. This indicates that MDF is likely more related to patient-specific characteristics (i.e., composition of lipids in tear film) than the SL fit itself.

Quantifying MDF

There is currently no universal method for quantifying MDF, and this is the first study to quantify MDF and compare it to lipid and protein concentrations in the FR. The subjective and objective methods of discriminating MDF severity used here were in strong agreement, although the objective method is able to more precisely quantify the severity of MDF that allowed more robust statistical comparison to the other outcomes. The subjective method used here had a total of 5 different categories of discrimination, which may be too many categories given the subjective similarities between categories. For example, grade 2 and 3, or grade 3 and 4, may be difficult to distinguish repeatedly. In the future, if this subjective method should be used (although the objective method is preferrable), we recommend distinguishing between 3 groups rather than 5.

Other groups have also begun to measure optical clarity of the FR with different techniques. Carracedo et al. quantified the optical density of the FR, also using OCT and ImageJ but measuring particles per mm^2, showing that the FR turbidity in keratoconic corneas increased by a factor of ~8x after 6-9 hours of lens wear and that greater turbidity correlated to a reduction in low contrast visual acuity[54]; they did not evaluate the composition or determine MDF in the study. Schornack et al. also measured FR turbidity, using Scheimpflug tomography images and using the optical density data in the software (measured as % density), finding that the optical density approximately doubled from ~5% to ~10% after 2-hours of SL wear[276]; they did not assess visual acuity or FR composition. Both of these studies are consistent with this study, finding a range of FR turbidities, but unlike these previous studies, the current study was specifically done to

quantify MDF severity to be compared to composition. The ImageJ protocol measured the mean gray density of the FR area in calibrated optical units, which is analogous to the optical density measurements used in the other studies. The intra- and inter-observer repeatability of the method used here was excellent and highly sensitive. In addition to the repeatability of the measurements, there was a strong correlation between the level of MDF seen in both eyes. This indicates that the two eyes of an individual experience a similar level of MDF severity, which is expected since the tear film composition would be expected to be similar in both eyes. When using the objective method described here to quantify MDF, it is recommended to use an OCT of high resolution and reduce background noise to a minimum when acquiring the image. Removing background noise was essential for each individual image because the noise was not consistent across acquisitions. Overall, the objective method used in this study can be considered a reliable and informative way to quantify MDF.

Fluid reservoir composition

Based on the MS data, the primary tear components among those tested that were correlated to MDF appear to be nonpolar lipids, specifically those that functionally prevent evaporation of the tear film. Due to the type of lipids seen in greater concentration in the FR (WE and CE), it is most likely that they are originating from the Meibomian glands (rather than from cell walls). Cell wall lipids are typically amphiphilic, whereas those observed here are highly nonpolar and are typically secreted by the Meibomian glands[86,101,270,277,278]. Lipids are hydrophobic fatty acids and their derivatives, and one of their primary collective functions is to reduce evaporation of the tear film. Two of the most compelling classes of lipids which showed the greatest correlations to MDF were the WE and CE,which are part of the fatty acyl sterol and sterol lipid categories, respectively. Both of these lipids are highly nonpolar and hydrophobic[99,130], and likely precipitating out of the aqueous-based FR as the lenses are being worn. Further, they are naturally known to compose up to 80% of tear film lipids[101,130]. All SL wearers appear to experience some amount of lipid

precipitation into the aqueous FR over time, as evidenced by the presence of some level of MDF (non-zero) scores in all subjects, and the presence of some levels of hydrophobic lipids in all samples. We propose that some level of MDF occurs in most if not all SL wearers, and simply that those individuals who experience a clinically significant amount of this lipid precipitation are considered as experiencing MDF.

The most abundant lipid species that were correlated with MDF were the WE, which made up approximately 10% of all lipids in the samples that showed greater MDF severity (compared to only 4% in the non-MDF samples). In the natural tear film, WE are prevalent, estimated to make up approximately 25% of normal tear lipids, although the studies vary widely[101,130,270,279]. This class of lipids, which are classically hydrophobic and highly nonpolar, are secreted from the Meibomian glands as part of meibum and largely believed to reduce evaporation and increase surface tension on the surface of the tears[98,99,101,130,270,272,280–284]. The entire fatty acyl family is characterized by long chains of repeating methylene groups which are fundamental in the hydrophobic nature of the molecules. They consist of a diverse group of lipid classes which includes fatty acids, alcohols, aldehydes, amines,and esters (WE are part of the fatty ester class)[282]. In addition to WE, several other classes from the fatty acyls were increased in MDF. Notably, the fatty amides and carnitines showed strongly positive correlations to MDF, although they collectively only comprised ~0.5% of total lipids detected. It is unclear what the significance of these lipids in the natural tears or FR are, although they are nonpolar which suggests they have a role at the surface of the tears reducing evaporation.

CE are not highly abundant in most bodily tissues and fluids. They are, however, abundant in meibum and sebum, often comprising up to 60% of the total tear lipids[101]. They are typically the most abundant lipid from the sterol category. In this study, although they were correlated to MDF, the CE only made up approximately 13% of the total lipids and were not the most abundant sterol. The secosteroids (Vitamin D derivatives) were greater in abundance overall. Both CE and WE

primarily originate in the Meibomian glands and are secreted as part of the meibum onto the ocular surface. The ester components of each class are hydrophilic, yet the fatty acid, fatty alcohol and cholesterol residues in the molecules create an extremely hydrophobic molecule[101]. Another interesting finding beyond the increased relative abundances were the ratios of saturated: unsaturated CE and WE that were measured. When considering both lipid classes, a greater ratio was significantly correlated to increasing MDF. This indicates that there are relatively more saturated forms of these lipid classes compared to the unsaturated forms in MDF. Since saturated lipids tend to have higher melting points compared to the unsaturated lipids, meaning they are more likely to be solid (rather than liquid) at the same temperature, this makes sense that greater relative amounts of saturated lipids could lead to more MDF. Ultimately the cause of the altered ratio is unclear, although it may be related to dysfunction of the Meibomian glands in some cases (see Clinical implications of findings).

Polar lipids in the tear film are less abundant than the nonpolar and act somewhat as an interface between nonpolar lipid and aqueous tear components[283,285,286]. Examples of polar lipids are the sphingolipids (sphingomyelins, ceramides) as well as the phosphatidylcholines found in the glycerophospholipid category. Sphingolipids, categorized based on a long-chain nitrogenous base as the core structure, made up approximately 12% of the lipids in the FR with ~11% as sphingomyelin, which is greater than would typically be expected in the natural tear film. Sphingomyelins are polar lipids that are found in cell membranes[280,287], but also may play a role in increasing surface tension and enhancing the structural stability of the tear fluid[268]. It could be that the sphingolipids are so much greater in abundance in the FR samples compared to that found in other studies evaluating natural tears because of epithelial cell membranes being broken down into the FR during prolonged SL wear.

Glycerolipids made up approximately 23% of the lipids detected in the FR, of which 21% were TAGs. Most studies that have measured TAG in the tears have measured it directly from meibum,

which typically contains less than 10% TAG[101,130]. The reason for increased abundance in these samples may be due to TAG produced outside of meibum, or simply because of trapped TAGs. Ultimately, they were found in high concentrations in most samples but were non-contributory toward increasing MDF severity. However, similarly to the (at least) low levels of other nonpolar lipids in all samples, they could certainly be contributing to the non-zero levels of MDF detected universally in these subjects.

Glycerophospholipids, which are glycerolipids that also have a phosphate group, were approximately 15% of all lipids detected, of which about 90% were a single species of lysophosphocholine (LPC), which to our knowledge has never been detected in the tears. This species of lipid is most commonly formed by enzymatic cleaving of a glycerophospholipid by the enzyme phospholipase A_2[288](PLA_2) although to our knowledge this has not been reported in the tears, and the PLA_2 proteins were detected minimally in these tear samples (<1 % of abundance, although they were present). These lipids were not correlated to MDF in this study, which is not surprising since they are largely polar and would not have the same degree of hydrophobic properties as the nonpolar lipids in the tears.

The protein analysis in this study showed relatively similar results between the MDF and non-MDF groups, with only sporadic or weak correlations between FR proteins and MDF. When significant correlations were observed, for example with select immunoglobulin fragments,they were detected in greater abundance in the non-MDF samples. The most abundant proteins in the normal tear film, while variable, include lactoferrin, lipocalin-1, lysozyme C, serum albumin, IG heavy constant alpha 1, prolactin-inducible protein, polymeric immunoglobulin receptor, immunoglobulin kappa constant, and zinc-alpha-2-glycoprotein[89,92–95]. This is in broad agreement with the results here, in which most of these proteins were among the most abundantly detected. Many of these large proteins are typically unaltered in contact lens wear[109,110,289], and although there has been a report of increased Lipocalin-1 in soft contact lens intolerance[113], none of these

proteins have been previously studied in SL wear. However, the most interesting finding in this data was that two of the Ig antibodies, which collectively made up approximately 6% of the detected proteins and peptides, were negatively correlated to increasing MDF. This was an unexpected finding, and ultimately unclear whether this is clinically meaningful. The presence of immunoglobulins in the tear film is well reported, and they can be altered in contact lens wear and disease[120,121,290,291]. One hypothesis for the reduced abundance of these immunoglobulins in MDF is that there could be an increase in activity of proteases and/or immune cells in MDF, which could degrade the immunoglobulins. Proteases (i.e., MMP-9) were not detected in these samples, but often go undetected in MS analysis when also evaluating for larger more abundant proteins (i.e., lactoferrin). However, this will be an important finding to follow up on in future studies that can confirm the reduced fragments and more specifically evaluate the role of proteases, cells or other components in the FR that could influence these proteins.

Since the protein and peptide abundances measured here are relative, and since the FR is such a unique tear environment, it is challenging to directly compare the results to other studies. However, another interesting finding that should be considered in the context of other tear studies was a high abundance of serum albumin detected in all the FR samples. On average, this was the second most abundant protein (after lactoferrin) in these FR samples, which is consistent with the abundance of albumin relative to other large proteins in other studies[89,275,291] , but unclear if it would be less without the use of a SL. The presence of high levels of albumin are often indicative of increased vascular permeability[292], which could be triggered by the landing of the SL on the spongy conjunctiva. In future studies the albumin could be compared to normal tear levels of albumin to assess if the vascular permeability is greater in the vessels contained within the FR. Again, these high levels of albumin were not specific to MDF, but rather a finding across all FR samples.

Using MS, it can be difficult to observe smaller, less abundant proteins without significant pre-

processing and specific protocols to remove the signals from the larger more abundant proteins. While these smaller proteins (i.e., cytokines, proteases) were not detected in the samples here, their concentrations are important to know in the context of MDF and future studies are necessary to take a more focused look at small inflammatory proteins in MDF.

Conjunctival compression

This study reports conjunctival curvature as a measure of compression with SL. This is a unique approach that was used because we found it to be more accurate and comparable between scans when using the sMap instrument. A greater change in curvature indicates greater compression, so a greater amount of curvature change after SL removal would indicate a deeper or tighter compression of the lens against the ocular surface. The compression observed here resulted in an average of -0.1 mm curvature change, slightly greater superior and nasally than temporally and inferiorly (which showed the least compression). The amount of compression showed a negative correlation to MDF, indicating that SL that caused a more compressive change in conjunctival shape were less associated with MDF. This was the opposite of the expected outcome but could be related to a more compressive landing area reducing the opportunity for tear exchange. Since the main cause of MDF is believed to come from lipids secreted by the Meibomian glands, perhaps the relatively more compressive lens fit restricts the influx of additional lipids throughout SL wear.

The compression observed in this study is relatively consistent with other studies which have used different technologies, although others have reported compression as µm of SAG (elevation) rather than curvature change. Curvature is used in this study Using OCT, Alonso-Caneiro et al. measured linear tissue compression following a short period of rotationally spherical SL wear and found an average tissue compression of 24 µm, greatest superiorly (50 µm) compared to inferior, nasal and temporal regions (13-20 µm)[38]. Three hours after lens removal the tissue compression

recovered by 50%, slower than observed in this study. The faster rebound measured here could be due to the use of toric lenses when indicated here, which may cause slightly less compression due to better alignment. Additionally, the measurement of anterior conjunctival curvature (measured here) could return to baseline prior to complete decompression (measured directly with OCT), which would be detectable on OCT and not the sMap. Future comparisons of OCT and scleral topography will better enlighten the ways that the data can be compared between studies.

Another study by Consejo et al. reported compression in µm using the only other type of commercially available anterior segment profilometer, the Eye Surface Profiler (ESP, Netherlands). They used the elevation measurement and determined a mean compression of 122 µm after 5 hours of SL wear (greatest superiorly) with only 23% recovery 3 hours after lens removal[252]. Macedo-de-Araujo et al. also used the ESP and reported the greatest compression nasally (103 µm) compared to temporally (84 µm)[243]; similarly, Courey et al.[293] examined the variation along the horizontal meridian using OCT and observed slightly more compression nasally than temporally for an 18 mm diameter SL (by ~20 µm). The differences in these studies are expected, due to variations in the types of SL used and the instrumentation used, none of which have been thoroughly compared. However, these studies all agree that conjunctival compression occurs variably and is typically greatest in the nasal and superior quadrants, which may be expected given the asymmetry of the surface[249].

Clinical implications of findings

The tear lipid findings have several implications of clinical significance. The Meibomian glands produce most of the lipids in the tears and the quality and quantity of this meibum can significantly affect tear film quality and cause dry eye[102]. For example, tear lipids are often irregular in patients with ocular surface disease, including dry eye[102,294,295] and specifically in Meibomian gland

dysfunction (MGD)[103,279,296,297]. Anecdotally, clinicians have linked the occurrence of MDF to patients with dry eye and MGD, and interestingly several studies have found specific increases and alterations in WE and CE lipids in patients with MGD[104,279,296]. This association would seem to suggest that patient with MGD may have a lipid profile that is most susceptible to developing MDF. It would be expected that the most common hydrophobic (nonpolar) lipids in the tear fluid would all be relatively increased in MDF, and if patients with MGD have a tendency toward having more nonpolar components such as WE and CE, they may experience MDF. It should also be noted that although the lipids that were observed in greater abundance in MDF were nonpolar, not all of the abundant nonpolar lipids were seen with greater abundance in MDF. For example, TAGs, which are nonpolar and were highly abundant in all FR samples, did not show an increase in MDF. However, TAGs are typically found in relatively low abundance in meibum[277] and may be originating from ocular surface cells. The lack of differences found in TAGs and the presence of differences in CE and WE in MDF provides additional support that this phenomenon is related to the composition of the meibum specifically.

Currently there are no evidence-based guidelines for managing MDF, although practitioners will often make several lens modifications to minimize MDF, including reducing corneal clearance, changing the shape of the LZR, changing the transition curves overlying the limbus, or modifying diameter. Based on this study and the current understanding of MDF, we recommend that the LZR of the lens be fit with alignment, and not changed based on MDF findings. Even with the significant correlation to a less compressed conjunctiva observed here, we do not recommend tightening a SL in MDF because of the other negative effects this may have on the conjunctiva. Further, it still isn't clear exactly how the pattern of conjunctival compression is related to MDF, so recommendations of what type of compression pattern to aim for are still not available. However, since the SL fit may clearly have some contribution to MDF severity, we do recommend that all lenses are fitted with a tight enough fit to avoid excessive movement, which is an obvious

indication of a loose-fitting lens. Although this study did not find an association with FR depth and MDF, it was not designed to test this and so may not have had great enough differences in FR depth to show a difference. Other studies have found increasing FR depth to be risk factor for MDF[135], and therefore we recommend this as a logical step to reduce symptoms MDF patients, as it reduces the overall thickness of the FR and therefore will decrease the total amount of FR turbidity.

Furthermore, the nonpolarity of the lipids detected in the MDF may provide support for the use of a filling solution that is more lipophilic to reduce MDF, although no specific solutions were tested here. Future studies may consider evaluating the use of preservative free formulations (i.e., artificial tears) that have nonpolar components. The inflammatory consequences of the lipid increases are unknown but there is no obvious functional characteristic of these lipids that indicate that are inflammatory in nature. However, further investigations into the proteins detected in the FR may provide a better understanding of the inflammatory environment in the FR and in MDF. While the results here do not alone allow conclusions to be drawn about the level of inflammation in the FR, the differences in select proteins (immunoglobulins) suggest that there are differences in the level of inflammation with increasing severity of MDF. These findings may indicate that there is in fact more inflammatory activity in MDF that is causing the degradation of immunoglobulins, although this will need to be confirmed with future studies into these proteins.

Limitations and future directions

There are some limitations to be noted in this study. First, this study assumes that a greater change in curvature is associated with a tighter lens of a deeper compression of the tissue. This is a reasonable assumption but should be tested in future studies that also evaluate compression using other methods (e.g., OCT). Second, the protein analysis was global but as performed was unable to detect smaller proteins such as cytokines and proteases. Future studies may consider

customized MS to detect the large as well as smaller proteins or using MS for large proteins and customized assays to detect smaller proteins of interest. However, both strategies would require larger volumes of sample to allow for broader testing. One of the greatest limitations in these studies and all other tear fluid studies is the volume of fluid available for analysis. Here we had sufficient volumes to avoid the need to pool inter-subject samples, but still pooled samples within eyes to reach necessary volumes to complete the testing.

This study showed that certain classes of lipids (i.e., WE) showed clear increases in MDF. When looking at each species of lipids, there were also select species from other classes and categories that were correlated. However, one should be careful about assessing each species and making strong conclusions from a single study. Lipids are commonly difficult to study and can be contaminated by the storage and process; further, they can break down during the processing and may be altered within classes to similar species. Therefore, it is more reliable to discuss large classes or groups of lipids to make conclusions about the data. Future studies that repeat these findings may better elucidate other lipid species that may be specific to MDF.

Support: NIH Grant P30 EY007551, NIH Grant S10 OD021758-01A1

Acknowledgement: The authors would like to acknowledge Visionary Optics, who supplied the SL used for this study.

Chapter 4. Intraocular pressure and optic nerve head morphology during scleral lens wear

Published September 2020 in Optometry Vision Science

Maria K Walker OD, MS, FAAO
Laura P Pardon OD, MS FAAO
Rachel Redfern OD, PhD, FAAO
Nimesh Patel OD, PhD, FAAO

Introduction

Scleral lens (SL) use has become increasingly widespread to correct vision and provide ocular surface protection for diseased eyes, with the benefits well-established by the visual quality and comfort they provide[17,48,60–62]. While examples of visual success are acclaimed with SL wear, and the capacity to rehabilitate the ocular surface is proven[67,71–73], alongside these successes are accounts of adverse events and an increasing concern for potential side effects[31,40,74–77,245]. Accordingly, there is an increasing interest in the effects of these custom devices on the ocular surface and adnexa[20,78]. With evidence of adverse effects, and considering the diseased eyes for which they are indicated[14,49,61,79–83], it is imperative to understand both the positive and negative ocular health impacts of the SL.

The SL fit is unique, vaulting over the cornea and landing on the conjunctival tissue adjacent to the limbus. The position of the lens on the eye is driven by a sub-atmospheric pressure beneath the lens[181,182], which forces the SL against the conjunctiva and causes compression as great as about 50 μm[38]. Beneath the conjunctiva lie the episcleral veins, and beneath that the trabecular meshwork, canals, ducts and channels of the aqueous humor outflow pathway. A disruption of aqueous dynamics could have an effect on intraocular pressure (IOP), a major risk factor for glaucoma. The landing of SLs over these important structures has given rise to concern that the SL can create resistance to aqueous humor outflow and lead to increased IOP[182,183]. Furthermore, greater amounts of SL settling would in theory lead to greater suction force that could exacerbate an increase in IOP[182].

Measuring IOP during SL wear presents a challenge since most clinical methods of measurement make direct contact with the cornea, which is covered by the SL. To manage this challenge, investigators have measured IOP using several different techniques: (1) by measuring the pressure over the cornea immediately after lens removal[298–301], (2) by using a corneal-calibrated device against the conjunctival tissue[298], and (3) by using a transpalpebral tonometer that

measures IOP through the eyelids[302]. The first modern study, conducted by Nau et al., used both the first and second technique with a pneumotonometer, calibrated for customary use against the cornea[298]. IOP was measured over the cornea before and after two hours of SL wear, and no difference was found before, during or after SL wear with either technique. A small pilot study by Vincent et al. found no significant increase in IOP after 3 or 8 hours of lens wear using the Ocular Response Analyzer (ORA, Reichert, Buffalo, New York) and a non-contact tonometer (TX-20P, Canon, Amstelveen, The Netherlands), respectively[300]. Another more recent study by Aitsebaomo et al. used iCare (iCare Finland Oy, Vantaa, Finland) immediately after lens removal[299], and a study by Michaud et al. used a transpalpebral tonometer (Diaton, DevelopAll Inc.) just prior to lens removal[302]. Shahnazi et al. measured IOP after lens removal in patients with ocular surface disease using a tonopen[301]. Each of these studies has variation in type of SLs worn, sample size, hours of lens wear, and technique used to measure IOP, which creates a challenge when comparing results from one study to the next.

The optic nerve head (ONH) is a relatively weak point in the otherwise rigid corneoscleral shell and, as a result, is particularly susceptible to the effects of IOP[303]. Accordingly, in response to acute IOP elevation with ophthalmodynamometry, changes in ONH structure (e.g., prelaminar tissue, neuroretinal rim thickness) can be detected[304–307]. Minimum rim width (MRW), quantified using optical coherence tomography, is a robust measure of the neuroretinal rim that has demonstrated excellent repeatability[185–187,308] and is sensitive for detecting subtle changes in optic nerve head structure caused by IOP increase. Changes in IOP can result in thinning of the MRW in as little as 5 minutes after IOP increase in primate models, although it takes approximately 2 hours to see the maximum change[309]. Although not typically measured during relatively minimal (<10 mmHg) changes in IOP, the dose dependent nature of MRW thinning is suggestive the MRW will show changes due to IOP changes of approximately 5 mmHg or greater. In this study, changes in the MRW are measured to indirectly assess fluctuations in IOP during SL wear.

The goals of the present study were to (1) assess changes in MRW over six hours of SL wear in order to indirectly determine whether SL wear influences IOP and (2) compare two techniques (Diaton and iCare) for measuring IOP during SL wear and determine their relationship to the MRW findings.

Methods

This study was done in compliance with the tenets of the Declaration of Helsinki and was approved by the Institutional Review Board at the University of Houston College of Optometry. A total of 27 healthy SL neophytes were recruited (26 completed), and all subjects signed an informed consent prior to enrollment. Sample size was determined for ANOVA, using a moderate effect size of f (0.3) with $\alpha = 0.05$ and power of 0.8. Potential subjects were excluded if they had a personal history of ocular hypertension or glaucoma, if their IOP measured greater than 20 mmHg in either eye on the day of enrollment, or if they had a history of ocular surgery (including refractive surgery such as LASIK) that could affect IOP readings.

The first study visits determined eligibility and selected the lens to be used on the experimental day. IOP was measured using iCare (Finland Oy, Vantaa, Finland) rebound tonometry. A SL fitting set (Zenlens RC for regular corneas, Alden Optical, Rochester, NY) was used to fit one randomly selected eye with a 15.4 mm diagnostic SL. Lenses were selected to vault the cornea by approximately 250 µm and provide clearance over the limbus, landing without obvious compression of the conjunctival blood vessels. All transition zone radii and landing zone radii had spherical curvatures for this study.

On the day of the experiment, subjects arrived at 7:30 am. Biomicroscopy and visual acuity were evaluated to confirm normal ocular health. After initial baseline testing, a SL was applied to the test eye at approximately 8:30 am and worn for a total of six hours. Measurements were taken at baseline (before and after SL application), after two and six hours of SL wear, and again

immediately after lens removal. The two principal data collected were IOP and optical coherence tomography derived MRW (primary outcome); additionally, anterior chamber depth and corneal thickness were measured (Lenstar LS900, Haag-Streit, Koeniz, Switzerland), as well as SL fluid reservoir depth (Spectralis OCT2, Heidelberg Engineering, Heidelberg, Germany).

Intraocular pressure measurements

During the experimental visit, IOP was measured with the iCare rebound tonometer and the Diaton transpalpebral tonometer. The iCare, which requires contact with the cornea, was used only before and after SL wear on the test eyes (control eyes were measured at each timepoint) and was measured within five seconds of SL removal when applicable. Measurements were repeated three times at each session and averaged for the final values. The Diaton was used on both eyes at all timepoints, while subjects laid in a supine position and were instructed to look at a target approximately 45 degrees down toward their feet. The instrument probe was placed 1-2 mm posterior to the eyelash margin on the outer eyelid, just above where the SL edge would land. Each instrument output represented a series of measurements analyzed and averaged by the instrument, and two measurements were obtained and averaged for each timepoint. The agreement of the two instruments was compared using a total of 100 matched measurements taken on the same eyes.

Minimum rim width measurement

Optical coherence tomography (Spectralis OCT2, Heidelberg Engineering, Heidelberg, Germany) was used to measure the change in MRW over six hours of SL wear. Global MRW was measured in both eyes at baseline (pre- and post-lens application for test eyes), at the two-hour and six-hour time points, and again in the test eye after SL removal. The Spectralis OCT system used for this study has a theoretical resolution of 7 µm. However, this axial resolution is for a single A-scan, and thickness measures are an average of several A-scans. Hence, with rigorous manual

segmentation, it is possible to detect changes smaller than the theoretical axial resolution. MRW has demonstrated excellent repeatability with a within-subject standard deviation between approximately 1-2 µm[310,311].

To quantify MRW, defined as the minimum distance from Bruch's Membrane opening (BMO) to the internal limiting membrane, a 24-line (15-degree) radial scan centered on the optic nerve head was acquired, and BMO and the inner limiting membrane were automatically identified (Glaucoma Module Premium Edition, version 6.0, Heidelberg Engineering, Heidelberg, Germany) (Figure *4.1*). The software will occasionally fail to correctly locate BMO, which can then be manually re-selected for the software to calculate MRW. Each scan was carefully inspected during this manual segmentation process and adjusted as needed by a single investigator (MKW), then verified by a second investigator (NP). Manual correction of automated segmentation is an essential step in analysis to ensure accurate BMO detection; however, pre- and post- segmentation correction values for global MRW still have excellent agreement as shown in other studies[187,311]. In order to minimize magnification effects with SL wear, all scans subsequent to the initial pre-lens baseline were obtained using the AutoRescan feature.

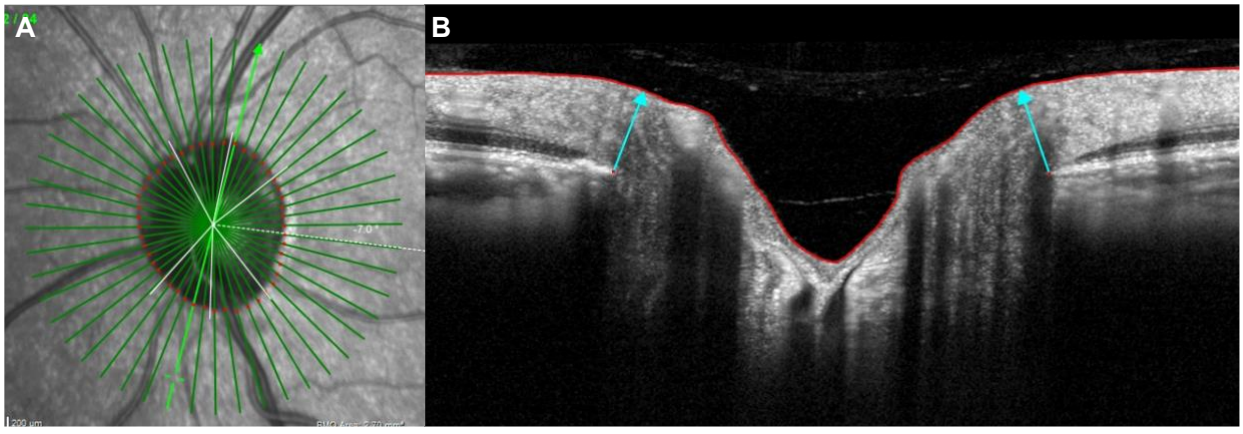

Figure 4.1. Acquisition of radial scans at the optic nerve head to measure minimum rim width. At each imaging session, test and control eyes underwent a 24-line radial scan of the optic nerve head. A fundus image shows the placement of the scan lines (A). Each of the 24 scan lines is an optical coherence tomography section at the nerve (B), shown with the MRW detection arrows in blue. The detection arrows can be manually adjusted as needed[187], and the program software automatically measures the length of the arrows for each scan. The global (average of all scans) MRW value was used for this study.

Statistical analysis

Normality of the data was tested using the D'Agostino-Pearson normality test. Mean IOP and MRW were compared between eyes before, during, and after SL wear, using repeated-measures ANOVA, paired t-test, and the non-parametric equivalents when appropriate. Linear regression and Pearson's correlation analyses were done to determine if there were associations between change in MRW, change in IOP, and change in the fluid reservoir depth. To compare these variables of different scales, values were normalized by calculating them as their percent change from baseline.

To assess the performance of the iCare and Diaton, a total of 100 IOP measurements taken on the same eyes with both instruments were compared using Bland-Altman analysis, linear regression, and Pearson's correlation coefficient. Additionally, repeatability was calculated for each instrument. All statistical analysis was completed using GraphPad Prism 7 (GraphPad Software, Inc, La Jolla, CA).

Results

A total of 26 adults (81% female) between the ages of 23 and 33 years with normal ocular health and no history of SL wear were included in this study. Mean central fluid reservoir depth was 221 µm (95% CI: 192 – 251 µm) at initial application and 148 µm (95% CI: 121 – 175 µm) after six hours of lens wear, settling an average of 73 µm (95% CI: 56 – 91 µm). Prior to SL application, mean central corneal thickness in test eyes was 540 µm (95% CI: 520 – 559 µm) and in the control eyes was 535 µm (95% CI: 513 – 557 µm), showing no difference between the eyes (P = 0.18). After 6 hours of SL wear, and measured within 5 minutes of lens removal, mean corneal thickness in test eyes was 537 µm (95% CI: 517 – 557 µm), and in control eyes was 523 µm (95% CI: 501 – 544 µm), significantly greater in the test eyes (P = 0.0001) but reduced from baseline in both eyes. Anterior chamber depth remained unchanged in test and control eyes throughout the

experimental visit: baseline: 3.133 mm (95% CI: 2.900 – 3.366 mm) in test eyes; 3.039 mm (95% CI: 2.937 – 3.141 mm) in control eyes (P = 0.50). Post-lens removal: 3.062 mm (95% CI: 2.953 – 3.172 mm) in test eyes; 3.010 mm (95% CI: 2.905 – 3.115 mm) in control eyes (P = 0.24).

Intraocular pressure

Mean IOP (iCare) on the morning of the experimental visit was 14 mmHg (95% CI: 12 – 15 mmHg) in both the test and control eyes. At the two-hour, six-hour, and post-lens timepoints, average IOP in the control eyes was 13 mmHg (95% CI at six-hours: 12 – 14 mmHg), showing no significant change after six hours (P = 0.19). Mean IOP in the test eyes, only measured again after SL removal, was 16 mmHg (95% CI: 14 – 18 mmHg), showing a +2 mmHg (95% CI: +1 to +3 mmHg) increase in IOP from baseline (P = .002) (Figure *4.2*).

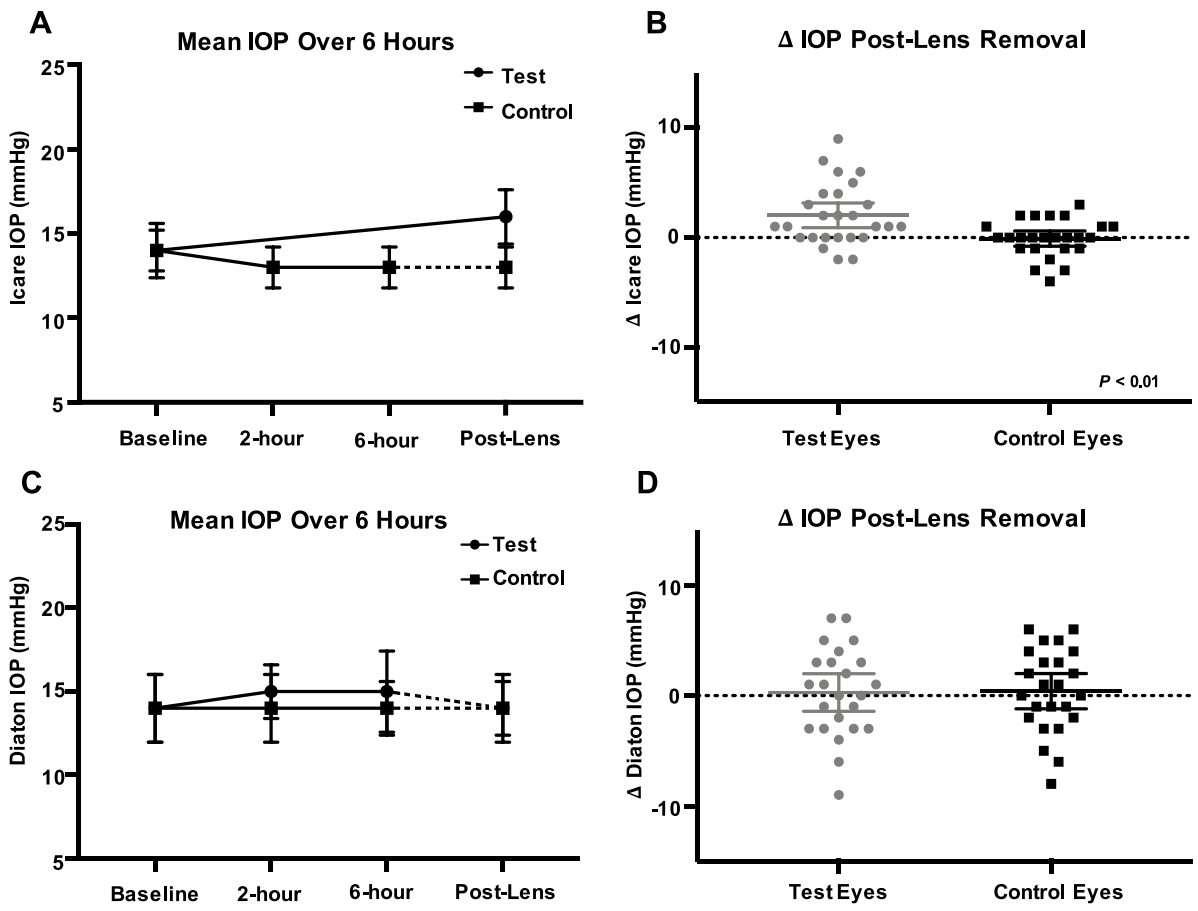

Figure 4.2. Mean intraocular pressure and changes during six hours of scleral lens wear, measured using iCare and Diaton. The mean IOP of the test and control eyes are plotted as the mean with 95% CI at each time point for the iCare (A) and Diaton (C), The change in IOP (**Δ** IOP) from baseline is shown for the iCare (B) and the Diaton (D) measured after SL removal for test and control eyes. Positive values indicate pressure increased from baseline. A dotted line indicates minimal time passed between measurements. IOP measured with iCare was significantly increased in the test eye after six hours of SL wear (P = 0.02). IOP: intraocular pressure.

IOP measured with the Diaton was 14 mmHg (95% CI: 12 – 16 mmHg) in both the test and the control eyes prior to SL application. After six hours of SL wear (pre-removal), it was 15 mmHg (95% CI: 13 – 18 mmHg) in the test eyes and 14 mmHg (95% CI: 12 – 16 mmHg) in the control eyes, not significantly different from each other (*P* = .35) or from their respective baseline measurements (*P* = .11 for test eyes; *P* = .71 for control eyes). After SL removal, the mean test eye measurement returned to 14 mmHg (95% CI: 12 to 16 mmHg). The mean IOP change with

Diaton was +0.3 mmHg (95% CI: -0.9 to +3.2 mmHg) in the test eyes, and +0.4 mmHg (95% CI: -0.8 to +1.7 mmHg) in the control eyes, showing no difference between the two eyes (*P* = .90).

A comparison of means between the iCare and Diaton for 100 IOP measurements showed no significant difference (Diaton: 15 mmHg (95% CI: 13 – 15 mmHg); iCare: 14 mmHg (95% CI: 14 – 15 mmHg); *P* = .35). The within-subject standard deviation was calculated (square root of the variance), then multiplied by 2.77 to determine repeatability.[264] For the Diaton, the repeatability was 8 mmHg, versus the iCare which had a repeatability of 2 mmHg. The instruments were also compared using Bland-Altman analysis which showed poor agreement and correlation of the instruments (regression slope = 0.22; R^2 = 0.03; Y-Intercept = 10.00; P = .07) (Figure *4.3*).

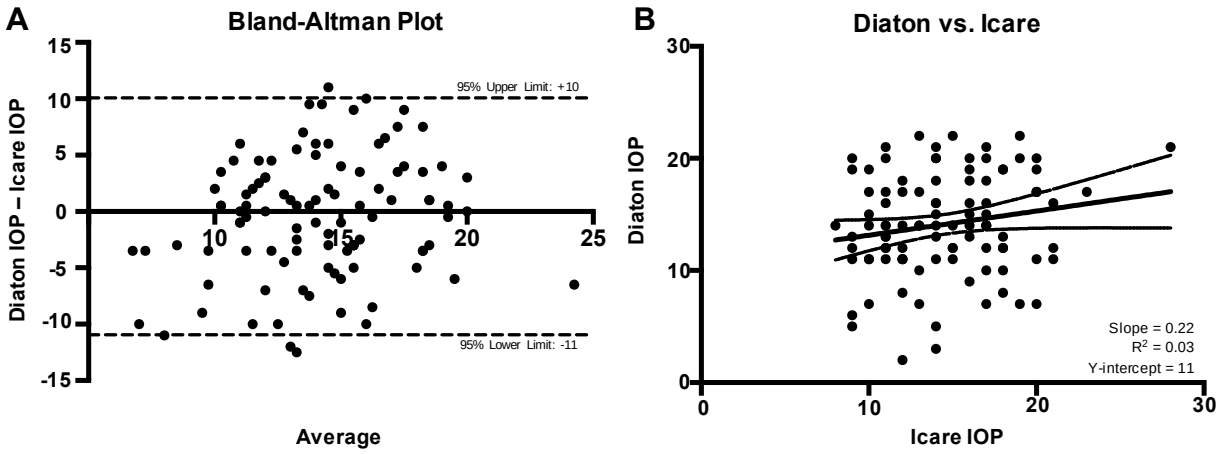

Figure 4.3. Bland-Altman and correlation plots between Diaton and iCare. A total of 100 measurements were used for the comparison, all taken with the iCare and Diaton on eyes that were not wearing SLs, were compared. The Bland-Altman plot (A) indicates a poor agreement between the Diaton and iCare. Each measurement was plotted against each other in the linear regression plot (B), which has a shallow slope that also shows poor agreement between the instruments. The 95% limits of agreement for each plot are shown by the dashed lines.

Minimum Rim Width

The mean MRW at baseline, measured between 8 am and 9 am, was 351 µm (95% CI: 330 – 372 µm) in test eyes and 344 µm (95% CI: 323 – 365 µm) in control eyes. Intrasubject values were highly correlated to each other at baseline (R^2 = 0.76; P < .001). After six hours and prior to

SL removal, MRW was 343 µm (95% CI: 323 – 363 µm) in test eyes and 338 µm (95% CI: 318 – 358 µm) in control eyes. This was a significant amount of MRW change from baseline in both the test (-8 µm; 95% CI: -11 to -6 µm) and the control eyes (-6 µm; 95% CI: -9 to -3 µm) (P < .01) (Figure 4.4). The difference in MRW change between eyes, calculated by subtracting the control eye thinning from the test eye thinning for each subject, was on average -2 µm (95% CI: -5 to 0 µm), indicating a slightly greater amount of thinning in the test eyes; however, this difference was not statistically significant (P = .09). After SL removal, MRW was repeated in test eyes and did not change significantly from the pre-SL removal measurements taken at six hours (P = .88).

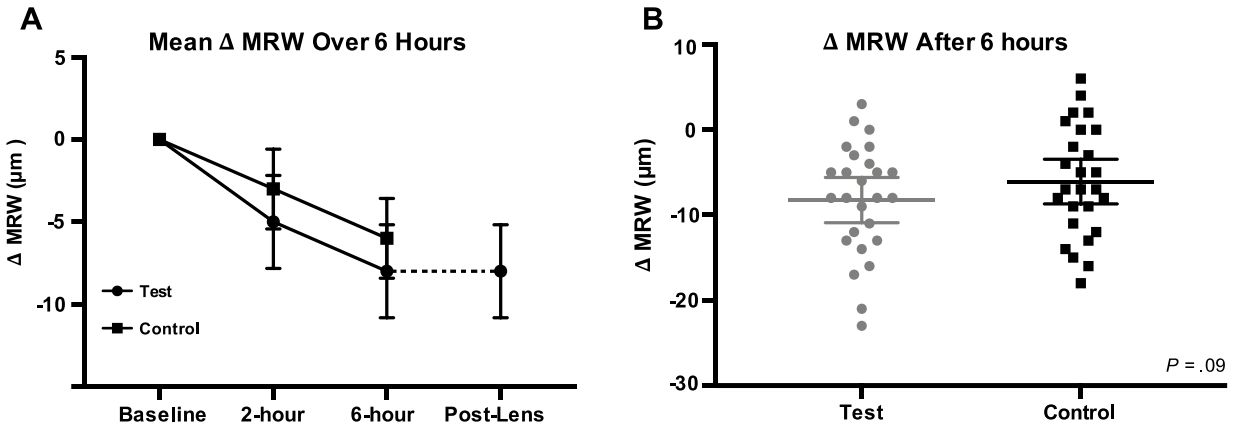

Figure 4.4. Mean minimum rim width changes. The MRW was measured over six hours of SL wear, measured with optical coherence tomography. Subjects wore a lens on one randomly selected eye for six hours and the fellow eye acted as the control. Mean change in minimum rim width from baseline (**Δ** MRW) is plotted as the mean with 95% CI at each time point (A) for the test and control eyes (a dotted line for test group plot indicates minimal time passed between measurements). The total change from baseline at six hours (before SL removal) is also shown (B) as a scatterplot of each test and control eye with whiskers showing the 95% CI for each group. Negative values indicate thinning of the MRW. MRW in the test eyes shows a slightly greater amount of thinning, although not representative of a significant difference (P = .09). MRW: minimum rim width.

There was individual variation observed in this data. While on average there was not a significant difference in the MRW with SL wear, 8 test eyes (31%) and 7 control eyes (27%) had greater than 10 µm of MRW thinning over the six-hour period. Most of the subjects with high amounts of thinning showed relatively symmetrical thinning between the eyes, although there was a trend of approximately 3 to 5 µm greater thinning in test eyes for several subjects (n = 10). Only two eyes,

both test eyes, showed greater than 20 µm thinning during the test period, but both fellow control eyes also showed higher than average amounts of thinning.

Linear regression and correlation analyses were done to evaluate associations between changes in MRW, IOP, and fluid reservoir depth. Change in MRW was not correlated with change in IOP (regression slope = 0.01; R^2 = 0.02; Y-Intercept = -0.02; *P* = .50) or change in fluid reservoir depth (regression slope = 0.002; R^2 = 0.0005; Y-Intercept = -0.02; *P* = .91). Additionally, there was no correlation between change in IOP (measured with iCare after lens removal) and change in fluid reservoir depth (regression slope = 0.31; R^2 = 0.11; Y-Intercept = 0.3; *P* = .10).

Discussion

In this study the effect of SL wear on the optic nerve head MRW and IOP were evaluated. Although there was a trend for increased thinning of the MRW in test eyes, the change for the six hours of SL wear was not statistically significant for these healthy eyes. However, there was a trend of greater thinning in the eyes wearing SLs that suggests certain individuals may be experiencing changes to the ONH structure due to an increase in IOP. Individuals in this study with the greatest magnitude of MRW thinning of the test or control eye were of greatest interest, as in theory they would be more likely to be sensitive to changes in IOP. However, in these individuals, the magnitude of MRW thinning was similar between the eyes.

Minimum rim width

Almost all eyes showed MRW thinning, regardless of SL wear. The normal eye exhibits diurnal changes in MRW throughout the day, on average showing approximately 8 µm of thinning between 7am and 7pm in young, healthy individuals without contact lens wear. However, there is considerable individual variability over a 12-hour period (range -31 to +1 µm)[310]. Therefore, this study used a control eye from the same individual to help reduce the effect of inter-subject variability. Ultimately, a normal eye appears to be quite capable of wearing a fitted SL and

maintaining a balance in IOP within limits that does not create significant mechanical stress at the ONH.

It is not surprising that we do not see a significant difference in MRW thinning between eyes, because normal individuals are quite capable of managing long-term IOP stress. The natural homeostasis of IOP is constantly tested by forces such as fluid intake, medications, body orientation, alcohol consumption, respiration, heart rate, exercise, and diurnal rhythms[158]. In response, the trabecular meshwork is capable of sensing a transient increase in outflow resistance and will respond by increasing pulsatile flow or reducing upstream resistance to avoid prolonged IOP increases that can create stress at the ONH[164,172,174,312]. However, glaucomatous eyes are often unable to self-regulate these stresses on IOP[171,174,313], therefore it is essential that these experiments be repeated in that population. Furthermore, individuals with collagen diseases such as keratoconus, a population with a high incidence of SL wear, may show a different response than seen with the normal eye[314].

Intraocular pressure

IOP was measured using two different methods. The Diaton, able to measure IOP as indicated during SL wear, seemed desirable to use but exhibited questionable reliability. This was in agreement with other studies that showed poor comparability to the gold standard Goldmann applanation tonometry[315–318]. The iCare, a validated instrument that is reasonably comparable to Goldmann applanation tonometry[319–321] was in part used here to offer potential validation of the Diaton. Our assessment of the instruments showed a large variability of the Diaton, which had a repeatability of 8 mmHg. Conversely, the iCare showed a better repeatability of 2 mmHg. There was also poor correlation between the iCare and the Diaton, suggesting poor accuracy of the Diaton, a conclusion that is in agreement with other studies[315–317]. We propose that the inconsistencies of the Diaton are in part due to variation in eyelid morphology between subjects,

such as eyelid thickness, elasticity, and other mechanical tissue properties. The Diaton data in this study also did not agree with the study by Michaud et al., which showed an approximately 5 mmHg increase after several hours of lens wear[302] Ultimately, the Diaton cannot be considered an accurate and reliable instrument for IOP assessment during SL wear.

After removal of the SLs, the Icare IOP was significantly greater in test eyes than control eyes. This is in relative agreement with the Aitsebaomo study, which also used iCare, although they saw an average increase about three times greater[299] However, the iCare data here does not agree with several studies that have used different methods of measuring IOP. Nau et al. found no increase using corneal pneumotonometry after two hours of SL wear[298] Vincent et al. saw a slight reduction after several hours of lens wear when measuring with an ocular response analyzer and a non-contact tonometer[300] and Shahnazi et al. also observed a slight decrease when measuring with tonopen in ocular surface disease patients[301]. The discrepancies in the studies may be due to the instruments used, the duration of SL wear (which was 2, 3-8, and 1-8 hours, respectively for the studies mentioned) or differences in the exact protocol for measuring IOP after SL removal (i.e., how long after removal was IOP measured?). If an increase in IOP is true, either due to SL wear or from the process of removing the lens itself, McMonnies et al. would predict that at removal the IOP would almost instantly return to baseline[182,322]. This study measured IOP within 5 seconds of SL removal, so may have still been able to capture an increase during SL wear, although this is ultimately unknown. The remaining questions are whether the increased Icare measurements are true, and if so, are they caused by prolonged IOP increase during SL wear, or caused by the process of lens removal itself?

Limitations of study

This study, while novel in technique, had several limitations that should be considered when designing similar studies. This study was short-term and in normal subjects; long-term studies in

diseased eyes may show different results, and this type of study should be repeated in individuals with glaucoma and keratoconus specifically. Another limitation is that normal diurnal changes in minimum rim with were not evaluated in test eyes in the absence of a SL. However, test eyes would be expected to follow a similar diurnal pattern to control eyes for a given individual, especially given the high correlation of MRW between eyes at baseline. Additionally, the duration of IOP increase measured with iCare after lens removal was not determined, and future studies should measure IOP for several minutes or longer after lens removal. Future studies may also benefit from careful biomicroscopic assessment of the anterior segment aqueous and episcleral veins beneath the SL landing zone, which can sometimes be observed for pulsatile blood flow patterns[172,312]. Lastly, a direct and accurate measure of IOP was still not obtained during SL wear, although we are not aware of an instrument that can safely accomplish this task.

Conclusions

This is the first study to our knowledge that evaluates the sensitive ONH tissue as an indirect measure of IOP during SL wear. This study suggests that SLs have a relatively small effect on IOP in the normal eye, and that any impacts of pressure fluctuation on the optic nerve are likely not significant for young, healthy eyes. This conclusion is supported by the insignificant difference in ONH MRW change in SL wearing eyes. The long-term effects of scleral lenses on IOP and ONH structure, especially in susceptible eyes, should be investigated.

Support: NIH Grant P30 EY007551, University of Houston GEAR grant

Acknowledgement: The authors would like to acknowledge Bausch & Lomb Specialty Vision Products, whose diagnostic fitting set was used for this study.

Chapter 5. Discussion

Summary

The studies completed in this dissertation represent an expansion of our understanding of how a SL affects the eye. We have shown that the FR is indeed altered in composition of immunomodulatory molecules compared to ocular surface tears, and have developed methods to image, quantify, and evaluate the composition of the FR. This work has determined the lipid profile in the FR was disrupted in subjects with MDF, whereas many proteins do not appear to be significantly altered. In addition to the progress in FR research we have made, we have also established a protocol for evaluating the downstream effects of the SL LZR on the sensitive ONH. By measuring the ONH during SL wear, we found enough variability and a trend toward ONH changes in the normal population to SL, which strongly suggests a need to evaluate this in the diseased (i.e., glaucoma, keratoconus) population.

In Chapter 2 the composition of the FR beneath the SL was evaluated. Measuring selected immunomodulatory molecules including interleukins (IL-4 and IL-8) and proteases (MMP-7, -9, and -10), we showed the FR composition is distinct from the ocular surface tears after several hours of SL wear. Given ocular surface cells readily produce cytokines and MMPs, these molecules could be secreted by corneal epithelial cells (and potentially conjunctival epithelial cells) and the SL could trap them within the FR. In Chapter 3, we took a deeper exploration into the lipid and larger protein components within the FR, comparing them between subjects with and without MDF using MS analysis. Additionally, we measured the amount of global conjunctival compression with SL and compared that to the composition of the FR to determine if conjunctival compression is associated with MDF. We found a moderately negative correlation between conjunctival compression and the occurrence of MDF, and identified select hydrophobic lipids (i.e., WE) that appear to be primary components of the turbid FR observed in MDF. In Chapter 4, the implications of the peripheral fit of a SL were further evaluated to explore downstream effects of the pressure exerted by the LZR of the SL. Specifically, we aimed to determine if the SL

increases IOP and deforms the pressure-sensitive tissue at the ONH. We showed no significant changes in MRW and found post-removal IOP increases of an average 2 mmHg after SL wear, indicating a need for further exploration with normal and diseased eyes.

Overall, these studies established novel protocols for testing important outcomes with SL, defining and exploring physiologic and mechanical effects of SL on the eye. This work is a step toward improving the understanding of the physiologic effects of the eye and raises additional questions about these same effects in a diseased population. Future studies will expand the evaluation of the tear and corneal inflammation present in SL wear and disease and will further evaluate implications of the SL LZR and its role in SL success.

Discussion of Chapter 2

The study completed in Chapter 2 supports the hypothesis that SL wear traps the normally refreshed tear film components in the FR leading to elevated levels of inflammatory mediators overlying the cornea and perilimbal conjunctiva. In testing this hypothesis, we investigated select inflammatory mediators in the FR during SL wear. Two interleukins were measured, IL-4 and IL-8, which both showed no change after several hours of SL wear. Of the proteases evaluated, MMP -9 and -10 showed significantly increased concentrations in the FR after 8 hours of SL wear, but MMP-7 did not.

Fluid reservoir collection and analysis

This study was the first to have collected the FR and compared it to ocular surface tears in SL wear, and this collection method shows great promise for future studies to examine the FR in diseased lens wearers. However, it can be technically challenging to collect usable samples of the natural and FR tears. In the FR tears, unlike collecting the natural tears, there is a finite volume and only one opportunity to collect during SL removal (i.e., it cannot be repeated until enough tears are captured). In some subjects, even when they have sufficient fluid under the SL, the FR

is not captured due to issues such as difficulty removing a SL, subject movement during collection, and simply removal too quick or at an angle that poorly facilitates FR capture. In order for a subjects' data to be included in the primary analysis, all 5 tear sample categories had to yield usable data (ocular surface tears at baseline and post SL wear on 2 separate days, as well as the FR on 2 separate days). A total of 10 out of the 15 subjects were eligible for cytokines/MMP comparison and no subjects qualified for TIMP assessment due to these volume constraints. However, this relatively small sample size was still large enough to detect the differences between samples that were most pronounced, such as MMP-10 data, which in post-hoc sample size calculations were at >80% power.

Baseline tears were collected in the morning of the first experimental day (prior to SL application) as a benchmark for each subject but were not used in the comparison or statistical analysis. We had also collected the ocular surface tears at one of the pre-SL visits, intending to use that as a no-SL control comparison, but there were not enough usable samples for the analysis. Therefore, the only usable pre-SL samples were those taken the morning prior to SL application, which could not reasonably be compared to the post-SL samples due to the timing and diurnal variations that would affect the comparison. As expected, the levels of pro-inflammatory cytokines in the ocular surface tears showed greater variability in the morning and were slightly greater than in the afternoon tears[96,323], although not significantly.

Many of the cytokines in the tear film are in the interleukin (IL) family, with master cytokines IL-1α and 1β being studied extensively in ocular surface disease[120,123,220,324–327]. IL-8 and IL-4 were measured because of their known associated with inflammation in contact lens wear[124,327–329]. While there was no significant change in either cytokine during SL wear in normal eyes, the variability in the data indicates that the study was not powered to detect a difference in these analytes, which were detected in low ranges with high variabilities. IL-8, which is involved in neutrophil recruitment and activation[328,330], was detected in low concentration or not at all in

several samples. IL-4, which was also not significantly greater in the FR but showed greater concentrations in the FR of select subjects, can be produced by corneal epithelial cells[331] and is most commonly associated with allergies and is a key regulator if IgE antibodies[331,332]. Although these findings were not significant, the increase in the FR that was observed with some subjects may indicate that some susceptible individuals may be producing these mediators and trapping them in the FR. The lack of a significant difference is related to the variability in the FR data. Given this variability, future studies aimed at monitoring FR cytokine levels would be well advised to consider using a larger sample size to increase statistical power. The subjects in this study were normal, and not expected to have excess production of IL-4 and IL-8. However, in subjects with diseases that may favor the production of these interleukins, this type of analysis should be repeated. This data also begs the exploration of additional cytokines in the interleukin family, since cytokines, proteases, and other inflammatory mediators in the tear fluid are dynamic and constantly interacting with each other, including via inhibitory pathways. However, in this study the primary objective was to look at MMPs, with a secondary goal of assessing a few cytokines, so the final mediators were selected based on accessibility of testing kits and given the limited volume of tears available (particularly with the ocular surface samples).

Proteases such as MMPs are among the most thoroughly studied in the tears and are variably present and often indicative of inflammation[271,333,334]. Their primary function is to break down extracellular matrix components, affecting tissue remodeling, cell migration, adhesion, and signaling[334,335]. MMP-9, the most ubiquitous MMP in the cornea, is elevated in inflammatory states such as during desiccating stress in dry eye disease[336,337], during recurrent corneal erosions[338], and in sub-inflammatory conditions such as keratoconus[339,340]. MMP-10, which showed the greatest increase in the FR, has not been extensively evaluated in the tears but is present in other tissues (i.e., lungs) during inflammation and tissue repair[341]. Its function is typically to facilitate wound healing and to dampen damaging inflammation; therefore, its increase is potentially a

positive one here that could mitigate the increase of other inflammatory components in the FR. In this study both MMP-9 and -10 showed significant increases in the FR when compared to the ocular surface tears. We propose two hypotheses for this: (1) the MMPs get trapped in the FR when the lens is applied and are slightly elevated on application due to it being in the morning; or (2) they are being produced by corneal epithelial cells during SL wear and then getting trapped in the FR (or both could be occurring). This could result in an upregulation of protease activity in the tears overlying the cornea in SL wear, or in the cornea itself, which could have potential negative sequelae, such as provocation of other inflammatory mediators, or breakdown of collagen and extracellular in the cornea. However, levels were highest after 1 day and reduced some after 4 days of wear, which may indicate an adaptive response that could be reduced as the eyes adapts to the SL over time. In addition, the physiologic significance of the increase in MMP-9 is difficult to assess since the TIMPs, which inhibit the activity of MMPs, were not able to be evaluated in these samples.

In order to fully understand the implication of increased MMP-9 and -10 in the FR it is important to measure the tissue inhibitors of MMP (TIMPs) activity in the fluid. MMP/TIMP ratios are calculated to understand the level of control of MMPs by their primary inhibitory regulators. While all TIMPs are capable of inhibiting MMP-9 and MMP-10, TIMP-1 and -2, respectively, are most commonly associated with inhibitory affinity. An increase in the MMP/TIMP ratio in the tears could be indicative of an increased inflammatory state[342]. In this study, TIMPs were only tested in selected samples when remaining volume after cytokines/MMPs analysis was available and so were not included in the initial analysis. In post-hoc analysis, however, the MMP/TIMP ratios were calculated for those samples that were available at each timepoint. The MMP-9 and -10 ratios with TIMP-1 and TIMP-2 ranged from 0.01 to 0.75 (Table 5.1). Mean T_b baseline ratios for MMP-9/TIMP-1 were 0.28 ± 0.16 and were 0.75 ± 0.44 and 0.41 ± 0.14 in the Tb and TFR after 8h, respectively. After 4d, the ratios were 0.06 ± 0.05 (T_b) and 0.37 ± 0.19 (T_{FR}). MMP-9/TIMP-2 were

similar. MMP-10 ratios were lower, ranging from 0.01 to 0.11 and 0.02 to 0.13 with TIMP-1 and TIMP-2, respectively. In general, TIMP/MMP usually remained less than 0.5, which is not particularly indicative of an inflammatory state; however, in the basal tears post-SL wear on Day 1 those ratios were higher. While the limited available data does not allow for any conclusive interpretation, larger studies including more subjects and simultaneous quantification of MMPs and TIMPs are needed to draw conclusions about TIMP regulation of MMPs during SL wear.

Table 5.1. MMP/TIMP ratios calculated for select subjects

Ratio	Baseline	8h post-SL wear		4d post-SL wear	
	T_b	T_b	T_{FR}	T_b	T_{FR}
	n=9	n = 12	n = 6	n = 8	n = 10
MMP-9 / TIMP-1	0.28 ± 0.16	0.75 ± 0.44	0.41 ± 0.14	0.06 ± 0.05	0.37 ± 0.19
MMP-9 / TIMP-2	0.36 ± 0.20	0.60 ± 0.30	0.50 ± 0.25	0.05 ± 0.04	0.42 ± 0.18
MMP-10 / TIMP-1	0.05 ± 0.02	0.07 ± 0.04	0.11 ± 0.03	0.01 ± 0.00	0.09 ± 0.03
MMP-10 / TIMP-2	0.05 ± 0.03	0.13 ± 0.10	0.11 ± 0.04	0.02 ± 0.00	0.12 ± 0.04

MMP-9 and MMP-10 ratios with TIMPs 1 and 2 are shown. Shown as mean ± SE for each of the5 tear sample categories (T_b and T_{FR} after 8h and 4d).

Comparison with other studies

A handful of other studies have evaluated the tears on the ocular surface (Table 5.2), although only one other study has evaluated the FR itself. That study, which was completed by Postnikoff et al. in 2019, found an increase in leukocytes in the FR, identified as CD66b+ granulocytes[135], although they did not find a significant increase in the MDF group. In a different study, Carracedo et al. evaluated the ocular surface tears of SL wearers with keratoconus, measuring a significant increase in MMP-9 after SL wear[39]. These MMP results are difficult to compare to our study that looked at normal eyes which have different baseline levels of MMPs[327,339,340,343], but based on our findings we may expect that MMP-9 in the FR may have been even higher in that cohort than in

the ocular surface tears. Given the role that MMP-9 appears to play in a myriad of corneal diseases, future studies are indicated to measure the FR proteases in each population.

Table 5.2. Tear composition studies with scleral lenses

Reference	Population	Outcome(s) Tested	Outcome	Clinical relevance
Composition of the tears				
Walker [344] 2020	10 normal subjects	IL-4, -8 MMP-2, -7, -9, -10	↑ MMP -9, -10 in FR No change in IL-4, IL-8 No change in MMP-2, -7	Inflammatory tear proteins may accumulate in the FR during SL wear
Postnikoff[135] 2019	24 SL subjects (mixed conditions)	Leukocytes	↑ CD45+ leukocytes and neutrophils in MDF	Inflammation may be increased during MDF
Carracedo[39] 2016	26 Kc subjects (w/ and w/o ICRS)	MMP-9 Ap4A	↑ MMP-9 in non-ICRS ↓ Ap4A in ICRS	SL reduce dry eye signs; MMP-9 may represent tear stagnation
Winder[132] 1977	5 subjects	Calcium	No difference between SL, SCL, or non-CL wearers	No effect of SL on tear calcium
Optical Density of the fluid reservoir				
Turhan[345] 2019	13 Kc subjects	Optical density	Optical density ↑ ~1%	FR turbidity during SL wear affects low contrast VA
Schornack[276] 2018	25 normal subjects	Optical density	Optical density ↑ 2x	Scheimpflug imaging can quantifying FR turbidity
Carracedo[54] 2017	26 Kc subjects (w/ and w/o ICRS)	FR turbidity	FR turbidity ↑ 8x	The turbidity increase may represent tear stagnation

IL: interleukin; MMP: matrix metalloproteinase; SL: scleral lens; FR: fluid reservoir; MDF: midday fogging; ICRS: intracorneal ring segments; Ap4A: diadenosine tetraphosphate; SCL: soft contact lens

A summary of the studies exploring the tear fluid composition and optical density of the tears during SL wear.

Origin of FR components and effects on the ocular surface

We predict that the composition of the FR is likely to contain increased levels of proteins that are produced by corneal and perilimbal conjunctival epithelial cells, given that there is very limited tear exchange between the FR and the outer ocular surface tears. It is unknown what effect(s) the chronic increase in MMPs or other tear proteins could have on the cornea, or on the diseases that SL are used to treat. It may be detrimental, but it also must be considered that it could be beneficial to the corneal health. The production of certain proteins may be induced to maintain corneal health in the presence of stagnant FR with potential cornea exposure to irritants related to the SL (coatings, deposits, preservatives from cleaning solutions). In this study, SL were cleaned with ClearCare, which is a peroxide system that neutralizes to sterile saline during the disinfection process, to reduce contaminants on the SL that could affect the response. Furthermore, the application solution was saline without a preservative, although the solution does contain boric acid to balance the pH.

Limitations of study

There were some limitations in this novel study that should be addressed and mitigated in future studies. The primary limitation was a relatively small sample size, and due to the challenges in obtaining usable samples tear samples, it can be difficult to gain usable datasets for all subjects. A small sample size with studies evaluating inflammatory mediators in the tears can be limiting due to the inherently high variability of inflammatory mediators in the tear fluid. In this study, this factor may have affected the outcomes for the mediators. However, for the mediators that showed the greatest changes, such as MMP-10, the relatively small sample size was still enough to detect significant changes and post hoc sample testing indicated that the findings for MMP-9 and -10 were powered at >75%. However, in the case of IL-4 and -8 for example, there may truly be a difference between the FR and ocular surface, yet the small sample size could have failed to

detect a change in this cohort. The TIMP data cannot be assessed using the current data available from this study, and should be evaluated in future evaluations of MMPs in the FR.

Discussion of Chapter 3

Chapter 3 showed the results of a study that evaluated lipid and protein content in the FR, comparing the findings to the amount of conjunctival compression to determine in part if a “tight fit” was associated with MDF. The purpose of this study was to (1) determine the composition of the FR in MDF, and (2) determine if greater changes in conjunctival curvature (a measure of compression) are associated with MDF, as has been suggested. It was determined that among lipids and proteins in the FR during MDF, hydrophobic lipids show the strongest correlation to increasing MDF. When compared to changes in conjunctival curvature during SL wear, findings were inconclusive but suggest that MDF may be negatively associated greater changes in conjunctival curvature.

Quantifying MDF

There are essentially two ways to classify MDF in research. First, the data could be approached as a nominal category of discrete data, and MDF graded subjectively into categories like in Chapter 3. This categorical approach can be clinically useful but is limited due to the variability within each group. In this approach, masked images were categorized (subjectively) by the examiner into groups of none, trace, mild, moderate, and severe MDF. All patients with scores less than or equal to 2 were considered “no MDF” and those greater than 2 were “MDF”. Based on the challenge in subjectively discriminating between different MDF levels, this method is not recommended for future studies, and instead the quantitative (ImageJ) method of MDF scoring was superior. Despite the limitations of the subjective method, when the quantitative scores of the subjects who were deemed “MDF” and ‘”no MDF” were averaged, the mean MDF score in the

MDF group was 60 ± 23 and in the non-MDF group it was 16 ± 7, indicating that the objective and subjective grading methods were somewhat comparable.

As a new technique for quantifying MDF, which has not been done in any peer-reviewed studies, it is important to establish the repeatability and reproducibility of the method, as well as compare it to any other available methods. In this study the measurements were taken twice by two different masked investigators, compared within and between investigators. The quantification technique proved to be extremely repeatable within examiners and reproducible between examiners. It should be noted that the variability between Day 1 and 4 was greatest for subjects that experienced MDF. The average SD of measurements between Day 1 and 4 in the MDF group was 13.0 and it was only 3.1 in the non-MDF group. This makes some sense, because MDF severity can be variable from day to day, although it was not necessarily expected to be more variable in the subjects with MDF. This is notable because it suggests that samples should not be pooled if possible, even if collected from the same eye. Despite this, the variability even in the MDF samples was considered within an acceptable range, since no subjects would have been in different grouping based on the variability. Based on the data, an approximate “cut off” for MDF may be around 35 units, with those less than 35 units being considered “non-MDF” and those greater considered to be experiencing true “MDF”. Future studies on broader populations of SL wearers are needed to establish the normative values of MDF in SL wear.

Fluid reservoir proteins and lipids

Mass spectrometry (MS) is a common technique used to measure proteins and lipids in the tears. This technology ionizes the molecules in a sample and then sends them into a vacuum where the mass and charge are detected. The analyzer is then able to distinguish ions by the mass-to-charge ratio (m/z) which is graphed as a spectrum of relative abundance vs m/z. The spectrum is compared to known standards to determine the analytes of interest represented.

The human tear film, which is only ~10 μm thick, contains thousands of proteins, peptides, lipids, electrolytes, gases, and metabolites. MS has been instrumental in determining what the composition of the natural tear fluid is. However, the FR is approximately 250 μm thick and presumably is mostly saline when the lens is applied. The difference between the FR and the tears was shown to be apparent in Chapter 2, and in Chapter 3 we explored the FR more extensively, using MS to identify the lipids and proteins it contains (with and without MDF). We found significant increases in wax esters (WE), fatty amides, saturated cholesterol esters (CE), and many other species of fatty acyls that were considered branch chain fatty acids. The commonality in most of these lipids is that they are highly nonpolar and hydrophobic.

Two aspects of the lipid results were somewhat surprising. First there were no detected O-acyl-w-hydroxy fatty acids (OAHFA) which are typically detected in human meibum samples, although they may be represented in some of fatty acyls that were detected. These lipids are similar in structure and conformation to WE and free fatty acids[101], which they may have been mistaken for in the MS findings. However, these lipids are polar so would not be expected to contribute to MDF and are typically only detected in small abundance in the tear fluid[102,270,277]. A second unexpected finding was that there was not an increase in TAGs in the MDF, which are hydrophobic nonpolar lipids that were abundant in the FR samples (~20%), yet not greater in the MDF samples. This doesn't necessary mean that the TAGs do not contribute to MDF, and in fact the TAGs could be contributing to the low grade level of turbidity that is observed in virtually all FR samples, but it does not appear that they are the primary contributor to MDF.

The findings here do not rule out the presence of other contributors to MDF such as smaller proteins, cells, or other forms of debris. Clinically MDF can look somewhat variable between patients, some appearing white and milky in appearance, or other times having a darker, browner hue[346], indicating the presence of possibly different contributors. Cellular contribution, for example, is unclear, and while some immune cells have been detected[135], there hasn't been an

evaluation of epithelial cells in the FR, which could be sloughed from the corneal epithelium or the perilimbal conjunctiva. In addition, the impact of edema or inflammation on MDF is still not defined, but there is no evidence of edema is related to MDF in this cohort. It is unknown exactly how the lipids and other components of MDF arise in the FR. They may be trapped there when SL are applied (and precipitate out over time) or could also be exchanging with the outer surface environment during SL wear. Tear exchange studies show that exchange with SL is, while variable, extremely low and in some cases undetectable[56–58,347], which seems to suggest that the primary contributors to MDF are in the FR when the SL is applied, representing the ocular surface tears at the time of application.

Conjunctival compression

Using the sMap to measure conjunctival compression is a novel technique that has not been published in the literature. However, the output is seemingly accurate and appears to change in the same expected direction in all individuals (steepening of the curvature), in a ring that corresponds to the landing of the lens. Although no specific repeatability measurements were taken in this study, the measurements at baseline (prior to SL wear) were compared to those 24 hours post-SL wear and were within approximately 0.05 mm of each other, indicating some level of repeatability of the instrument and consistency of the conjunctival shape (without SL wear). While the instrument appears relatively consistent in measuring, this should be studies further and the accuracy of the measurements compared to other techniques (i.e., OCT, Pentacam®, Eaglet) could be established in future studies. In comparing the sMap to other techniques, it is important to note that with the compression software the sMap is unable to measure the SAG at the compression ring, which is what is used in the other studies. This study measures the curvature, which steepens away from the observer and flattens back post-SL removal. The SAG differs in that is measures the depth of sinking in the SL compression ring. Both techniques are representative of the change in tissue morphology, but they have not been compared.

It is understandable to predict that there would be a relationship between the amount of conjunctival compression with SL wear and the composition of the FR. The conjunctival tissue that is adjacent to the corneal limbus, which contains secretory cells (i.e., goblet cells) and capillaries that contribute to the tear fluid[348,349]. In other tissues, transient compression or mechanical disruption of a blood vessel can change its permeability to inflammatory mediators[350], leading to the hypothesis that limbal blood vessels could be provoked into releasing inflammatory mediators if compressed by a SL. Further, as a patient blinks while the SL is on the eye, and the SL is continuously pressed against the conjunctiva and superficial blood vessels, it could alter vessel permeability and facilitate inflammatory mediator secretion into the FR. This is further evidenced by the increase in bulbar and limbal hyperemia observed after SL removal[351], indicating compression or interaction between the SL and blood vessels during lens wear. In Chapter 3, the amount of compression was evaluated by measuring the change in curvature (shape) of the tissue after the SL was removed from the eye.

The compression ring beneath the LZR of a SL is easy to appreciate following SL removal. Following lens removal, macroscopic changes such as a compression ring, or local regions of conjunctival indentation may be observed, which may or may not stain with NaFl. Based on other studies, we know these changes are predominantly superficial at the level of the conjunctiva and are presumably related to the gradual settling of the lens; a reduction in central clearance of ~100-200 µm over the course of the day is typically observed during SL wear[139,140,352–355]. Despite these tissue alterations during and following lens wear, patients may often be asymptomatic due to the limited innervation and therefore low sensitivity of the conjunctiva[50]. However, there has been hypotheses that suggest that a lens which is tighter on the eye (i.e., causes greater compression of the tissue) will be associated with MDF. The root of this hypothesis is seeded in the common belief among SL practitioners that MDF is caused by mucin; the belief is that a SL compresses the conjunctiva, inducing goblet cells to secrete mucin into the FR that creates the turbidity

observed in MDF. This is a logical path of thought, but the results seen in Chapter 3 directly contradict this theory. We found that the opposite relationship was true in this cohort, and subjects with greater changes in conjunctival curvature during SL were associated with lower levels of MDF. More studies are needed to confirm or conflict with this finding.

Future directions of fluid reservoir research

Current research on the FR is in a beginning stage and there is much to learn and explore. The volume of tear/saline within the FR is much greater (>100 µL) than that which exists normally on the ocular surface (7-10 µL[51,356]), with minimal tear exchange in a well-fitted SL[55,56,58]. Now that the protocols are established and some normative data has been established, we can begin to implement these to study disease states. Beyond analyzing the components of the FR, this research will also lead to studying ways to manipulate the FR composition and explore the potential therapeutic uses of the SL. In addition, this work can aid in the development of novel application solutions for the SL, which are being designed to provide maximal nutritional support to the cornea.

In expanding the evaluation of the inflammatory components within the FR, several additional cytokines that are relevant to ocular surface disease and contact lens inflammation should be quantified. These include but are not limited to: Interferon (IFN)-ɣ, a pro-inflammatory mediator that is increased in keratoconus[220]; CCL5 (RANTES), an immune cell chemoattractant; tumor necrosis factor (TNF)-α and β, which are considered master cytokines are often increased in disease[220,339,340,357], as well as the myriad of cytokines from the IL family (i.e., IL-1α, -1β, -2, -6, -12, etc.). These and other mediators have a long history of being studies in other types of contact lens wear but have yet to be studies in SL wear. Further, given the presence of some hyperemia indicating blood vessel dilation, more efforts should be taken to understand the cellular and protein components in the blood vessels that could be leaking out and affecting the FR

composition. When the SL applies pressure to the conjunctiva, the perilimbal blood vessels in the conjunctiva could be stimulated to release inflammatory cells and mediators. For examples, mast cells could degranulate as a response to SL wear, which could be related to the increase in IL-4 that was observed with some subjects in Chapter 2. In addition, cells in the conjunctival stroma could migrate through the epithelium and into the FR. These pathways should be explored, and therapeutics (i.e., mast cell stabilizers) that could affect this response could be evaluated. As this research expands, it should be measured on normal and also on disease groups, specifically keratoconus (the most common indication for SL[61,358]) and other diseases causing irregular astigmatism, as well as ocular surface diseases like Sjögren's syndrome, which is also notorious for harboring abnormal quantities of inflammatory mediators in the tear fluid[224,326,359].

Another interesting area of research for the FR is in evaluating mucins. Tear mucins are hydrophilic glycoproteins[84,85,360], and at least 7 mucins are present in the tears and ocular surface epithelia, distinguished as either secreted (MUC2, MUC5AC, MUC5B, MUC7) or membrane associated (MUC1, MUC4, MUC16). MUC5AC is the most abundant secretory mucin in the tears, secreted from conjunctival goblet cells[361]. Mucins in SL wear are not particularly well studied, although there is one recent study that evaluated goblet cells and mucin clouds using conjunctival impression cytology in SL wear[362]. They found no difference in goblet cells density or mucin cloud amplitude after SL wear. Mucins have also been popularly hypothesized to be increased in individuals who experience MDF, stemming from the hypothesis that compressed goblet cells in the conjunctiva secreted mucin into the FR[363]. However, the study presented in Chapter 3 seems to indicate that this is unlikely, although the mucins were not specifically targeted in the testing (no mucins were detected in the MS protein analysis, but they are not always detectable in standard MS technique). There was also pilot study with 5 patients done by the author in 2014 that looked at mucins using MS and did not detect them[248], lending evidence toward them not

being causative of MDF. Regardless, more studies evaluating the mucins in the FR are needed, as well as further assessments of goblet cell viability and activity during SL wear.

Metabolites and minerals are additional targets that could be explored in future FR research. Approximately 100 minerals and metabolites have been identified in the tear film including amino acids, electrolytes, and arachidonic acid derivatives[89,114]. Two studies have previously evaluated metabolites in SL wear. Back in 1977, a study that measured tear calcium levels observed no differences between patients wearing soft, corneal, or SL, when compared to non-lens wearers[132]. More recently, Carracedo et al. found a reduced concentration of diadenosine tetraphosphate (Ap_4A), a nucleotide associated with dry eye disease[133], after 8 hours of SL wear in keratoconus patients. It is unclear what this decrease meant clinically, although it could be related to the lack of shear forces generated by the eyelids during blinking[39]. SL wear is not clear and would be interesting to assess.

Due to the current belief of minimal tear exchange with most lens designs, some researchers and clinicians have begun to investigate the possibility of using the FR as a “depot” for medications or solutions that may provide antimicrobial protection or nutritional support for the eye. Laballe et al. investigated concentrations of a fluoroquinolone antibiotic drop that could be achieved in ocular tissue using a SL reservoir[62]. Ciralsky et al developed a protocol for continuous wear of a SL to treat persistent epithelial defects[364]. SL have also been used to deliver topical bevacizumab to the ocular surface to treat corneal neovascularization in the management of five patients with severe corneal neovascularization[64,141]. Future studies building on these early studies may stimulate additional interest in using SL in the delivery of ocular medications.

Discussion of Chapter 4

Moving into Chapter 4, we began to explore the downstream effects of the landing area of the SL, which applies pressure on the conjunctiva and sclera overlying the areas of aqueous humor (AH)

outflow from the anterior segment. The hypothesis is that the LZR of a SL, in overlying the AH outflow pathway, impedes AH outflow and increases IOP, causing subtle changes at the ONH. The approach was inspired by studies done with primate models showing that increasing IOP causes thinning of the tissue at the rim of the ONH (termed the minimum rim width, or "MRW"). We applied a diagnostic SL to one eye of a subject and evaluated IOP and MRW in both eyes over a 6-hour period of time, with the non-lens wearing eye acting as a control. The IOP was monitored every 2 hours with a rebound tonometer (iCare), which could only be used when the SL was not on the eye (i.e., only taken on control eyes during SL wear), therefore not allowing any measurements of the test eye during SL wear. We also measured IOP with a newer instrument, the Diaton transpalpebral tonometer, which measures IOP over the eyelid on the superior portion of the conjunctiva/sclera. This would appear to address the dilemma of measuring IOP during SL wear, since this instrument can be used as indicated while the SL is on eye; however, the results of this instrument were not repeatable or comparable to the iCare (which is a commonly used instrument in research and has been shown to have comparable to results to other techniques). Ultimately, this study showed no significantly greater thinning of the MRW in test eyes, and a significant increase in IOP (2 mmHg, on average) after SL removal post-6 hours of wear.

The hypothesis that SL wear can influence IOP is not novel, nor is the attempt to test it. In 1951, Huggert reported that IOP increased by up to 30 mmHg in patients wearing glass SL for 25 minutes[180]. Miller, Carroll and Holmberg hypothesized that the suction force holding a SL on the eye (which they referred to as "scleral cling") could lead to compression of episcleral vasculature and could therefore impede the evacuation of aqueous from the eye through those vascular structures[181]. However, it is difficult to predict exactly where the anatomy of the different anatomical structures of the AH outflow pathway will be compared to the SL landing zone.

Sixty years after the initial work of Ascher and Huggert using glass SL, several recent studies have investigated the effect of modern highly oxygen permeable SL on IOP (Table 5.3). The greatest obstacle in studying the effect of a SL on IOP is the challenge in making direct contact with the cornea during lens wear, and there is no safe established way to directly measure IOP during SL wear in a human eye. As such, there is no standard methodology for measuring IOP during SL wear. Indeed, several different types of instruments have been used to measure IOP including the Schiotz tonometer[365], pneumotonometer[298,366], iCare rebound tonometer[299,367,368], Tonopen[301], Diaton transpalpebral tonometer[366,367,369], as well as Goldmann applanation tonometry[370]. Measurements have been taken before, during, and after SL wear using lenses of different diameters, peripheral curves, and even lenses with fenestrations have been used (Table 5.3), all in an attempt understand the impact of a SL on IOP. There are certain advantages and justifications for each method that has been used, such as a strong history of use on the conjunctiva (i.e., pneumotonometry), or being able to measure the most quickly (i.e., iCare), or simply being the gold standard for measuring IOP when there is no lens on the eye (i.e., Goldmann[371]). However, there are also disadvantages with each method, with the strongest being that none of these instruments are calibrated and reliable to measure IOP during SL wear. This creates an inherent yet unknown variability between studies. In addition to the variability in instruments used, the timing of the measurements, as well as the location of the eye where the measurements were made, also vary between studies.

The study completed in Chapter 4 attempted to test several of the methods used in other studies, as well as to use a novel method of indirect IOP assessment by directly observing changes to the ONH. This study was the first of two in the peer-reviewed literature that have evaluated the ONH directly during SL wear to indirectly assess changes in IOP. This new technique shows great promise in how we can assess the pressure in the eye during SL wear and evaluate the structural impact of a SL on the eye.

Table 5.3. Modern studies on IOP in SL wear

Author Year	Study Population	Lens Method	Study Design & Results
Nau[298] 2016	29 participants Ages: 29 ± 6 Normal neophytes	15.0 mm *PT*	IOP measured pre, post-1h, -2h, and post-SL removal; one test eye, other control No difference between peripheral IOP in study vs. control eye at any point during the study; No difference between baseline and any other time points in the study eye
Vincent[300] 2017	12 subjects (2 groups) Normal neophytes	16.5 mm *ORA; NCT*	IOP measured pre- and post-SL wear (post 3, 8 hours), control day (no SL) and test day Group 1 (ORA) and Group 2 (NCT) showed no difference between days
Aitsebaomo[299] 2019	9 subjects Age range: 25-30 Normal neophytes	15.8 mm *iCare*	IOP measured pre- and post-SL wear; one eye test, control eye wearing soft lens IOP change in test eye: +5.81 ± 1.62 mmHg; control eye: -0.62 ± 0.88 mmHg
Michaud[302] 2019	21 subjects Ages: 24 ± 4 Normal neophytes	15.8-,18-mm *DTT*	IOP measured pre, post-4-5h, and post SL removal; IOP measured without lens as control Small: IOP increased 10.1 ± 1.9 to 14.4 ± 5.1 mmHg; Large: 9.24 ±2.1 to 14.4 ±4.8 mmHg
Porcar[372] 2019	74 subjects Normal and Kc Habitual wearers	12.6-13.5 mm* ORA	IOP measured pre-dispense and immediately after removal (post-8h wear) after 1 year of daily wear. No differences in IOP after 1 year of SL wear in any groups
Shahnazi[301] 2019	25 subjects Habitual wearers	17.0-18.0 mm* *Tonopen*	Retrospective review of patients with IOP measured pre- and post-SL wear (variable wear) No differences in IOP (decreased an average of -0.89 mmHg, P > 0.05)
Kramer[370] 2020	32 subjects Habitual wearers	Custom SL* *GAT*	IOP measured pre-dispense and after SL removal after 1 and 6 months of daily wear No differences in IOP observed at either time point
Cheung[368] 2020	50 subjects Ages: 23 ± 4 Normal neophytes	16.5 mm (central fenestration) *iCare*	IOP measured pre, immediately post-application, and post 1-2 minutes of wear, OD only IOP increased 3.6 ± 2.2 mmHg during SL wear. No change from baseline post-SL removal
Obinwanne[365] 2020	20 subjects Ages: 28 ± 4 Normal neophytes	16.0 mm *STI*	IOP measured pre-, 10 minutes post-application, post- 2, -4h SL wear, 10 minutes post-removal. No significant differences noted over study period

Fogt[366] 2020	20 subjects Ages: 29 ± 9 Normal neophytes	15.2-,18-mm *PT; DTT*	IOP measured pre, immediately post-application, post-1h, and post-removal; each lens worn (randomly) in succession for 1 hour (OD only). PT: No change; DTT: Significant increase in IOP with both lenses
Walker[367] 2020	26 subjects Age range: 23-33 Normal neophytes	15.4 mm *iCare; DTT MRW*	IOP and MRW measured, pre, post-2, -4, -6h wear, and immediately post-removal No significant change in MRW; +2 mmHg increase in IOP post-SL removal (iCare)
Samaha[369] 2021	20 subjects Ages: Normal neophytes	16.0 mm *NCT; MRW*	IOP and MRW measured at baseline, 2h, 6h on test day and compared to no-lens data on same eye. Significantly greater MRW thinning (by -3.35 ± 2.2 µm) in the test condition

ORA: ocular response analyzer; NCT: non-contact tonometer; DTT: Diaton transpalpebral tonometer; GAT: Goldmann applanation tonometry; STI: Schiotz-tonometer Improved; PT: pneumotonometer; Kc: keratoconus
*indicates that study was done using the subjects' habitual, customized SL (a range of brands, diameters, and other SL parameters)

Methods to measure IOP during SL wear

As mentioned, evaluating IOP during SL wear is challenged by the placement of the lens overlying the cornea during lens wear. In Chapter 4 we measured IOP using two methods: the Diaton transpalpebral tonometer and the iCare rebound tonometer, the first of which was measured throughout lens wear and the latter was measured via the cornea pre-application and post-removal of the SL. No significant changes in IOP were noted in the Diaton readings, and an average increase of +2 mmHg was found using the iCare. The usability of using each of these two techniques is evaluated here.

Transpalpebral tonometry measures the elastic resistance of the eye through the upper lid and sclera using the ballistic principle of a free-falling object of known weight onto the tissue. This method requires that the instrument be held in vertical orientation, with the head tilted back and eyes depressed approximately 45 degrees. Comparisons between Goldmann applanation tonometry and transpalpebral tonometry have yielded mixed results. Current consensus suggests that transpalpebral tonometry may be most appropriately used as a screening tool[373], but should not be considered as equivalent to Goldmann applanation tonometry[316,374–376]. Nonetheless, the instrument used to perform transpalpebral tonometry (Diaton, BiCom, Inc, Long Beach, NY) is readily available, relatively inexpensive, and is easy to use. The Diaton has been used in patients who do not have viable corneas for testing IOP, for example patients who have a keratoprosthesis implanted and no longer have a true cornea, and so it is natural that researchers have turned to this instrument for the purpose of evaluating IOP in SL wear. In SL wear it appears to show some potential use, as some studies have shown moderate reliability in its use but determining the repeatable use of it is essential before it can be used reliably in clinical trials. The Bland-Altman comparisons in Chapter 4 showed it has virtually no correlation to iCare taken under normal measurement conditions (no SL in place). However, this does not mean that the instrument may

not work in certain populations when used by a trained investigator. It simply means that the data from the Diaton in this study is not considered reliable nor precise enough to sensibly interpret.

The iCare, which has a long history of use in research, been shown to be comparable to the Tonopen and Goldmann tonometry[320,377,378] and was therefore considered the gold standard here. This instrument consists of two coaxial coils within a probe shaft that bounces a magnetized probe off the cornea and detects the probe deceleration that is caused as it hits the eye. This instrument is also the only readily available device that is portable and can be used without topical anesthetic, allowing measurements to truly be taken immediately post-SL removal. However, the iCare cannot be reliably used when the SL is on the eye, so it is still limiting in that regard. In post-hoc testing, we took a deeper look at the iCare results to better understand if there was a relationship between post-removal IOP and MRW, and also to evaluate the influence of central corneal thickness (CCT) on IOP measurements. To do so, we focused on the subjects that had equal or greater than +4 mmHg increase in IOP post-SL removal. There were 7 subjects (27%) who had a +4 mmHg or greater increase in iCare reading immediately post SL removal. The control eyes, in contrast, showed no average increase in IOP readings after the test period (mean change was 0) with a range of -4 to +2 mmHg IOP change. This shows a clear increase in IOP readings post removal in the SL eye, which was statistically and clinically significant; however, it is unclear what this change truly means. One cause for the increase could have been corneal swelling during SL wear, which is known to occur at low levels during SL wear[28,30,32,35,353,379] and which could induce artificially greater IOP measurements[380]. To assess this, we evaluated the change in central corneal thickness (CCT) and compared it to the increased IOP (Table 5.4). However, five out of the seven high IOP eyes had less than 10 µm increase in CCT, and two of them actually showed a decrease in CCT after SL wear.

Comparing the IOP to MRW, we expected that the subjects with increased IOP post-SL removal would also show more thinning of the MRW, if both measures were representing an IOP increase

during SL wear. However, there was no correlation between change in IOP and MRW thinning (r = -0.13; P = 0.52), and in fact the subjects with the greatest amount of post-removal IOP increase showed lesser than average MRW differences between the test and control eyes. However, this study was not powered nor designed to test this measure, so this should be more carefully explored in follow up studies to make conclusions.

The corneas of the subjects in this study were on the relatively thin side of normal (535 µm) compared to some literature showing the normal mean closer to 550 µm[51]. However, this could be due to the instrument used to measure CCT, which was the Lenstar, which in a recent study showed slightly lesser values when compared to 3 other CCT measuring instruments[381]. The slightly lower values observed in this study may have been an instrument bias. Overall, the corneas in this study were considered normal and did not show clinically significant swelling or signs of pathology.

Table 5.4. iCare, MRW and corneal thickness compared

Subject ID / EYE	iCare (mmHg)	MRW* (µm)	CCT (µm)
3 / OD	+4	+1	+6
11 / OD	+4	-22	-6
18 / OD	+5	+4	+32
13 / OS	+6	-2	+7
27 / OS	+6	-2	+29
24 / OD	+7	-1	-10
16 / OS	+9	+2	+9

*MRW shown as difference in thinning between test and control eye; negative values indicate greater thinning in the test eye; MRW: minimum rim width; CCT: central corneal thickness

The 7 subjects who showed a +4 or greater increase in iCare tonometry immediately post-SL removal are compared to the MRW and CCT thicknesses.

In this study the IOP post-SL removal increased by an average of +2 mmHg, which is clinically significant for many individuals. For example, patients with glaucoma, or those who may be predisposed to glaucomatous risks based on their anatomy and physiology. Due to the unique fit of the SL and the proposed mechanism for increasing IOP, at-risk individuals may not always be

identifiable with current glaucoma risk factor assessments. But still the question remains, is the increase measured due to a true prolonged increase in SL wear, or perhaps due to the force of removing the lens that causes a brief, acute increase? We still don't know the answer based on this or other studies, but we can begin to predict possible scenarios that can be tested, such as the following:

1) The IOP increase is true but acute and caused by the mechanical forces of removing the SL.
2) The IOP increase is true, and IOP is increased during SL wear, but the increase is not a great enough increase to cause downstream ONH deformation in these young, healthy eyes.
3) The IOP increase is true, and the measurements are a combination of slowly prolonged increases due to SL but also an added increase due to the forces of removal.

In summary, the direct measurements of IOP in this study confirmed that the Diaton cannot be considered reliable in the current research to evaluate increased IOP with SL wear, and the iCare is a reliable measure of post-removal IOP. However, the true meaning of the increase in iCare tonometry seen in this study, and the clinical implications of such, remain somewhat unclear. One future goal for studies should be to measure the iCare readings again after 5 minutes post removal, or measure with Goldmann tonometry as well, which will help to determine the true cause for the increase post-SL wear. Additionally, a SL animal model would be quite appropriate to study these changes.

MRW measurements

This study was the first to use MRW as a surrogate for evaluating IOP during SL wear. MRW has been shown to have excellent repeatability and sensitivity to detect subtle changes due to fluctuations in IOP[184–187]. In animal models, changes can be noted within minutes of IOP change and are shown to be dose-dependent[184], likely affected by IOP fluctuations as little as 5 mmHg. In normal eyes, MRW decreases over the course of the day without any exogenous influences or

an increase in IOP, but it is believed that if IOP is increasing that the magnitude of thinning will be greater. The motivation to use this technique during SL wear is that it can be done while the SL is on the eye, and furthermore is a direct measure of the implied consequence of increased IOP, which is pressure-induced stress at the ONH. To date, two research groups, including ours, have used this technique to assess the effect of SL wear on the sensitive ONH. In 2020, Samaha & Michaud also published changes in MRW using the Spectralis OCT, in 20 young, healthy participants over the course of 6 hours of 16.0-mm SL wear in the right eye only[369]. In both MRW studies, thinning over the course of the day was expected and observed in most eyes, and there was greater MRW thinning in the test condition (SL wear). Samaha & Michaud found a statistically greater decrease (-3.35 ± 6.32 μm) in the test condition, which was similar to our finding of approximately 2 μm greater thinning in the test eyes, although it did not reach statistical significance in our cohort. The results of these studies, while differing in magnitude, agree that there is evidence of an increased IOP that can affect the ONH during SL wear. The differences in the magnitude may be attributable to the primary difference between the two studies, which was the determination of a control. We used the non-SL wearing eye as a control, measured on the same day as the test eye, and they measured the test eye on a previous day as the control. One of the justifications for using the same eye on a different day as a control is that there could be a consensual response of one eye to the other eye in response to an increase in IOP or MRW. Although it is unknown if this consensual response would be stimulated with SL wear or at the level of the MRW, ocular consensual responses to stimuli are known to occur (i.e., during post-surgical inflammation)[382]. Additionally, a different subject group wearing different types of SL could have affected the results, and ultimately both studies provide justification that this should be looked at over a wider population of potential SL wearers. Certainly, a good control when using this methodology is essential, since MRW has quite large natural diurnal fluctuations that must be considered.

An important consideration in understanding the MRW data is to consider whether this can be used to calculate the magnitude of IOP change that corresponds to a change in MRW. This is challenging to interpret, because the size and depth of an individual ONH, as well as properties and forces of surrounding tissues, could potentially be involved. However, in the Samaha study, the authors did attempt to correlate change in IOP with change in MRW by referencing a study of primates in which IOP was raised from 10-60 mmHg (in 10 mmHg increments) while assessing changes in MRW[184]. Based upon their calculations, they suggested that a 0.61-micron change in MRW represented a 1 mmHg increase in IOP. Application of this formula to data collected resulted in wide variability of predicted change in IOP during lens wear, from an increase of 14.75 mmHg to a decrease of 21.31 mmHg. In some cases, predicted IOP based upon the change in MRW observed resulted in an estimation of a negative IOP. This variability further suggests that there are additional forces involved, and a direct relationship between MRW and IOP in humans has yet to be established.

In regard to variability of the MRW data, there was an appreciable amount of variation in the data. While on average there was not a significant difference in the MRW with SL wear, 8 test eyes (31%) and 7 control eyes (27%) had greater than 10 µm of MRW thinning over the six-hour period. Most of the subjects with high amounts of MRW thinning showed relatively symmetrical thinning between the eyes, although there was approximately 3 to 5 µm greater thinning in test eyes for 38% of subjects (n = 10). Only two eyes, both test eyes, showed greater than 20 µm thinning during the test period (-21 and -23 µm), although both fellow control eyes did show greater than average amounts of thinning (-13 and -14 µm thinning, respectively). In summary, the IOP increases associated with the changes in MRW are unclear and are likely to have individual variations (just as other ONH parameters do), as are the physiologic risks for developing glaucoma in those that experience those greater amounts of MRW thinning.

The individual variation in the impact of SL on MRW and IOP is also likely to be a function of the

ocular biomechanics, specifically in the scleral tissue. The biomechanical properties of the sclera (e.g., its stiffness or distensibility which refers to tissue resistance or susceptibility to deformation forces) vary with age, ethnicity, glaucoma, and refractive error. Therefore, scleral lens settling dynamics, tissue compression, and any change in intraocular pressure during SL wear may vary significantly with respect to these factors. Although these properties were not evaluated here, future studies should seek to explore these variations in scleral biomechanics that could impact the deformation of tissue and ultimately the ONH deformation during SL wear.

Clinical implications of findings

Maintaining a steady IOP is a vital homeostatic process and dysregulation can result in ocular hypertension and potentially glaucoma. The potential to disrupt this natural homeostasis with a SL is a major clinical concern. As it stands currently, a consensus has yet to be reached on whether SL wear does, in fact, result in an increase in IOP in the short or long term. However, the research has allowed us to improve the tools and diagnostic techniques as well as our interpretation of them, and while there is progress yet to be made, clinical guidelines can begin to be formed with the currently available data.

The current evidence is supportive of a clinical recommendation to measure baseline IOP prior to initiating SL in all patients. We do not recommend use of the Diaton, which has been used in several studies but each pointing out the questionable reliability. Peripheral pneumotonometry may be the best current option for measuring IOP during SL wear, and although the normative range of this has not been established, it can be used for pre- and post-SL comparison as a reasonable screening tool. To measure IOP immediately post-removal we recommend iCare due to the ease and speed of acquisition. Any increase in IOP, either chronically during SL wear or due to the removal process, will be expected to return to a baseline state essentially immediately

after the inducing force is removed[322]. Therefore, the proximity of measurement to the removal is likely an important factor in getting any real data about the SL and IOP.

It should be noted that the purpose of measuring IOP is to screen for one of the major risk factors for glaucoma. However, IOP alone cannot be used to diagnose glaucoma. It is just one of the parameters assessed; corneal thickness, optic nerve structure, and visual function are also assessed in individuals considered to be at risk for disease. It is also worth noting that standard IOP assessment through the cornea may yield inaccurate results when performed in eyes with abnormal corneas (such as keratoconus, S/P keratoplasty, corneal dystrophy). Given that most patients who wear SL have some form of corneal pathology, SL prescribers may be well advised to consider not just IOP, but also additional risk factors for glaucoma when evaluating relative risks and benefits of SL wear for their patients, particularly if patients have other risk factors for the disease.

The MRW at the ONH may be the most useful tool for monitoring the effects of (potentially) chronic elevated IOP during SL wear. Based on the MRW data, we recommend a baseline and follow-up high-resolution optic nerve scans in SL patients when available. The MRW parameter is relatively novel and may not be available on many commercially available instruments, so we recommend practitioners follow the standard of care OCT testing for glaucoma which is a retinal nerve fiber layer (RNFL) scan. However, the dynamic changes in MRW may be more sensitive than the RNFL measure in early detection of glaucomatous ONH change, so this should be the test selected when available[383]. Similar to IOP monitoring, this should be repeated as needed depending on the glaucomatous risk factors for an individual.

Even with an increase in the resistance overlying the AH outflow pathways, and a potential stimulus to increase IOP, the normal human eye is not without homeostatic mechanisms that could potentially regulate IOP during SL wear. In a normal environment, without any type of

contact lens wear, several intrinsic and extrinsic factors exist that could potentially affect IOP homeostasis. For example, fluctuations in IOP occur due to influences such as fluid intake, medications, body orientation, alcohol consumption, respiration, heart rate, exercise, and diurnal rhythms[313]. While these factors affecting IOP are numerous, the AH outflow pathway, specifically the TM, is capable of modulating pulsatile flow to maintain a steady IOP in healthy eyes. In a properly functioning system, the mechanotransduction cells in the TM sense the resistance of AH increasing during these situations and adjusts in response to increased outflow pressure to regulate IOP[174]. Therefore, healthy eyes could in theory be able to maintain IOP in response to external forces, which is likely the case given that we do not see drastic increases in glaucoma in SL wearers. However, the individual response to mechanical force to the anterior segment is variable, with equal pressure to the anterior segment creating different IOP responses[322], and furthermore the effects of chronic IOP increases can take years or decades to manifest, which may not yet be apparent in the relatively new modernized SL designs. Other factors such as age[384] and disease state, specifically glaucoma, can affect the functionality of the IOP homeostatic system. Glaucomatous eyes may have defective autoregulatory mechanisms[172,174,313,385] and therefore be more susceptible to a potential increase in IOP during SL wear. Examination of the influence of SL wear on IOP in eyes with glaucoma would provide insight into the potential risks of SL wear in this population.

Future directions of intraocular pressure research

The physiological impact of SL wear on AH dynamics is a topic of considerable interest in the SL community. While it is possible that SL application, wear, or removal may introduce a challenge to these homeostatic mechanisms, the neuroregulatory system may be sufficiently robust to adjust to any alteration in IOP due to SL wear, at least in the short term in healthy individuals. However, in patients with glaucoma or other vulnerable compensatory mechanisms, the autoregulation system may not be able to adequately control IOP in the presence of a significant

exogenous challenge such as a SL. Additionally, while short-term variations in IOP associated with SL wear provide some insight the physiological impact of these lenses on homeostatic processes that control aqueous flow, long-term assessment of factors associated with IOP regulation in SL wearers may provide more clinically relevant information. With this in mind, future studies should evaluate IOP during SL wear in individuals who are at risk for glaucoma. Long-term clinical studies could also provide additional insight into potential increased risk for glaucoma associated with SL wear.

The landing of the SL onto the ocular surface is certainly an aspect to consider when evaluating the change in IOP and ONH morphology with SL wear. In Chapter 4, the LZR was evaluated using slit lamp biomicroscopy, which showed no real differences in grossly evaluated (blood vessel) compression. All lenses were explicitly fitted with spherical or toric LZRs to ensure proper alignment of the lens on the ocular surface, so it is not surprising that there were no compression patterns observed using the relatively low-resolution qualitative assessment done with the biomicroscope. However, other techniques such as OCT imaging could allow more reliable quantification of changes in tissue thickness or elevation associated with SL wear. The OCT images taken in the study in Chapter 4 were not assessed due to limitations in the consistency of the measurement location. The images were taken using a single line raster, and there was no active effort to measure the exact same location at the follow-up scans. Therefore, these images cannot reliably be assessed in this study, although ongoing analysis of these images using Matlab software may allow us to better calculate the volumetric area beneath the lens to better measure compression of the conjunctiva, episcleral, and scleral tissue, including assessment of compression at the level of episcleral veins, Schlemm's canal, and the trabecular meshes.

Another factor that bears attention is the individual variations in scleral and conjunctival anatomy. The scleral stroma is composed primarily of dense bundles of collagen of varying fibril diameter in a random arrangement with a similar percentage and type of collagen observed anteriorly and

posteriorly[386]. Near the limbus scleral collagen bundles are arranged in concentric circles, which is thought to allow some flexibility in response to changes in IOP or biomechanical stress transmitted from the extraocular muscles[153]. The biomechanical properties of the sclera (e.g., its stiffness or distensibility which refers to tissue resistance or susceptibility to deformation forces) vary with age, ethnicity, glaucoma, and refractive error[155,387]. Consequently, SL settling dynamics, tissue compression and any change in IOP during lens wear may vary significantly with respect to these factors, due to associated differences in scleral composition and biomechanical properties. However, the majority of tissue changes observed during SL wear appear to be superficial to the scleral stroma[38]. Future studies should explore the biomechanics of the scleral and evaluate the impact of biomechanics on the transferring of pressure and impact of the SL landing zone. Since most work examining scleral biomechanics typically considers the scleral tissue surrounding the optic nerve in relation to glaucoma development (in experimental animal models or using in-vitro techniques)[153], the data presented in this study may not directly translate to the anterior sclera at the location of the LZR. Future studies will explore this more comprehensively.

Conclusions

The studies completed in this dissertation represent novel approaches to studying the impact of a SL on the eye, showing that the FR is distinct from the ocular surface basal tears and may harbor a unique inflammatory environment, perhaps most uniquely in the presence of altered lipid profiles of the FR in MDF. This is an exciting and expanding time and there is much work to do to enhance the understanding of this environment of tears beneath the SL, as well as a great potential for expanding the therapeutic capabilities of this contact lens modality. In addition to FR analysis, a method to evaluate downstream effects such as IOP and ONH morphology has been established here and suggests that, while the SL appears to have minimal effect on ocular pressure homeostasis in normal eyes, it should be investigated further in SL wearers.

References

1. Fick, A. A contact-lens (translated by May CH). *Archives of Ophthalmology* **17**, 215–216 (1888).

2. Pearson, R. M. Karl Otto Himmler, manufacturer of the first contact lens. *Contact Lens & Anterior Eye* **30**, 11–16 (2007).

3. Müller, A. Brillengläser und Hornhautlinsen. Inaugural dissertation, University of Kiel. (1889).

4. Pearson, R. M. The Sämisch case and the Müllers of Wiesbaden. *Optometry and Vision Science* **86**, 157–164 (2009).

5. Panas, P. Traitement optique du kératocône. *Annales d'Oculistique* **99**, 293 (1888).

6. Haas, E. Les verres de contact. *Supplement to Bulletin de la Société d'Ophtalmologie de Paris* 1–160 (1937).

7. Dohme, B. Demonstration eines Patienten mit Zeiβchen Kontaktgläsern bei Keratokonus. *Klinische Monatsblätter für Augenheilkunde.* **68**, 650 (1922).

8. Hartinger, H. Zur Berichtigung der Fehlsichtigkeiten mittels der geschliffenen Zeissischen Haftgläser. Klinische Monatsblätter für Augenheilkunde. *Klinische Monatsblätter für Augenheilkunde.* **84**, 115–119 (1930).

9. Csapody, I. Abgüsse der lebenden Augenoberfläche für Verordnung von Kontaktgläsern. *Klinische Monatsblätter für Augenheilkunde.* **82**, 818–822 (1929).

10. Dallos, J. The individual fitting of contact glasses. *Transactions of the Ophthalmogical Society of the United Kingdom* **57**, 509–520 (1938).

11. Thier, P. Contactglazen, vervaardigd van harsproducten. *Nederlands tijdschrift voor geneeskunde* **83**, 4161 (1939).

12. Reich, L. The Rynco RX-56 lens. *Journal of the American Optometric Association* **47**, 300 (1976).

13. Ezekiel, D. F. Gas permeable haptic lenses. *Journal of the British Contact Lens Association* **6**, 158–161 (1983).

14. Takahide, K. *et al.* Use of fluid-ventilated, gas-permeable scleral lens for management of severe keratoconjunctivitis sicca secondary to chronic graft-versus-host disease. *Biology of Blood and Marrow Transplantation* **13**, 1016–1021 (2007).

15. Tan, D. D. T., Pullum, K. W. K. & Buckley, R. J. Medical applications of scleral contact lenses: 1. A retrospective analysis of 343 cases. *Cornea* **14**, 130–7 (1995).

16. Rosenthal, P., Cotter, J. M. & Baum, J. Treatment of persistent corneal epithelial defect with extended wear of a fluid-ventilated gas-permeable scleral contact lens. *American Journal of Ophthalmology* **130**, 33–41 (2000).

17. van der Worp, E. *et al.* Modern Scleral Contact Lenses: A Review. *Contact Lens & Anterior Eye* **37**, 240–250 (2014).

18. Ozek, D., Kemer, O. E. & Altiaylik, P. Visual performance of scleral lenses and their impact on quality of life in patients with irregular corneas. *Arquivos Brasileiros de Oftalmologia* **81**, 475–480 (2018).

19. Downie, L. E. & Lindsay, R. G. Contact lens management of keratoconus. *Clinical and Experimental Optometry* **98**, 299–311 (2015).

20. Povendano-Montero, F. *et al.* Bibliometric Study of Scientific Research on Scleral Lenses. *Eye & Contact Lens* **44 Suppl 2**, S285–S291 (2018).

21. Vincent, S. J. The rigid lens renaissance: A surge in sclerals. *Contact Lens & Anterior Eye* **41**, 139–143 (2018).

22. Nau, C. B. *et al.* Demographic Characteristics and Prescribing Patterns of Scleral Lens Fitters: The SCOPE Study. *Eye & Contact Lens* **44 Suppl 1**, S265–S272 (2017).

23. Pullum, K. W. The unique role of scleral lenses in contact lens practice. *Contact Lens & Anterior Eye* **22 Suppl 1**, S26-34 (1999).

24. Pullum, K. W. & Buckley, R. J. A study of 530 patients referred for rigid gas permeable scleral contact lens assessment. *Cornea* **16**, 612–622 (1997).

25. Tan, D. T., Pullum, K. W. & Buckley, R. J. Medical Applications of Scleral Contact Lenses: 2. Gas-Permeable Scleral Contact Lenses. *Cornea* **14**, 130–137 (1995).

26. Kok, J. H. & Visser, R. Treatment of ocular surface disorders and dry eyes with high gas-permeable scleral lenses. *Cornea* **11**, 518–522 (1992).

27. Schein, O. D., Rosenthal, P. & Ducharme, C. A gas-permeable scleral contact lens for visual rehabilitation. *American Journal of Ophthalmology* **109**, 318–322 (1990).

28. Giasson, C. J., Morency, J., Melillo, M. & Michaud, L. Oxygen tension beneath scleral lenses of different clearances. *Optometry and Vision Science* **94**, 466–475 (2017).

29. Jaynes, J. J. M., Edrington, T. B. T. & Weissman, B. A. Predicting scleral GP lens entrapped tear layer oxygen tensions. *Contact Lens & Anterior Eye* **38**, 44–47 (2015).

30. Michaud, L., van der Worp, E., Brazeau, D., Warde, R. & Giasson, C. J. Predicting estimates of oxygen transmissibility for scleral lenses. *Contact Lens & Anterior Eye* **35**, 266–271 (2012).

31. Aguilella-arzo, M., Edrington, T. B., Weissman, B. A. & Compan, V. Modeling Corneal Oxygen with Scleral Gas Permeable Lens Wear. *Optometry and Vision Science* **93**, 1339–1348 (2016).

32. Tan, B. *et al.* Effects of scleral-lens oxygen transmissibility on corneal thickness: A pilot study. *Contact Lens & Anterior Eye* **42**, 366–372 (2019).

33. Compan, V. *et al.* Oxygen diffusion and edema with modern scleral rigid gas permeable contact lenses. *Investigative Ophthalmology & Visual Science* **55**, 6421–6429 (2014).

34. Vincent, S. J., Alonso-Caneiro, D. & Collins, M. J. The time course and nature of corneal oedema during sealed miniscleral contact lens wear. *Contact Lens & Anterior Eye* **42**, 49–54 (2019).

35. Kim, Y. H., Tan, B., Lin, M. C. & Radke, C. J. Central Corneal Edema with Scleral-Lens Wear. *Current Eye Research* **43**, 1305–1315 (2018).

36. Pullum, K. W. & Stapleton, F. J. Scleral lens induced corneal swelling: what is the effect of varying Dk and lens thickness? *Contact Lens & Anterior Eye* **23**, 259–63 (1997).

37. Mountford, J., Carkeet, N. & Carney, L. Corneal thickness changes during scleral lens wear: Effect of gas permeability. *International Contact Lens Clinic* **21**, 19–22 (1994).

38. Alonso-Caneiro, D., Vincent, S. J. & Collins, M. J. Morphological changes in the conjunctiva, episclera and sclera following short-term miniscleral contact lens wear in rigid lens neophytes. *Contact Lens & Anterior Eye* **39**, 53–61 (2016).

39. Carracedo, G. *et al.* Short-term Effect of Scleral Lens on the Dry Eye Biomarkers in Keratoconus. *Optometry and Vision Science* **93**, 150–157 (2015).

40. Nixon, A. D., Barr, J. T. & VanNasdale, D. A. Corneal epithelial bullae after short-term wear of small diameter scleral lenses. *Contact Lens & Anterior Eye* **40**, 116–126 (2017).

41. Serramito, M. *et al.* Posterior cornea and thickness changes after scleral lens wear in keratoconus patients. *Contact Lens & Anterior Eye* **42**, 85–91 (2019).

42. Serramito-Blanco, M. *et al.* Anterior corneal curvature and aberration changes after scleral lens wear in keratoconus patients with and without ring segments. *Eye & Contact Lens* **45**, 141–148 (2019).

43. Vincent, S. J., Alonso-Caneiro, D. & Collins, M. J. Corneal changes following short-term miniscleral contact lens wear. *Contact Lens & Anterior Eye* **37**, 461–468 (2014).

44. Vincent, S. J., Alonso-Caneiro, D. & Collins, M. J. Miniscleral lens wear influences corneal curvature and optics. *Ophthalmic and Physiological Optics* **36**, 100–111 (2016).

45. Kim, S. *et al.* Fitting miniscleral contact lenses in Korean patients with keratoconus. *Clinical & Experimental Optometry* **100**, 375–379 (2017).

46. Pecego, M., Barnett, M., Mannis, M. J. & Durbin-Johnson, B. Jupiter Scleral Lenses: the UC Davis Eye Center experience. *Eye & Contact Lens* **38**, 179–182 (2012).

47. Rathi, V. M., Mandathara, P. S. & Dumpati, S. Contact lens in keratoconus. *Indian Journal of Ophthalmology* **61**, 410–5 (2013).

48. Bergmanson, J. P., Walker, M. K. & Johnson, L. A. Assessing scleral contact lens satisfaction in a keratoconus population. *Optometry and Vision Science* **93**, 855–860 (2016).

49. Pullum, K. W., Whiting, M. A. & Buckley, R. J. Scleral contact lenses: the expanding role. *Cornea* **24**, 269–277 (2005).

50. Norn, M. S. Conjunctival sensitivity in normal eyes. *Acta Ophthalmologica* **51**, 58–66 (1973).

51. Bergmanson, J. P. G. *Clinical Ocular Anatomy and Physiology*. vol. 27 (Texas Eye Research and Technology Center, 2021).

52. Walker, M., Bergmanson, J. P., Marsack, J. D., Miller, W. & Johnson, L. Complications and Fitting Challenges Associated with Scleral Contact Lenses: A Review. *Contact Lens & Anterior Eye* **39**, 88–96 (2016).

53. Ne, L. *et al.* Midday Visual Fogging in Scleral Lens Wearers – Does Fit Matter. *Contact Lens Spectrum* vol. 54 (2012).

54. Carracedo, G. *et al.* Post-lens tear turbidity and visual quality after scleral lens wear. *Clinical & Experimental Optometry* **100**, 577–582 (2017).

55. Tse, V., Tan, B., Kim, Y. H., Zhou, Y. & Lin, M. C. Tear dynamics under scleral lenses. *Contact Lens & Anterior Eye* **42**, 43–48 (2019).

56. Skidmore, K. v., Walker, M. K., Marsack, J. D., Bergmanson, J. P. G. & Miller, W. L. A measure of tear inflow in habitual scleral lens wearers with and without midday fogging. *Contact Lens & Anterior Eye* **42**, 36–42 (2019).

57. Morrison, S. *et al.* Tear Exchange Beneath Scleral Lenses? Poster presented at *Global Specialty Lens Symposium*. Las Vegas, NV (2015).

58. Paugh, J. R. *et al.* Silicone Hydrogel and Rigid Gas-Permeable Scleral Lens Tear Exchange. *Eye & Contact Lens* **44**, 97–101 (2018).

59. Chhabra, M., Prausnitz, J. M. & Radke, C. J. Modeling corneal metabolism and oxygen transport during contact lens wear. *Optometry and Vision Science* **86**, 454–466 (2009).

60. Visser, E.-S., Visser, R., van Lier, H. J. J. & Otten, H. M. Modern Scleral Lenses Part I: Clinical Features. *Eye & Contact Lens* **33**, 13–20 (2007).

61. Dimit, R., Gire, A., Pflugfelder, S. C. & Bergmanson, J. P. G. Patient Ocular Conditions and Clinical Outcomes using a PROSE Scleral Device. *Contact Lens & Anterior Eye* **36**, 159–163 (2013).

62. Laballe, R. *et al.* Preclinical assessment of scleral lens as a reservoir-based ocular therapeutic system. *Contact Lens & Anterior Eye* **39**, 394–396 (2016).

63. Jacobs, D. S. & Rosenthal, P. Boston scleral lens prosthetic device for treatment of severe dry eye in chronic graft-versus-host disease. *Cornea* **26**, 1195–1199 (2007).

64. Yin, J. & Jacobs, D. S. Long-term outcome of using Prosthetic Replacement of Ocular Surface Ecosystem (PROSE) as a drug delivery system for bevacizumab in the treatment of corneal neovascularization. *Ocular Surface* **17**, 134–141 (2019).

65. Basu, S. *et al.* Chronic Ocular Sequelae of Stevens-Johnson Syndrome in Children: Long-term Impact of Appropriate Therapy on Natural History of Disease. *American Journal of Ophthalmology* **May**, 7–28 (2018).

66. Weyns, M., Koppen, C. & Tassignon, M. J. Scleral contact lenses as an alternative to tarsorrhaphy for the long-term management of combined exposure and neurotrophic keratopathy. *Cornea* **32**, 359–361 (2013).

67. Heur, M., Bach, D., Theophanous, C. & Chiu, G. B. Prosthetic Replacement of the Ocular Surface Ecosystem Scleral Lens Therapy for Patients with Ocular Symptoms of Chronic Stevens-Johnson syndrome. *American Journal of Ophthalmology* **158**, 49–54 (2014).

68. Rosenthal, P. & Croteau, A. Fluid-ventilated, gas-permeable scleral contact lens is an effective option for managing severe ocular surface disease and many corneal disorders that would otherwise require penetrating keratoplasty. *Eye & Contact Lens* **31**, 130–134 (2005).

69. Barnett, M., Ross, J. & Durbin-Johnson, B. Preliminary Clinical Exploration of Scleral Lens Performance on Normal Eyes. *Journal of Contact lens Research and Science* **2**, (2018).

70. Vincent, S. J. & Fadel, D. Optical considerations for scleral contact lenses: A review. *Contact Lens & Anterior Eye* **42**, 598–613 (2019).

71. Visser, E.-S., van der Linden, B. J., Otten, H. M., van der Lelij, A. & Visser, R. Medical Applications and Outcomes of Bitangential Scleral Lenses. *Optometry and Vision Science* **90**, 1078–1085 (2013).

72. Alipour, F., Kheirkhah, A. & Jabarvand Behrouz, M. Use of Mini Scleral Contact Lenses in Moderate to Severe Dry Eye. *Contact Lens & Anterior Eye* **35**, 272–276 (2012).

73. Visser, E.-S. S., Visser, R., van Lier, H. J. J. & Otten, H. M. Modern scleral lenses part II: patient satisfaction. *Eye & Contact Lens* **33**, 21–25 (2007).

74. Fernandes, M. & Sharma, S. Polymicrobial and Microsporidial Keratitis in a Patient using Boston Scleral Contact Lens for Sjogren's Syndrome and Ocular Cicatricial Pemphigoid. *Contact Lens & Anterior Eye* **36**, 95–97 (2013).

75. Rathi, V. M., Mandathara, P. S., Vaddavalli, P. K., Srikanth, D. & Sangwan, V. S. Fluid Filled Scleral Contact Lens in Pediatric Patients: Challenges and Outcome. *Contact Lens & Anterior Eye* **35**, 189–192 (2012).

76. Michaud, L. For a Better Understanding of Scleral Contact Lens-related Pathophysiology. *Investigative Ophthalmology & Visual Science* **55**, 6430 (2014).

77. Isozaki, V. L. & Chiu, G. B. Transient corneal epithelial bullae associated with large diameter scleral lens wear: A case series. *Contact Lens & Anterior Eye* **41**, 463–468 (2018).

78. Davies, I. Scleral publications & contact lens category growth. *Contact Lens & Anterior Eye* **42**, 234–235 (2019).

79. Rathi, V. M., Mandathara, P. S., Taneja, M., Dumpati, S. & Sangwan, V. S. Scleral lens for keratoconus: Technology update. *Clinical Ophthalmology* **28**, 2013–2018 (2015).

80. Barnett, M. & Mannis, M. J. Contact Lenses in the Management of Keratoconus. *Cornea* **30**, 1510–1516 (2011).

81. Severinsky, B., Behrman, S., Frucht-Pery, J. & Solomon, A. Scleral Contact Lenses for Visual Rehabilitation after Penetrating Keratoplasty: Long-term outcomes. *Contact Lens & Anterior Eye* **37**, 196–202 (2014).

82. Bavinger, J. C., DeLoss, K. & Mian, S. I. Scleral Lens use in Dry Eye Syndrome. *Current Opinion in Ophthalmology* **26**, 319–24 (2015).

83. Schornack, M., Baratz, K., Patel, S. & Maguire, L. Jupiter Scleral Lenses in the Management of Chronic Graft versus Host Disease. *Eye & Contact Lens* **34**, 302–305 (2008).

84. Hollingsworth, M. A. & Swanson, B. J. Mucins in cancer: Protection and control of the cell surface. *Nature Reviews Cancer* **4**, 45–60 (2004).

85. Moniaux, N., Escande, F., Porchet, N., Aubert, J. P. & Batra, S. K. Structural organization and classification of the human mucin genes. *Frontiers in Bioscience* **6**, 1192-206 (2001).

86. Nicolaides, N. *et al.* Meibomian gland studies: comparison of steer and human lipids. *Investigative Ophthalmology & Visual Science* **20**, 522–536 (1981).

87. Cher, I. A new look at lubrication of the ocular surface: fluid mechanics behind the blinking eyelids. *Ocular Surface* **6**, 79–86 (2008).

88. Ewen King-Smith, P., Hinel, E. A. & Nichols, J. J. Application of a novel interferometric method to investigate the relation between lipid layer thickness and tear film thinning. *Investigative Ophthalmology & Visual Science* **51**, 2418–2423 (2010).

89. Zhou, L. *et al.* In-depth analysis of the human tear proteome. *Journal of Proteomics* **75**, 3877–3885 (2012).

90. Zhou, L. *et al.* Identification of tear fluid biomarkers in dry eye syndrome using iTRAQ quantitative proteomics. *Journal of Proteome Research* **8**, 4889–4905 (2009).

91. Wong, T. *et al.* Proteomic profiling of inflammatory signaling molecules in the tears of patients on chronic glaucoma medication. *Investigative Ophthalmology & Visual Science* **52**, 7385–7391 (2011).

92. Zhou, L. *et al.* Proteomic analysis of human tears: defensin expression after ocular surface surgery. *Journal of Proteome Research* **3**, 410–416 (2004).

93. Molloy, M. P. *et al.* Establishment of the human reflex tear two-dimensional polyacrylamide gel electrophoresis reference map: New proteins of potential diagnostic value. *Electrophoresis* **18**, 2811–2815 (1997).

94. Sack, R. A., Tan, K. O., Tan, A., Kah Ooi Tan & Tan, A. Diurnal tear cycle: Evidence for a nocturnal inflammatory constitutive tear fluid. *Investigative Ophthalmology & Visual Science* **33**, 626–640 (1992).

95. Fluckinger, M., Haas, H., Merschak, P., Glasgow, B. J. & Redl, B. Human tear lipocalin exhibits antimicrobial activity by scavenging microbial siderophores. *Antimicrobial Agents and Chemotherapy* **48**, 3367–3372 (2004).

96. Markoulli, M., Papas, E., Cole, N. & Holden, B. A. The diurnal variation of matrix metalloproteinase-9 and its associated factors in human tears. *Investigative Ophthalmology & Visual Science* **53**, 1479–1484 (2012).

97. Brown, S. H. J. *et al.* A comparison of patient matched meibum and tear lipidomes. *Investigative Ophthalmology & Visual Science* **54**, 7417–7423 (2013).

98. Rantamaki, A. H. *et al.* Human tear fluid lipidome: From composition to function. *PLoS ONE* **6**, e19553 (2011).

99. Butovich, I. A. On the lipid composition of human meibum and tears: Comparative analysis of nonpolar lipids. *Investigative Ophthalmology & Visual Science* **49**, 3779–3789 (2008).

100. Ham, B. M., Jacob, J. T. & Cole, R. B. MALDI-TOF MS of phosphorylated lipids in biological fluids using immobilized metal affinity chromatography and a solid ionic crystal matrix. *Analytical Chemistry* **77**, 4439–4447 (2005).

101. Butovich, I. A. Tear film lipids. *Experimental Eye Research* **117**, 4–27 (2013).

102. Lam, S. M. *et al.* Meibum lipid composition in Asians with dry eye disease. *PLoS One* **6**, e24339 (2011).

103. Borchman, D., Yapper, M. & Foulks, G. Changes in Human Meibum Lipid with Meibomian Gland Dysfunction using Principal Component Analysis Douglas. *Experimental Eye Research* **91**, 246–256 (2010).

104. Borchman, D., Foulks, G., Yappert, M. & Milliner, S. Differences in human meibum lipid composition with meibomian gland dysfunction using NMR and principal component analysis. *Investigative Ophthalmology & Visual Science* **53**, 337–347 (2012).

105. Rohit, A., Willcox, M. & Stapleton, F. Tear lipid layer and contact lens comfort: a review. *Eye & Contact Lens* **39**, 247–53 (2013).

106. Kuo, M. T. *et al.* Tear proteomics approach to monitoring Sjögren syndrome or dry eye disease. *International Journal of Molecular Sciences* **20**, (2019).

107. Versura, P. *et al.* Predictive role of tear protein expression in the early diagnosis of Sjögren's syndrome. *Annals of Clinical Biochemistry* **55**, 561–570 (2018).

108. Velasco Cabrera, M. J. *et al.* Lactoferrin in tears in contact lens wearers. *Eye & Contact Lens* **23**, 127–129 (1997).

109. Glasson, M. J., Stapleton, F., Keay, L., Sweeney, D. & Willcox, M. D. P. Differences in Clinical Parameters and Tear Film of Tolerant and Intolerant Contact Lens Wearers. *Investigative Ophthalmology & Visual Science* **44**, 5116–5124 (2003).

110. Glasson, M. J., Stapleton, F., Keay, L. & Willcox, M. D. P. The effect of short-term contact lens wear on the tear film and ocular surface characteristics of tolerant and intolerant wearers. *Contact Lens & Anterior Eye* **29**, 41–47 (2006).

111. Redls, B., Holzfeind, P. & Lottspeichq, F. cDNA Cloning and Sequencing Reveals Human Tear Prealbumin to Be a Member of the Lipophilic-ligand Carrier Protein Superfamily. *Journal of Biochemistry*. **5**, 267 (1992).

112. Gachon, A.-M. F. & Lacazette, E. Tear lipocalin and the eye's front line of defense. *British Journal of Ophthalmology* **82**, 453–5 (1998).

113. Glasson, M., Stapleton, F. & Willcox, M. Lipid, lipase and lipocalin differences between tolerant and intolerant contact lens wearers. *Current Eye Research* **25**, 227–235 (2002).

114. Nichols, J. J. & Green-Church, K. B. Mass spectrometry-based proteomic analyses in contact lens-related dry eye. *Cornea* **28**, 1109–1117 (2009).

115. Pflugfelder, S. C., Jones, D., Ji, Z., Afonso, a & Monroy, D. Altered cytokine balance in the tear fluid and conjunctiva of patients with Sjögren's syndrome keratoconjunctivitis sicca. *Current Eye Research* **19**, 201–211 (1999).

116. Shinzawa, M. *et al.* Epidermal Fatty Acid-Binding Protein: A Novel Marker in the Diagnosis of Dry Eye Disease in Sjogren Syndrome. *International Journal of Molecular Sciences* **19**, (2018).

117. Koo, B. S., Lee, D. Y., Ha, H. S., Kim, J. C. & Kim, C. W. Comparative analysis of the tear protein expression in blepharitis patients using two-dimensional electrophoresis. *Journal of Proteome Research* **4**, 719–724 (2005).

118. Sharif, R. *et al.* Prolactin-Induced Protein is a novel biomarker for Keratoconus. *Experimental Eye Research* **179**, 55–63 (2019).

119. Masoudi, S., Stapleton, F. J. & Willcox, M. D. P. Contact lens-induced discomfort and protein changes in tears. *Optometry and Vision Science* **93**, 955–962 (2016).

120. McKay, T., Serjersen, H., Hjortdal, J., Zieske, J. & Karamichos, D. Characterization of Tear Immunoglobulins in a Small-Cohort of Keratoconus Patients. *Scientific Reports* **10**, 9426 (2020).

121. Maurya, R. P. *et al.* Immunoglobulin Concentration in Tears of Contact Lens Wearers. *Journal of Ophthalmic and Vision Research* **9**, 320–323 (2014).

122. Willcox, M. D., Zhenjun, Z., Naduvilath, T. & Jara, P. L. Cytokine changes in tears and relationship to contact lens discomfort. *Molecular Vision* **21**, 293–305 (2015).

123. Gad, A., Vingrys, A. J., Wong, C. Y., Jackson, D. C. & Downie, L. E. Tear film inflammatory cytokine upregulation in contact lens discomfort. *Ocular Surface* **17**, 89–97 (2019).

124. González-Pérez, J. *et al.* Tear film inflammatory mediators during continuous wear of contact lenses and corneal refractive therapy. *British Journal of Ophthalmology* **96**, 1092–1098 (2012).

125. Poyraz, C., Irkec, M. & Mocan, M. C. Elevated tear interleukin-6 and interleukin-8 levels associated with silicone hydrogel and conventional hydrogel contact lens wear. *Eye & Contact Lens* **38**, 146–9 (2012).

126. López-de la Rosa, A., González-García, M. J., Calonge, M. & Enríquez-de-Salamanca, A. Tear Inflammatory Molecules in Contact Lens Wearers: A Literature Review. *Current Medicinal Chemistry* **27**, 523–548 (2019).

127. Baleriola-lucas, C., Fukuda, M., P Willcox, M. D., Sweeney, D. F. & Holden, B. A. Fibronectin Concentration in Tears of Contact Lens Wearers. *Experimental Eye Research* **64** (1997).

128. Fung, K. Y. C., Morris, C., Sathe, S., Sack, R. & Duncan, M. W. Characterization of the in vivo forms of lacrimal-specific proline-rich proteins in human tear fluid. *Proteomics* **4**, 3953–3959 (2004).

129. Mckown, R. L. *et al.* Lacritin and Other New Proteins of the Lacrimal Functional Unit. *Experimental Eye Research* **88**, 848–858 (2009).

130. Pucker, A. D. & Nichols, J. J. Analysis of meibum and tear lipids. *Ocular Surface* **10**, 230–250 (2012).

131. Chen, L., Zhou, L., Chan, E. C. Y., Neo, J. & Beuerman, R. W. Characterization of the human tear metabolome by LC-MS/MS. *Journal of Proteome Research* **10**, 4876–4882 (2011).

132. Winder, A. F., Ruben, M. & Sheraidah, G. A. Tear calcium levels and contact lens wear. *British Journal of Ophthalmology* **61**, 539–543 (1977).

133. Peral, A., Carracedo, G., Acosta, M. C., Gallar, J. & Pintor, J. Increased levels of diadenosine polyphosphates in dry eye. *Investigative Ophthalmology & Visual Science* **47**, 4053–4058 (2006).

134. Harthan, J. *et al.* Scleral Lens Prescription and Management Practices: The SCOPE Study. *Eye & Contact Lens* **44 Suppl 1**, S228–S232 (2018).

135. Postnikoff, C. K. *et al.* Identification of leukocytes associated with midday fogging in the post-lens tear film of scleral contact lens wearers. *Investigative Ophthalmology & Visual Science* **60**, 226–233 (2019).

136. Rathi, V. M., Mandathara, P. S., Dumpati, S. & Sangwan, V. S. Change in vault during scleral lens trials assessed with anterior segment optical coherence tomography. *Contact Lens & Anterior Eye* **40**, 157–161 (2017).

137. Sonsino, J. & Mathe, D. S. Central vault in dry eye patients successfully wearing scleral lens. *Optometry and Vision Science* **90**, e248-51 (2013).

138. Nau, C. B. & Schornack, M. M. Region-Specific Changes in Postlens Fluid Reservoir Depth Beneath Small-Diameter Scleral Lenses Over 2 Hours. *Eye & Contact Lens* **Sep**, Suppl1: S210-S215 (2018)

139. Vincent, S. J., Alonso-Caneiro, D. & Collins, M. J. The temporal dynamics of miniscleral contact lenses: Central corneal clearance and centration. *Contact Lens & Anterior Eye* **41**, 162–168 (2018).

140. Kauffman, M. J., Gilmartin, C. A., Bennett, E. S. & Bassi, C. J. A Comparison of the short-term settling of three scleral lens designs. *Optometry and Vision Science* **91**, 1462–1466 (2014).

141. Lim, M., Jacobs, D. S., Rosenthal, P. & Carrasquillo, K. G. The boston ocular surface prosthesis as a novel drug delivery system for bevacizumab. *Seminars in Ophthalmology* **24**, 149–155 (2009).

142. Lim, P., Ridges, R., Jacobs, D. S. & Rosenthal, P. Treatment of persistent corneal epithelial defect with overnight wear of a prosthetic device for the ocular surface. *American Journal of Ophthalmology* **156**, 1095–1101 (2013).

143. Ling, J. D., Gire, A. & Pflugfelder, S. C. PROSE therapy used to minimize corneal trauma in patients with corneal epithelial defects. *American Journal of Ophthalmology* **155**, 615–619, 619 e1–2 (2013).

144. Brennan, N. A. & Chantal Coles, M. L. Extended wear in perspective. *Optometry and Vision Science* **74**, 609–23 (1997).

145. Lin, M. C. & Polse, K. A. Hypoxia, overnight wear, and tear stagnation effects on the corneal epithelium: Data and proposed model. *Eye & Contact Lens* **33**, 387–381 (2007).

146. Bonanno, J. A. & Polse, K. A. Corneal acidosis during contact lens wear: Effects of hypoxia and CO2. *Investigative Ophthalmology & Visual Science* **28**, 1514-1220 (1987).

147. Bonanno, J. Contact lens induced corneal acidosis. *Eye & Contact Lens* **22**, 70–4 (1996).

148. McKinney, A. *et al.* The Cause of Midday Visual Fogging in Scleral Gas Permeable Lens Wearers. *Investigative Ophthalmology & Visual Science* **54**, ARVO E-Abstract 5483 (2013).

149. Schornack, M. M. *et al.* Factors associated with patient-reported midday fogging in established scleral lens wearers. *Contact Lens & Anterior Eye* **43**, 602–608 (2020).

150. Harvey, T. M., Alzaga Fernandez, A. G., Patel, R., Goldman, D. & Ciralsky, J. Conjunctival anatomy and physiology. in *Ocular surface disease: Cornea, conjunctiva and tear film* (eds. Holland, E. J., Mannis, M. J. & Lee, W. B.) 23–28 (Elsevier, 2013).

151. Snell, R. S. & Lemp, M. A. The eyeball. in *Clinical Anatomy of the Eye* (eds. Snell, R. & Lemp, M.) 133–210 (Blackwell Science, 1998).

152. Lawrenson, J. G. & Ruskell, G. L. The structure of corpuscular nerve endings in the limbal conjunctiva of the human eye. *Journal of Anatomy* **177**, 75–84 (1991).

153. Boote, C. *et al.* Scleral structure and biomechanics. *Progress in Retinal and Eye Research* **Jan**, 100733 (2020).

154. Morrison, J. C. & van Buskirk, E. M. Anterior collateral circulation in the primate eye. *Ophthalmology* **90**, 707–715 (1983).

155. Elsheikh, A. *et al.* Regional variation in the biomechanical properties of the human sclera. *Experimental Eye Research* **90**, 624–633 (2010).

156. Clayson, K. *et al.* Corneoscleral stiffening increases IOP spike magnitudes during rapid microvolumetric change in the eye. *Experimental Eye Research* **165**, 29–34 (2017).

157. Gabelt, B. T., Kiland, J., Tian, B. Y. & Kaufman, P. Aqueous Humor: Secretion and Dynamics. in *Duane's Clinical Ophthalmology* (eds. Tasman, W. & Jaeger, E. A.) vol. 2 (Lippincott Williams & Wilkins, 2006).

158. Abu-Hassan, D. W., Acott, T. S. & Kelley, M. J. The Trabecular Meshwork: A Basic Review of Form and Function. *Journal of Ocular Biology* **2**, 1–22 (2014).

159. Lütjen-Drecoll, E. & Lutjen-Drecoll, E. Functional morphology of the trabecular meshwork in primate eyes. *Progress in Retinal and Eye Research* **18**, 91–119 (1999).

160. Ethier, C. R., Kamm, R. D., Palaszewski, B. A., Johnson, M. C. & Richardson, T. M. Calculations of flow resistance in the juxtacanalicular meshwork. *Investigative Ophthalmology & Visual Science* **27**, 1741–1750 (1986).

161. Mcewen, W. K. Application of Poiseuille's law to aqueous outflow. *American Journal of Ophthalmology* **60**, 290–294 (1958).

162. Acott, T. S. & Kelley, M. J. Extracellular matrix in the trabecular meshwork. *Experimental Eye Research* **86**, 543–561 (2008).

163. Bill, A. & Svedbergh, B. Scanning electron microscopic studies of the trabecular meshwork and the canal of schlemm - an attempt to localize the main resistance to outflow of aqueous humor in man. *Acta Ophthalmologica* **50**, 295–320 (1972).

164. Roy Chowdhury, U. *et al.* Aqueous humor outflow: dynamics and disease. *Investigative Ophthalmology & Visual Science* **56**, 2993–3003 (2015).

165. Vittal, V., Rose, A., Gregory, K. E., Kelley, M. J. & Acott, T. S. Changes in gene expression by trabecular meshwork cells in response to mechanical stretching. *Investigative Ophthalmology & Visual Science* **46**, 2857–2868 (2005).

166. Kim, S. H., Turnbull, J. & Guimond, S. Extracellular matrix and cell signaling: the dynamic cooperation of integrin, proteoglycan and growth factor receptor. *Journal of Endocrinology* **209**, 139–151 (2011).

167. Bradley, J. M. B. *et al.* Effects of mechanical stretching on trabecular matrix metalloproteinases. *Investigative Ophthalmology & Visual Science* **42**,1505–1513 (2001).

168. Yue, B. Y. J. T. The extracellular matrix and its modulation in the trabecular meshwork. *Survey of Ophthalmology* **40**, 379–390 (1996).

169. Ashton, N. Anatomical study of Schlemm's canal and aqueous veins by means of neoprene casts. Part I. Aqueous veins. *British Journal of Ophthalmology* **35**, 291–303 (1951).

170. Dvorak-Theobald, G. Further studies on the canal of Schlemm; its anastomoses and anatomic relations. *American Journal of Ophthalmology* **39**, 65–89 (1955).

171. Johnstone, M., Jamil, A. & Martin, E. Aqueous Veins and Open Angle Glaucoma. *Glaucoma: A Practical Evidence-Based Approach to Patient Care* 65–78 (2010).

172. Johnstone, M., Martin, E. & Jamil, A. Pulsatile flow into the aqueous veins: manifestations in normal and glaucomatous eyes. *Experimental Eye Research* **92**, 318–27 (2011).

173. Ascher, K. W. The aqueous veins. I. Physiologic importance of the visible elimination of intraocular fluid. *American Journal of Ophthalmology* **192**, xxix–liv (1942).

174. Carreon, T., van der Merwe, E., Fellman, R. L., Johnstone, M. & Bhattacharya, S. K. Aqueous outflow - A continuum from trabecular meshwork to episcleral veins. *Progress in Retinal and Eye Research* **57**, 108–133 (2017).

175. Bill, A. Uveoscleral drainage of aqueous humor: physiology and pharmacology. *Progress in Clinical Biology Research* **312**, 417–427 (1989).

176. Bill, A. & Phillips, C. I. Uveoscleral drainage of aqueous humour in human eyes. *Experimental Eye Research* **12**, 275–281 (1971).

177. McDougal, D. H. & Gamlin, P. D. Autonomic control of the eye. *Comprehensive Physiology* **5**, 439–473 (2015).

178. Willcox, M. D. P. Characterization of the normal microbiota of the ocular surface. *Experimental Eye Research* **117**, 99–105 (2013).

179. Gabelt, B. T., Karurman, P. L. & Kaufman, P. L. Production and Flow of Aqueous Humor. in *Adler's Physiology of the Eye* (2011).

180. Huggert, A. Increase of the intraocular pressure when using contact glasses. *Acta Ophthalmologica* **29**, 475–81 (1951).

181. Miller, D., Carroll, J. M. & Holmberg, A. Scleral lens cling measurement. *American Journal of Ophthalmology* **65**, 929–930 (1968).

182. McMonnies, C. W. A hypothesis that scleral contact lenses could elevate intraocular pressure. *Clinical and Experimental Optometry* **99**, 594–596 (2016).

183. Fadel, D. & Kramer, E. Potential contraindications to scleral lens wear. *Contact Lens & Anterior Eye* **42**, 92–103 (2019).

184. Patel, N., McAllister, F., Pardon, L. & Harwerth, R. The effects of graded intraocular pressure challenge on the optic nerve head. *Experimental Eye Research* **169**, 79–90 (2018).

185. Enders, P. *et al.* Intraday Repeatability of Bruch's Membrane Opening-based Neuroretinal Rim Measurements. *Investigative Ophthalmology & Visual Science* **58**, 5195–5200 (2017).

186. Gupta, L. *et al.* Reproducibility of Minimum Rim Width and Retinal Nerve Fibre Layer Thickness using the Anatomic Positioning System in Glaucoma Patients. *Canadian Journal of Ophthalmology* **54**, 335–341 (2019).

187. Park, K., Kim, J. & Lee, J. Reproducibility of Bruch Membrane Opening-Minimum Rim Width Measurements with Spectral Domain Optical Coherence Tomography. *Journal of Glaucoma* **26**, 1041–1050 (2017).

188. Romero-Jiménez, M. & Flores-Rodríguez, P. Utility of a semi-scleral contact lens design in the management of the irregular cornea. *Contact Lens & Anterior Eye* **36**, 146–150 (2013).

189. Schornack, M. M., Baratz, K. H., Patel, S. V & Maguire, L. J. Jupiter scleral lenses in the management of chronic graft versus host disease. *Eye & Contact Lens* **34**, 302–305 (2008).

190. Chahal, H. S. *et al.* Scleral Contact Lenses in an Academic Oculoplastics Clinic: Epidemiology and Emerging Considerations. *Ophthalmic Plastic and Reconstructive Surgery* **34**, 231-236 (2017).

191. Schornack, M. M. & Baratz, K. H. Ocular cicatricial pemphigoid: the role of scleral lenses in disease management. *Cornea* **28**, 1170-1172 (2009).

192. Wiwanitkit, V. Scleral lenses and ocular cicatricial pemphigoid. *Cornea* **29**, 1330 (2010)

193. Takahide, K. *et al.* Use of Fluid-Ventilated, Gas-Permeable Scleral Lens for Management of Severe Keratoconjunctivitis Sicca Secondary to Chronic Graft-versus-Host Disease. *Biology of Blood and Marrow Transplantation* **13**, 1016–1021 (2007).

194. Dimit, R., Gire, A., Pflugfelder, S. C. & Bergmanson, J. P. G. Patient ocular conditions and clinical outcomes using a PROSE scleral device. *Contact Lens & Anterior Eye* **36**, 159–163 (2013).

195. Ye, P., Sun, A. & Weissman, B. a. Role of mini-scleral gas-permeable lenses in the treatment of corneal disorders. *Eye & Contact Lens* **33**, 111–113 (2007).

196. Bergmanson, J., Walker, M. K. & Johnson, L. A. Assessing Scleral Contact Lens Satisfaction in a Keratoconus Population. *Optometry and Vision Science* **93**, 855–860 (2016).

197. Visser, E.-S., Visser, R., van Lier, H. J. J. & Otten, H. M. Modern scleral lenses part II: patient satisfaction. *Eye & Contact Lens* **33**, 21–25 (2007).

198. Walker, M. K., Bergmanson, J. P., Miller, W. L., Marsack, J. D. & Johnson, L. A. Complications and fitting challenges associated with scleral contact lenses: A review. *Contact Lens & Anterior Eye* **39**, 88-96 (2015).

199. Rathi, V. M., Mandathara, P. S., Vaddavalli, P. K., Srikanth, D. & Sangwan, V. S. Fluid filled scleral contact lens in pediatric patients: challenges and outcome. *Contact Lens & Anterior Eye* **35**, 189–92 (2012).

200. Bruce, A. S. & Nguyen, L. M. Acute red eye (non-ulcerative keratitis) associated with mini-scleral contact lens wear for keratoconus. *Clinical and Experimental Optometry* **96**, 245–248 (2013).

201. Fadel, D. & Kramer, E. Potential contraindications to scleral lens wear. *Contact Lens & Anterior Eye* **42**, 92-103 (2019).

202. El-Ruby, A. Advantages and Disadvantages of scleral and corneal contact lenses. *Bulletin of Ophthalmological Society of Egypt* **64**, 233–5 (1971).

203. Nixon, A. D., Barr, J. T. & VanNasdale, D. A. Corneal epithelial bullae after short-term wear of small diameter scleral lenses. *Contact Lens & Anterior Eye* **40**, 116–126 (2017).

204. Tse, V., Tan, B., Kim, Y. H., Zhou, Y. & Lin, M. C. Tear dynamics under scleral lenses. *Contact Lens & Anterior Eye* **42**, 43-48 (2019).

205. Michaud, L., van der Worp, E., Brazeau, D., Warde, R. & Giasson, C. J. Predicting estimates of oxygen transmissibility for scleral lenses. *Contact Lens & Anterior Eye* **35**, 266–271 (2012).

206. Vincent, S. J., Alonso-caneiro, D., Collins, M. J., Beanland, A. & Lam, L. Hypoxic Corneal Changes following Eight Hours. *Optometry and Vision Science* **93**, 293–299 (2016).

207. Sticca, M. P. *et al.* Acanthamoeba keratitis in patients wearing scleral contact lenses. *Contact Lens & Anterior Eye* **41**, 307-310 (2018).

208. Zimmerman, A. B. & Marks, A. Microbial Keratitis Secondary to Unintended Poor Compliance with Scleral Gas-Permeable Contact Lenses. *Eye & Contact Lens* **40**, e1–e4 (2014).

209. Hill, G., Michaud, L. & Jedlicka, J. Addressing scleral lens clinical concerns. *Optometry Times* 2016–2018 (2016).

210. Tse, V., Tan, B., Kim, Y. H., Zhou, Y. & Lin, M. C. Tear dynamics under scleral lenses. *Contact Lens & Anterior Eye* **42**, 43-48 (2019).

211. Skidmore, K. V., Walker, M. K., Marsack, J. D., Bergmanson, J. P. G. & Miller, W. L. A measure of tear inflow in habitual scleral lens wearers with and without midday fogging. *Contact Lens & Anterior Eye* **42**, 36-42 (2019).

212. Caroline, P. & Andre, M. How Much Tear Exchange Occurs Beneath Scleral Lenses. *Contact Lens Spectrum* **29**, 64 (2014).

213. Paugh, J. R. *et al.* Silicone Hydrogel and Rigid Gas-Permeable Scleral Lens Tear Exchange. *Eye & Contact Lens* **44**, 1 (2018).

214. Ko, L., Maurice, D. & Ruben, M. Fluid exchange under scleral contact lenses in relation to wearing time. *The British Journal of Ophthalmology* **54**, 486-489 (1970).

215. Carracedo, G. *et al.* Post-lens tear turbidity and visual quality after scleral lens wear. *Clinical and Experimental Optometry* **100**, 577–582 (2017).

216. Postnikoff, C. K. *et al.* Identification of leukocytes associated with midday fogging in the post-lens tear film of scleral contact lens wearers. *Investigative Ophthalmology & Visual Science* **60**, 226-233 (2019).

217. Compa˜n, V. *et al.* Oxygen diffusion and edema with modern scleral rigid gas permeable contact lenses. *Investigative Ophthalmology & Visual Science* **55**, 6421–6429 (2014).

218. Weissman, B. a. & Ye, P. Calculated tear oxygen tension under contact lenses offering resistance in series: Piggyback and scleral lenses. *Contact Lens & Anterior Eye* **29**, 231–237 (2006).

219. Giasson, C. J., Morency, J., Melillo, M. & Michaud, L. Oxygen tension beneath scleral lenses of different clearances. *Optometry and Vision Science* **94**, 466–475 (2017).

220. Jun, A. S. *et al.* Subnormal cytokine profile in the tear fluid of keratoconus patients. *PLoS ONE* **6**, (2011).

221. Lema, I. *et al.* Inflammatory response to contact lenses in patients with keratoconus compared with myopic subjects. *Cornea* **27**, 758–763 (2008).

222. Balasubramanian, S. A., Mohan, S., Pye, D. C. & Willcox, M. D. P. Proteases, proteolysis and inflammatory molecules in the tears of people with keratoconus. *Acta Ophthalmologica* **90**, e303-309 (2012).

223. Corrales, R. M. *et al.* Desiccating stress stimulates expression of matrix metalloproteinases by the corneal epithelium. *Investigative Ophthalmology & Visual Science* **47**, 3293-3302 (2006).

224. Tishler, M. *et al.* Elevated tear interleukin-6 levels in patients with Sjögren syndrome. *Ophthalmology* **105**, 2327–9 (1998).

225. Nichols, J. J. *et al.* The TFOS International Workshop on Contact Lens Discomfort: Executive summary. *Investigative Ophthalmology & Visual Science* **54**, TFOS7-TFOS13 (2013).

226. Julious, S. A. Sample size of 12 per group rule of thumb for a pilot study. *Pharmaceutical Statistics* **4**, 287-291 (2005).

228. Acera, A., Vecino, E. & Duran, J. A. Tear MMP-9 levels as a marker of ocular surface inflammation in conjunctivochalasis. *Investigative Ophthalmology & Visual Science* **23**, 8285-8291 (2013).

229. Leonardi, A., Sathe, S., Bortolotti, M., Beaton, A. & Sack, R. Cytokines, matrix metalloproteases, angiogenic and growth factors in tears of normal subjects and vernal keratoconjunctivitis patients. *Allergy* **64**, 710-717 (2009).

230. Fujishima H., Takeuchi T., Shinozaki N., Saito I. & Tsubota, K. Measurement of IL-4 in tears of patients with seasonal allergic conjunctivitis and vernal keratoconjunctivitis. *Clinical & Experimental Immunology* **102**, 395-398 (2008).

231. Elner, V. *et al.* Human corneal interleukin-8. IL-1 and TNF-induced gene expression and secretion. *American Journal of Pathology* **139**, 977–88 (1991).

232. Kaufman, H. E. The practical detection of mmp-9 diagnoses ocular surface disease and may help prevent its complications. *Cornea* **32**, 211–6 (2013).

233. Messmer, E. M., von Lindenfels, V., Garbe, A. & Kampik, A. Matrix Metalloproteinase 9 Testing in Dry Eye Disease Using a Commercially Available Point-of-Care Immunoassay. *Ophthalmology* **123**, 2300-2308 (2016).

234. Markoulli, M., Papas, E., Cole, N. & Holden, B. A. The diurnal variation of matrix metalloproteinase-9 and its associated factors in human tears. *Investigative Ophthalmology & Visual Science* **53**, 1479-1484 (2012).

235. Matsumura, T. *et al.* Changes in matrix metalloproteinases in diabetes patients' tears after vitrectomy and the relationship with corneal epithelial disorder. *Investigative Ophthalmology & Visual Science* **56**, 3559-3564 (2015).

236. Corrales, R. M. *et al.* Desiccating stress stimulates expression of matrix metalloproteinases by the corneal epithelium. *Investigative Ophthalmology & Visual Science* **47**, 3293-3302 (2006).

237. McMahan, R. S. *et al.* Stromelysin-2 (MMP10) Moderates Inflammation by Controlling Macrophage Activation. *Journal of immunology* **197**, 899-909 (2016).

238. Skidmore, K. V., Walker, M. K., Marsack, J. D., Bergmanson, J. P. G. & Miller, W. L. A measure of tear inflow in habitual scleral lens wearers with and without midday fogging. *Contact Lens & Anterior Eye* **42**, 36-42 (2019).

239. Markoulli, M., Papas, E., Cole, N. & Holden, B. A. The diurnal variation of matrix metalloproteinase-9 and its associated factors in human tears. *Investigative Ophthalmology & Visual Science* **21**, 1479-1484 (2012).

240. Sack, R. A., Kah Ooi Tan & Tan, A. Diurnal tear cycle: Evidence for a nocturnal inflammatory constitutive tear fluid. *Investigative Ophthalmology & Visual Science* **33**, 626-640 (1992).

241. Leonardi, A., Tasinato, A., Fregona, I., Plabani, M. & Secchi, A. MMP-1, MMP-9 and TIMP-1 Tear Levels and Activity in Vernal Keratoconjunctivitis. ARVO Annual Meeting Abstract. *Investigative Ophthalmology & Visual Science* **43**, 110 (2002).

242. Lemp, M. A. *et al.* The definition and classification of dry eye disease: Report of the definition and classification subcommittee of the international Dry Eye WorkShop (2007. *Ocular Surface* **5**, 75-92 (2007).

243. Juliana Macedo-de-Araújo, R. *et al.* In vivo assessment of the anterior scleral contour assisted by automatic profilometry and changes in conjunctival shape after miniscleral contact lens fitting. *Journal of Optometry* **12**, 131–140 (2019).

244. Pucker, A. D. *et al.* Assessment of a practitioner's perception of scleral contact lens complications. *Contact Lens & Anterior Eye* **42**, 15-19 (2019).

245. Walker, M. K., Bergmanson, J., Miller, W., Marsack, J. & Johnson, L. Complications and fitting challenges associated with scleral contact lenses: A review. *Contact Lens & Anterior Eye* **39**, 88–96 (2016).

246. Barnett, M. Foggy with No Chance of Moisture. *Review of Cornea and Contact Lenses* (2018).

247. Caroline, P. P. & Andre, M. Cloudy Vision with Sclerals. *Contact Lens Spectrum* **27**, 56 (2012).

248. Walker, M. K. *et al.* Laboratory Analysis of Scleral lens Tear Reservoir Clouding. Poster presented at the *Global Specialty Lens Symposium.* Las Vegas, NV (2014).

249. Consejo, A., Behaegel, J., van Hoey, M., Iskander, D. R. & Rozema, J. J. Scleral asymmetry as a potential predictor for scleral lens compression. *Ophthalmic and Physiological Optics* **38**, 609–616 (2018).

250. Walker, M. K., Schornack, M. M. & Vincent, S. J. Anatomical and physiological considerations in scleral lens wear: Conjunctiva and sclera. *Contact Lens & Anterior Eye* **43**, 517-528 (2020).

251. Vincent, S. J., Alonso-Caneiro, D., Collins, M. J., Alonso-Caneiro, D. & Collins, M. J. Optical coherence tomography and scleral contact lenses: clinical and research applications. *Clinical and Experimental Optometry* **102**, 224–241 (2019).

252. Consejo, A. *et al.* Anterior eye surface changes following miniscleral contact lens wear. *Contact Lens & Anterior Eye* **42**, 70–74 (2019).

253. DeNaeyer, G. & Sanders, D. R. sMap3D Corneo-Scleral Topographer Repeatability in Scleral Lens Patients. *Eye & Contact Lens* **44 Suppl 1**, S259–S264 (2018).

254. Lippman, R. FDA Clinical Trials and the Regulatory Process A look at how initiatives being implemented by the FDA affect clinical investigation of contact lenses. *Contact Lens Spectrum* **27**, 34–39 (2012).

255. Nichols, J., Mitchel, G. & King-Smith, P. The Impact of Contact Lens Care Solutions on the Thickness of the Tear Film and Contact Lens. *Cornea* **24**, 825–832 (2005).

256. Berntsen, D. *et al.* Subjective Comfort and Physiology with Modern Contact Lens Care Products. *Optometry and Vision Science* **93**, 809–819 (2016).

257. Terry, R. *et al.* CCLRU standards for success of daily and extended wear contact lenses. *Optometry and Vision Science* **70**, 234–43 (1993).

258. Bailey, I. L., Bullimore, M. A., Raasch, T. W. & Taylor, H. R. Clinical grading and the effects of scaling. *Investigative Ophthalmology & Visual Science* **32**, 422–32 (1991).

259. Rodriguez, J. D., Johnston, P. R., Ousler, G. W., Smith, L. M. & Abelson, M. B. Automated grading system for evaluation of ocular redness associated with dry eye. *Clinical Ophthalmology* **3**, 1197–1204 (2013).

260. Keller, A., Nesvizhskii, A., Kolker, E. & Aebersold, R. Empirical statistical model to estimate the accuracy of peptide identifications made by MS/MS and database search. *Analytical Chemistry* **74**, 5383–92 (2002).

261. Nesvizhskii, A., Keller, A., Kolker, E. & Aebersold, R. A statistical model for identifying proteins by tandem mass spectrometry. *Analytical Chemistry* **75**, 4646–58 (2003).

262. Read, S. A. *et al.* Diurnal variation of anterior scleral and conjunctival thickness. *Ophthalmic and Physiological Optics* **36**, 279–289 (2016).

263. Bartlett, J. W. & Frost, C. Reliability, repeatability and reproducibility: Analysis of measurement errors in continuous variables. *Ultrasound in Obstetrics and Gynecology* **31**, 466–475 (2008).

264. Bland, J. M. & Altman, D. G. Measurement error. *British Medical Journal* **313**, 744 (1996).

265. Lenders, J. W. M., Williams, T. A., Reincke, M. & Gomez-Sanchez, C. E. 8-Oxocortisol and 18-hydroxycortisol: is there clinical utility of these steroids? *European Journal of Endocrinology* **178**, R1-R9 (2017).

266. Freel, E. M. *et al.* Studies on the Origin of Circulating 18-Hydroxycortisol and 18-Oxocortisol in Normal Human Subjects. *The Journal of Endocrinology and Metab*olism **89**, 4628-4633 (2004).

267. Aitzetmüller, K. & Koch, J. Liquid chromatographic analysis of sebum lipids and other lipids of medical interest. *Journal of Chromatography B: Biomedical Sciences and Applications* **145**, 195–202 (1978).

268. Olżyńska, A. & Cwiklik, L. Behavior of sphingomyelin and ceramide in a tear film lipid layer model. *Annals of Anatomy* **210**, 128–134 (2017).

269. Glasgow, B. J. & Abduragimov, A. Interaction of Ceramides and Tear Lipocalin Ben. *Biochimica et Biophysica Acta* **1863**, 399–408 (2018).

270. Butovich, I. A., Wojtowicz, J. C. & Molai, M. Human tear film and meibum. Very long chain wax esters and (O-acyl)-omega-hydroxy fatty acids of meibum. *Journal of Lipid Research* **50**, 2471–2485 (2009).

271. Sack, R. A. *et al.* Towards a closed eye model of the pre-ocular tear layer. *Progress in Retinal and Eye Research* **19**, 649–668 (2000).

272. Bron, A. J., Tiffany, J. M., Gouveia, S. M., Yokoi, N. & Voon, L. W. Functional aspects of the tear film lipid layer. *Experimental Eye Research* **78**, 347–360 (2004).

273. Ochieng, J. & Chaudhuri, G. Cystatin superfamily. *Journal of Health Care for the Poor and Underserved* **21**, 51–70 (2010).

274. Parthiban, N. *et al.* Quantitative profiling of tear proteome reveals down regulation of zinc alpha-2 glycoprotein in Aspergillus flavus keratitis patients. *Experimental Eye Research* **186**, 107700 (2019).

275. Dor, M. et al. Investigation of the global protein content from healthy human tears. *Experimental Eye Research* **179**, 64-74 (2018).

276. Schornack, M. M. & Nau, C. B. Changes in Optical Density of Postlens Fluid Reservoir During 2 Hours of Scleral Lens Wear. *Eye & Contact Lens* **44 Suppl 2**, S344–S349 (2018).

277. Chen, J., Green-Church, K. B. & Nichols, K. K. Shotgun lipidomic analysis of human meibomian gland secretions with electrospray ionization tandem mass spectrometry. *Investigative Ophthalmology & Visual Science* **51**, 6220–6231 (2010).

278. Butovich, I. A., Uchiyama, E., di Pascuale, M. A. & McCulley, J. P. Liquid chromatography-mass spectrometric analysis of lipids present in human meibomian gland secretions. *Lipids* **42**, 765–776 (2007).

279. Borchman, D., Ramasubramanian, A., Foulks, G. N. & Boulevard, M. A. Human Meibum Cholesteryl and Wax Ester Variability with Age, Sex, and Meibomian Gland Dysfunction. *Investigative Ophthalmology & Visual Science* **60**, 2286-2293 (2019).

280. Nagyová, B. & Tiffany, J. M. Components responsible for the surface tension of human tears. *Current Eye Research* **19**, 4–11 (1999).

281. Berger, R. E. & Corrsin, S. A surface tension gradient mechanism for driving the pre-corneal tear film after a blink. *Journal of Biomechanics* **7**, 225–238 (1974).

282. Eoin Fahy, Dawn Cotter, Manish Sud, and S. S. Lipid classifications, structures and tools. *Biochimica et Biophysica Acta* **1811**, 637–647 (2011).

283. Wizert, A., Robert Iskander, D., Cwiklik, L. & Roccatano, D. Organization of Lipids in the Tear Film: A Molecular- Level View. *PLoS One* **9**, e92461 (2014).

284. Köfeler, H. C. Branched fatty acids. in *Encyclopedia of Lipidomics* 1–3 (2016).

285. Telenius, J., Koivuniemi, A., Kulovesi, P., Holopainen, J. M. & Vattulainen, I. Role of Neutral Lipids in Tear Fluid Lipid Layer: Coarse-Grained Simulation Study. *Langmuir* **28**, 17092-17100 (2012).

286. Shine, W. E. & Mcculley, J. P. Polar lipids in human meibomian gland secretions. *Current Eye Research* **36**, 89-94 (2009).

287. Dean, A. W. & Glasgow, B. J. Mass spectrometric identification of phospholipids in human tears and tear lipocalin. *Investigative Ophthalmology & Visual Science* **53**, 1773–1782 (2012).

288. ben Bacha, A., Abid, I. & ben Bacha, A. Secretory Phospholipase A 2 in Dromedary Tears: a Host Defense Against Staphylococci and Other Gram-Positive Bacteria. *Applied Biochemistry and Biotechnology* **169**, 1858–1869 (2013).

289. Carney, F. P., Morris, C. A. & Willcox, M. D. P. Effect of hydrogel lens wear on the major tear proteins during extended wear. *Clinical & Experimental Ophthalmology* **25 Suppl 1**, S36-8 (1997).

290. Farris, R. L. Tear analysis in contact lens wearers. *Transactions of the American Ophthalmological Society* **83**, 501–45 (1985).

291. Acera, A. *et al.* Changes in tear protein profile in keratoconus disease. *Eye* **25**, 1225–1233 (2011).

292. Bill, A. Capillary Permeability to and Extravascular Dynamics of Myoglobin, Albumin and Gammaglobulin in the Uvea. *Acta Physiologica Scandinavica* **73**, 204–219 (1968).

293. Courey, C., Courey, G. & Michaud, L. Conjunctival inlapse: nasal and temporal conjuctival shape variations associated with scleral lens wear. *Journal of Contact Lens Research and Science* **2**, e-38 (2018).

294. Foulks, G. N. The Correlation Between the Tear Film Lipid Layer and Dry Eye Disease. *Survey of Ophthalmology* **52**, 369–374 (2007).

295. Bland, H. C., Moilanen, J. A., Ekholm, F. S. & Paananen, R. O. Investigating the Role of Specific Tear Film Lipids Connected to Dry Eye Syndrome: A Study on O-Acyl-omega-hydroxy Fatty Acids and Diesters. *Langmuir* **35**, 3545–3552 (2019).

296. Joffre, C. *et al.* Differences in meibomian fatty acid composition in patients with meibomian gland dysfunction and aqueous-deficient dry eye. *British Journal of Ophthalmology* **92**, 116–119 (2008).

297. Hetman, Z. A. & Borchman, D. Concentration dependent cholesteryl-ester and wax-ester structural relationships and meibomian gland dysfunction. *Biochemistry and Biophysics Reports* **21**, (2020).

298. Nau, C. B. C., Schornack, M. M. M., McLaren, J. W. J. & Sit, A. J. A. Intraocular Pressure After 2 Hours of Small-Diameter Scleral Lens Wear. *Eye & Contact Lens* **42**, 350–353 (2016).

299. Aitsebaomo, A., Wong-Powell, J., Miller, W. L. & Amir, F. Influence of Scleral Lens on Intraocular Pressure. *Journal of Contact Lens Research and Science* **3**, e1–e9 (2019).

300. Vincent, S. J., Alonso-Caneiro, D. & Collins, M. J. Evidence on Scleral Contact Lenses and Intraocular Pressure. *Clinical and Experimental Optometry* **100**, 87–88 (2017).

301. Shahnazi, K. C., Isozaki, V. L. & Chiu, G. B. Effect of Scleral Lens Wear on Central Corneal Thickness and Intraocular Pressure in Patients with Ocular Surface Disease. *Eye & Contact Lens* **46**, 341-347 (2019).

302. Michaud, L., Samaha, D. & Giasson, C. J. Intra-ocular pressure variation associated with the wear of scleral lenses of different diameters. *Contact Lens & Anterior Eye* **42**, 104–110 (2019).

303. Downs, J. C. Optic Nerve Head Biomechanics in Aging and Disease. *Experimental Eye Research* **Apr**, 19–29 (2015).

304. Fazio, M. A., Johnstone, J. K., Smith, B., Wang, L. & Girkin, C. A. Displacement of the Lamina Cribrosa in Response to Acute Intraocular Pressure Elevation in Normal Individuals of African and European Descent. *Investigative Ophthalmology & Visual Science* **57**, 3331–9 (2016).

305. Bedggood, P. *et al.* Optic Nerve Tissue Displacement during Mild Intraocular Pressure Elevation: its Relationship to Central Corneal Thickness and Corneal Hysteresis. *Ophthalmic and Physiological Optics* **38**, 389–399 (2018).

306. Agoumi, Y. *et al.* Laminar and prelaminar tissue displacement during intraocular pressure elevation in glaucoma patients and healthy controls. *Ophthalmology* **118**, 52–59 (2011).

307. Tun, T. A. *et al.* Association of Functional Loss with the Biomechanical Response of the Optic Nerve Head to Acute Transient Intraocular Pressure Elevations. *JAMA Ophthalmology* **136**, 184–192 (2018).

308. Schrems-Hoesl, L., Schrems, W., Laemmer, R., Kruse, F. & Mardin, C. Precision of Optic Nerve Head and Retinal Nerve Fiber Layer Parameter Measurements by Spectral-domain Optical Coherence Tomography. *Journal of Glaucoma* **27**, 407–414 (2018).

309. Pardon, L. P., Harwerth, R. S. & Patel, N. B. Neuroretinal Rim Response to Transient Changes in Intraocular Pressure in Healthy Non-human Primate Eyes. *Experimental Eye Research* **193**, 107978 (2020).

310. Pardon, L., McAllister, F., Cheng, H. & Patel, N. Minimum Rim Width Decreases over a 12-hour Daytime Period in Healthy Individuals. *Optometry and Vision Science* **95**, 180035 (2018).

311. Almobarak, F. A. *et al.* Automated Segmentation of Optic Nerve Head Structures with Optical Coherence Tomography. *Investigative Ophthalmology & Visual Science* **55**, 1161–8 (2014).

312. Xin, C. *et al.* Aqueous outflow regulation: Optical coherence tomography implicates pressure-dependent tissue motion. *Experimental Eye Research* **158**, 171–186 (2017).

313. Acott, T. S. *et al.* Intraocular pressure homeostasis: maintaining balance in a high-pressure environment. *Journal of Ocular Pharmacology and Therapeutics* **30**, 94–101 (2014).

314. Loukovitis, E. *et al.* Genetic Aspects of Keratoconus: A Literature Review Exploring Potential Genetic Contributions and Possible Genetic Relationships with Comorbidities. *Ophthalmology and Therapy* **7**, 263–292 (2018).

315. Li, Y., Shi, J., Duan, X. & Fan, F. Transpalpebral Measurement of Intraocular Pressure using the Diaton Tonometer versus Standard Goldmann Applanation Tonometry. *Graefe's Archive for Clinical & Experimental Ophthalmology* **248**, 1765–70 (2010).

316. Doherty, M. D., Carrim, Z. I. & O'Neill, D. P. Diaton Tonometry: An Assessment of Validity and Preference against Goldmann Tonometry. *Clinical & Experimental Ophthalmology* **40**, e171-5 (2012).

317. Wisse, R. P., Peeters, N., Imhof, S. M. & van der Lelij, A. Comparison of Diaton Transpalpebral Tonometer with Applanation Tonometry in Keratoconus. *International Journal of Ophthalmology* **9**, 395–8 (2016).

318. Toker, M. I., Vural, A., Erdogan, H., Topalkara, A. & Arici, M. K. Central Corneal Thickness and Diaton Transpalpebral Tonometry. *Graefe's Archive for Clinical & Experimental Ophthalmology* **246**, 881–889 (2008).

319. Suman, S., Agrawal, A., Pal, V. K. & Pratap, V. B. Rebound Tonometer: Ideal Tonometer for Measurement of Accurate Intraocular Pressure. *Journal of Glaucoma* **23**, 633–7 (2014).

320. Li, B. Z. *et al.* Comparison of iCare Rebound Tonometer and Goldmann Applanation Tonometer after Descemet's Stripping with Automated Endothelium Keratoplasty. *Chinese Journal of Ophthalmology* **49**, 257–62 (2013).

321. Pronin, S., Brown, L., Megaw, R. & Tatham, A. J. Measurement of intraocular pressure by patients with glaucoma. *JAMA Ophthalmology* **135**, 1030-1036 (2017).

322. McMonnies, C. W. & Boneham, G. C. Experimentally Increased Intraocular Pressure using Digital Forces. *Eye & Contact Lens* **33**, 124–129 (2007).

323. Thakur, A., Willcox, M. D. P. & Stapleton, F. The proinflammatory cytokines and arachidonic acid metabolites in human overnight tears: Homeostatic mechanisms. *Journal of Clinical Immunology* **18**, 61–70 (1998).

324. Lee, S. Y. *et al.* Analysis of tear cytokines and clinical correlations in Sjogren syndrome dry eye patients and non-Sjogren syndrome dry eye patients. *American Journal of Ophthalmology* **156**, 247-253 (2013).

325. Kallinikos, P., Morgan, P. & Efron, N. Assessment of stromal keratocytes and tear film inflammatory mediators during extended wear of contact lenses. *Cornea* **25**, 1–10 (2006).

326. Yoon, K. C., Jeong, I. Y., Park, Y. G. & Yang, S. Y. Interleukin-6 and tumor necrosis factor-alpha levels in tears of patients with dry eye syndrome. *Cornea* **26**, 431–437 (2007).

327. Balasubramanian, S. A., Mohan, S., Pye, D. C. & Willcox, M. D. P. Proteases, proteolysis and inflammatory molecules in the tears of people with keratoconus. *Acta Ophthalmologica* **90**, 303–309 (2012).

328. Thakur, A. & P Willcox, M. D. Chemotactic Activity of Tears and Bacteria Isolated During Adverse Responses. *Experimental Eye Research* **66**, 129-137 (1998).

329. Ionescu, I. C. *et al.* Overexpression of Tear Inflammatory Cytokines as Additional Finding in Keratoconus Patients and Their First-Degree Family Members. *Mediators of Inflammation* **2018**, 1–9 (2018).

330. Koch, A. E. *et al.* Interleukin-8 as a macrophage-derived mediator of angiogenesis. *Science* **258**, 1798-1801 (1992).

331. Fujishima, H., Takeuchij, T. T., Shinozaki, N., Saito, I. & Tsubota, K. Measurement of IL-4 in tears of patients with seasonal allergic conjunctivitis and vernal keratoconjunctivitis. *Clinical & Experimental Immunology* **102**, 395-398 (1995).

332. Leonardi, A., Sathe, S., Bortolotti, M., Beaton, A. & Sack, R. Cytokines, matrix metalloproteases, angiogenic and growth factors in tears of normal subjects and vernal keratoconjunctivitis patients. *Allergy* **64**, 710-717 (2009).

333. Balasubramanian, S. A., Pye, D. C. & Willcox, M. D. P. Effects of eye rubbing on the levels of protease, protease activity and cytokines in tears: Relevance in keratoconus. *Clinical and Experimental Optometry* **96**, 214–218 (2013).

334. Page-McCaw, A., Ewald, A. J. & Werb, Z. Matrix metalloproteinases and the regulation of tissue remodelling. *Nature Reviews Molecular Cell Biology* **8**, 221-223 (2007).

335. Sivak, J. M. & Fini, M. E. MMPs in the eye: Emerging roles for matrix metalloproteinases in ocular physiology. *Progress in Retinal and Eye Research* **21**, 1-14 (2002).

336. Corrales, R. M. *et al.* Desiccating stress stimulates expression of matrix metalloproteinases by the corneal epithelium. *Investigative Ophthalmology & Visual Science* **47**, 3293-3302 (2006).

337. Kaufman, H. E. The practical detection of mmp-9 diagnoses ocular surface disease and may help prevent its complications. *Cornea* **32**, 211–6 (2013).

338. Garrana, R. M. R., Zieske, J. D., Assouline, M. & Gipson, I. K. Matrix metalloproteinases in epithelia from human recurrent corneal erosion. *Investigative Ophthalmology & Visual Science* **40**, 1266–1270 (1999).

339. Lema, I., Duran, J. A. & Durán, J. A. Inflammatory molecules in the tears of patients with keratoconus. *Ophthalmology* **112**, 654–659 (2005).

340. Lema, I., Sobrino, T., Durán, J. a, Brea, D. & Díez-Feijoo, E. Subclinical keratoconus and inflammatory molecules from tears. *The British Journal of Ophthalmology* **93**, 820–824 (2009).

341. Vandivort, T. *et al.* Stromelysin-2 (MMP-10) facilitates clearance and moderates inflammation and cell death following lung exposure to long multiwalled carbon nanotubes. *International Journal of Nanomedicine* **12**, 1019–1031 (2017).

342. Leonardi, A., Tasinato, A., Fregona, I., Plabani, M. & Secchi, A. MMP-1, MMP-9 and TIMP-1 Tear Levels and Activity in Vernal Keratoconjunctivitis. ARVO Annual Meeting Abstract. *Investigative Ophthalmology & Visual Science* **43**, 110 (2002).

343. Galvis, V. *et al.* Keratoconus: an inflammatory disorder? *Eye* **29**, 843–859 (2015).

344. Walker, M. K., Lema, C., Redfern, R. & Lema, C. Scleral lens wear: Measuring inflammation in the fluid reservoir. *Contact Lens & Anterior Eye* **43**, 577-584 (2020).

345. Akkaya Turhan, S., Dizdar Yigit, D. & Toker, E. Impact of Changes in the Optical Density of Postlens Fluid on the Clinical Performance of Miniscleral Lenses. *Eye & Contact Lens* **46**, 353-358 (2019).

346. Johns, L. Scleral Lenses, Turbid Clouding. *I-site Newsletter* online (2014).

347. Muntz, A., Subbaraman, L. N., Sorbara, L. & Jones, L. Tear exchange and contact lenses: a review. *Journal of Optometry* **8**, 2–11 (2015).

348. Gipson, I. K. & Inatomi, T. Cellular origin of mucins of the ocular surface tear film. *Advances in Experimental Medicine and Biology* **438**, 221-227 (1998).

349. Soriano-Romaní, L. *et al.* Novel anti-inflammatory liposomal formulation for the pre-ocular tear film: In vitro and ex vivo functionality studies in corneal epithelial cells. *Experimental Eye Research* **154**, 79-87 (2017).

350. Lu, X. & Kassab, G. S. Integrins mediate mechanical compression-induced endotheliumdependent vasodilation through endothelial nitric oxide pathway. *Journal of General Physiology* **146**, 221-232 (2015).

351. Macedo-de-Araújo, R. J., Amorim-de-Sousa, A., van der Worp, E. & Gonzalez-Meijome, J. M. Clinical Findings and Ocular Symptoms Over 1 Year in a Sample of Scleral Lens Wearers. *Eye & Contact Lens* **46**, e40-e55 (2019).

352. Otchere, H., Jones, L. W. & Sorbara, L. Effect of Time on Scleral Lens Settling and Change in Corneal Clearance. *Optometry and Vision Science* **94**, 908–913 (2017).

353. Esen, F. & Toker, E. Influence of apical clearance on mini-scleral lens settling, clinical performance, and corneal thickness changes. *Eye & Contact Lens* **43**, 230–235 (2017).

354. Bray, C., Britton, S., Yeung, D., Haines, L. & Sorbara, L. Change in over-refraction after scleral lens settling on average corneas. *Ophthalmic and Physiological Optics* **37**, 467–472 (2017).

355. Caroline, P. J. & Andre, M. Scleral lens settling. *Contact Lens Spectrum* **27**, 56 (2012).

356. Li, M. *et al.* Daytime variations of tear osmolarity and tear meniscus volume. *Eye & Contact Lens* **38**, 282–7 (2012).

357. Narayanan, S., Corrales, R. M., Farley, W., McDermott, A. M. & Pflugfelder, S. C. Interleukin-1 receptor-1-deficient mice show attenuated production of ocular surface inflammatory cytokines in experimental dry eye. *Cornea* **27**, 811–7 (2008).

358. Schornack, M. M. & Patel, S. v. Scleral lenses in the management of keratoconus. *Eye & Contact Lens* **36**, 39–44 (2010).

359. Aluru, S. V. *et al.* Tear Fluid Protein Changes in Dry Eye Syndrome Associated with Rheumatoid Arthritis: A Proteomic Approach. *Ocular Surface* **15**, 112–129 (2017).

360. Gendler, S. J. & Spicer, A. P. Epithelial mucin genes. *Annual Review of Physiology* **57**, 607–634 (1995).

361. Gipson, I. K. Distribution of mucins at the ocular surface. *Experimental Eye Research* **78**, 379–388 (2004).

362. Macedo-De-Araújo, R. J., Serramito-Blanco, M., van der Worp, E., Carracedo, G. & González-Méijome, J. M. Differences between inferior and superior bulbar conjunctiva goblet cells in scleral lens wearers: A pilot study. *Optometry and Vision Science* **97**, 726–731 (2020).

363. Caroline, P. & Andre, M. Cloudy Vision with Sclerals. *Contact Lens Spectrum* **27**, 56 (2012).

364. Ciralsky, J. B. *et al.* Treatment of Refractory Persistent Corneal Epithelial Defects: A Standardized Approach Using Continuous Wear PROSE Therapy. *Ocular Immunology and Inflammation* **23**, 219-224 (2014).

365. Obinwanne, C. J., Echendu, D. C., Agbonlahor, O. & Dike, S. Changes in scleral tonometry and anterior chamber angle after short-term scleral lens wear. *Optometry and Vision Science* **97**, 720–725 (2020).

366. Fogt, J. S. *et al.* Comparison of pneumatonometry and transpalpebral tonometry measurements of intraocular pressure during scleral lens wear. *Optometry and Vision Science* **97**, 711–719 (2020).

367. Walker, M., Pardon, L., Redfern, R. & Patel, N. Intraocular pressure and optic nerve head morphology during scleral lens wear. *Optometry and Vision Science* **97**, 661-668 (2020).

368. Cheung, S. Y., Collins, M. J. & Vincent, S. J. The impact of short-term fenestrated scleral lens wear on intraocular pressure. *Contact Lens & Anterior Eye* **43**, 585–588 (2020).

369. Samaha, D. & Michaud, L. Bruch membrane opening minimum rim width changes during scleral lens wear. *Eye & Contact Lens* **47**, 295–300 (2020).

370. Kramer, E. G. & Vincent, S. J. Intraocular pressure changes in neophyte scleral lens wearers: A prospective study. *Contact Lens & Anterior Eye* **43**, 609–612 (2020).

371. Amm, M. & Hedderich, J. Transpalpebrale tonometrie mit einem digitalen, tragbaren tonometer in gesunden augen und nach perforierender keratoplastik. *Ophthalmologe* **102**, 70-76 (2005).

372. Porcar, E., Montalt, J. C., España-Gregori, E. & Peris-Martínez, C. Impact of Corneoscleral Contact Lens Usage on Corneal Biomechanical Parameters in Keratoconic Eyes. *Eye & Contact Lens* **45**, 318-323 (2019).

373. Latina, M., Shazly, T., Iospa, R. & Chynn, E. Accuracy of transpalpebral tonometer compared to Goldmann applanation tonometer in normal and glaucomatous eyes. *Investigative Ophthalmology & Visual Science* **50**, ARVO Abstract 2843 (2009).

374. Lam, A. K. C., Lam, C. H. & Chan, R. The validity of a digital eyelid tonometer (TGDc-01) and its comparison with Goldmann applanation tonometry - a pilot study. *Ophthalmic and Physiological Optics* **25**, (2005).

375. Troost, A. Transpalpebral tonometry: reliability and comparison with Goldmann applanation tonometry and palpation in healthy volunteers. *British Journal of Ophthalmology* **89**, 280-283 (2005).

376. A. Troost, K. Specht, F. Krummenauer, S.H. Yun, O. S. Deviations between transpalpebral tonometry using TGDc-01 and Goldmann applanation tonometry depending on the IOP level. *Graefes Archives of Clinical & Experimental Ophthalmology* **243**, 853–858 (2005).

377. Vincent, S. J., Vincent, R. A., Shields, D. & Lee, G. A. Comparison of intraocular pressure measurement between rebound, non-contact and Goldmann applanation tonometry in treated glaucoma patients. *Clinical & Experimental Ophthalmology* **40**, e163-170 (2012).

378. Salvetat, M. L. *et al.* Comparison of iCare tonometer and Goldmann applanation tonometry in normal corneas and in eyes with automated lamellar and penetrating keratoplasty. *Eye* **25**, 642–650 (2011).

379. Fisher, D., Collins, M. J. & Vincent, S. J. Post-lens fluid reservoir thickness and corneal edema during closed eye scleral lens wear. *Contact Lens & Anterior Eye* **44**, 102–107 (2021).

380. Herndon, L. W. Measuring intraocular pressure-adjustments for corneal thickness and new technologies. *Current Opinion in Ophthalmology* **17**, 115–119 (2006).

381. Can, E., Eser-Ozturk, H., Duran, M., Cetinkaya, T. & Ariturk, N. Comparison of central corneal thickness measurements using different imaging devices and ultrasound pachymetry. *Indian Journal of Ophthalmology* **67**, 496–499 (2019).

382. El-Harazi, S., Feldman, R., Ruiz, R., Villanueva, G. & Chuang, A. Consensual inflammation following ocular surgery. *Ophthalmic Surgical Lasers* **30**, 254–9 (1999).

383. Cho, H.-K. & Kee, C. Rate of Change in Bruch's Membrane Opening-Minimum Rim Width and Peripapillary RNFL in Early Normal Tension Glaucoma. *Journal of Clinical Medicine* **9**, 1–13 (2020).

384. Fautsch, M. P. *et al.* Aqueous humor outflow: what do we know? Where will it lead us? *Investigative Ophthalmology & Visual Science* **47**, 4181–4187 (2006).

385. Ascher, MD. The Aqueous Veins: Biomicroscopic Study of the Aqueous Humor Elimination. *Medical Journal of Australia* **2**, 1-19 (1962).

386. Keeley, F. W., Morin, J. D. & Vesely, S. Characterization of collagen from normal human sclera. *Experimental Eye Research* **39**, 533–542 (1984).

387. Grytz, R. *et al.* Age- and race-related differences in human scleral material properties. *Investigative Ophthalmology & Visual Science* **55**, 8163–8172 (2014).